"Characterizing Natural Gas Hydrates in the Deep Water Gulf of Mexico: Applications for Safe Exploration and Production Activities Semi-Annual Report"

Report Type: Semi-Annual
No: 41330R10

Starting	**October 2005**
Ending	**March 2006**

Author:
Emrys Jones

June 2006

DOE Award Number: DE-FC26-01NT41330

Submitting Organization:
Chevron Energy Technology Company
1500 Louisiana Street
Houston, TX 77002

DISCLAIMER

ABSTRACT

In 2000, Chevron began a project to learn how to characterize the natural gas hydrate deposits in the deepwater portions of the Gulf of Mexico. A Joint Industry Participation (JIP) group was formed in 2001, and a project partially funded by the U.S. Department of Energy (DOE) began in October 2001. The **primary objective** of this project is to develop technology and data to assist in the characterization of naturally occurring gas hydrates in the deep water Gulf of Mexico (GOM). These naturally occurring gas hydrates can cause problems relating to drilling and production of oil and gas, as well as building and operating pipelines. Other objectives of this project are to better understand how natural gas hydrates can affect seafloor stability, to gather data that can be used to study climate change, and to determine how the results of this project can be used to assess if and how gas hydrates act as a trapping mechanism for shallow oil or gas reservoirs.

During October 2005 – March 2006, the JIP concentrated on:

- Conducting experiments on the cores collected;
- Analyzing the log data collected;
- Revising the project work plan and budget to complete Phase II.
- Holding JIP and contractor meetings to discuss results of Leg 1.

More information can be found on the JIP website.

https://cpln-www1.chevrontexaco.com/cvx/gasjip.nsf

Table of Contents

LIST of TABLES & FIGURES

Appendix A. Science Plan

APPENDIX B. Georgia Tech Pressure Core Measurements, pp. 22-44

Appendix C. Geotek Pressure Coring and Core Logging Report, pp. 45-131

section ends. Temperatures were picked from maxima in data.
Figure EXPL-12. Infrared thermal images of (at top) the ice trough, half-filled with ice and (at bottom) a core that was recently handled by a gloveless individual. Both ice and people can change the temperature of cores and potentially disturb remnant thermal anomalies from gas hydrate dissociation.
Figure EXPL-13. MSCL-S inside the 20-foot unrefrigerated logging container on the *Uncle John* during the GOM-JIP Expedition.
Figure EXPL-14. Complete data set for Core KC151-3-20H, showing influence of gas expansion on data. From left, RGB data from line scan image, spectral color data from Minolta color spectrophotometer, gamma density, resistivity, magnetic susceptibility (loop sensor), magnetic susceptibility (point sensor), natural gamma radioactivity, temperature, line scan image, and infrared image.
Figure EXPL-15. MSCL-P with Geotek P-wave Central Measurement Chamber in place (yellow arrow). The Georgia Tech measurement chamber (not in use) is sitting behind the Geotek CMC.
Figure EXPL-16. MSCL-XYZ installed in the DSDP West Coast Repository at the Scripps Institution of Oceanography, where the split cores from the GOM-JIP were logged. The MSCL-XYZ is configured for natural gamma measurements in this photo.
Figure AT-1. Plot of temperature data from infrared imaging, which takes the temperature of the core liner, and from direct measurement of the center of the core at core section ends for the top of Hole AT13-2. Two-dimensional infrared image is shown to the right of the plot.
Figure AT-2. Plot of temperature data from infrared imaging, which takes the temperature of the core liner, and from direct measurement of the center of the core at core section ends for the bottom of Hole AT13-2. Two-dimensional infrared image is shown to the right of the plot.
Figure AT-3. Gamma density (green line) and infrared image for Core AT13-2-8H. Sharply bounded cold regions are voids, but the voids had shifted by the time the gamma density is measured. Gamma density was not calibrated for air, so empty liner appears to have negative densities.
Figure AT-4. Temperature data for Core AT13-2-11H, including infrared image. Internal temperatures and core liner temperatures from infrared scanning did not match due to handling of the core.
Figure AT-5. Temperature data from the Seabird CTD cast over Site AT13.
Figure AT-6. Temperature and pressure data versus time for Core AT13-2-7P. The retrieval of the tool up the drill pipe is bounded by green dashed lines.
Figure AT-7. MSCL-S data, including gamma density, P-wave velocity, magnetic susceptibility, and electrical resistivity, for Hole AT13-2.
Figure AT-8. Line scan color image taken with the MSCL-XYZ using the Geoscan camera of a typical core section seen during the GOM-JIP Expedition (Section AT13-2-4H-5): clay with gas expansion voids. Pixels are 100 microns on a side. Color fringing on edges of image results from registration of camera CCDs.
Figure AT-9. MSCL-XYZ data summary plot, including magnetic susceptibility and color spectrophotometry, for Hole AT13-2.
Figure AT-10. ROV push core AT14-7PC, collected in fiberglass liner, in the MSCL-S. Small fiberglass core sections had end-caps taped on for logging to prevent the core from

oozing out of the liner.
Figure AT-11. MSCL-S data summary plot, including gamma density, P-wave velocity, and magnetic susceptibility, for push core AT14-7PC.
Figure ATM-1. Data from pressure core ATM2-5P, collected from 26.82 mbsf at a pressure of 130 bar. Figure shows gamma density data, collected in the MSCL-V; P-wave velocity, collected in the MSCL-P; and linear X-ray scan, collected in the X-ray CT scanner. Low density/high velocity zone at 27 cm core depth, corresponding to odd X-ray texture, may be a hydrate-bearing layer.
Figure ATM-2. Plot of temperature data from infrared imaging, which takes the temperature of the core liner, and from direct measurement of the center of the core at core section ends for the top of Hole ATM1. Two-dimensional infrared image is shown to the right of the plot.
Figure ATM-3. Plot of temperature data from infrared imaging, which takes the temperature of the core liner, and from direct measurement of the center of the core at core section ends for the top of Hole ATM2. Two-dimensional infrared image is shown to the right of the plot.
Figure ATM-4. Plot of gamma density and infrared-derived temperature for core ATM1-2H, showing difficulty in distinguishing cold regions that correspond to voids from cold regions that correspond to hydrate. Voids had shifted an unknown distance between the two measurements.
Figure ATM-5. Temperature from infrared track (blue) and pore water salinity (red) for Hole ATM1. Freshening trend from 8-15 mbsf is not reflected in the recorded thermal anomalies.
Figure ATM-6. Temperature from infrared track (blue) and pore water salinity (red) for Hole ATM2. The two pore water freshening anomalies in bottom core (arrows; ATM2-3H) may correspond to negative thermal anomalies.
Figure ATM-7. Temperature data from the temperature shoe fitted on the FHPC for cores ATM1-5H and ATM2-3H.
Figure ATM-8. Temperature and pressure data versus time for Core ATM2-5P. The retrieval of the tool up the drill pipe is bounded by green dashed lines.
Figure ATM-9. MSCL-S data, including gamma density, P-wave velocity, magnetic susceptibility, and electrical resistivity, for Hole ATM1.
Figure ATM-10. MSCL-S data, including gamma density, P-wave velocity, magnetic susceptibility, and electrical resistivity, for Hole ATM2.
Figure ATM-11. MSCL-XYZ data summary plot, including magnetic susceptibility and color spectrophotometry, for Holes ATM1&2.
Figure KC151-1. Data from pressure core KC151-3-11P, collected from 227.08 mbsf at a pressure of 160 bar. Figure shows gamma density data, collected in the MSCL-V; P-wave velocity &amplitude, collected in the MSCL-P; and linear X-ray scan, collected in the X-ray CT scanner. Top two-thirds and bottom third of core are distinct in density and velocity.
Figure KC151-2. Data from pressure core KC151-3-13R, collected from 235.92 mbsf at a pressure of 160 bar. Figure shows gamma density data, collected in the MSCL-V; P-wave velocity and amplitude, collected in the MSCL-P; and linear X-ray scan, collected in the X-ray CT scanner. Lower half of core is distinguished by low P-wave amplitudes, slightly lower P-wave velocity and more variable density. High-velocity spike at center

of core may have been a thin hydrate vein.

Figure KC151-3. Gamma density data from pressure core KC151-3-13R, collected on repetitive scans during depressurization. Legend shows density scan number and pressure. Each scan is offset from the next by 0.2 g/cc. The high-velocity spike in Figure KC151-2 may correspond to the crack in the core that formed at about 35 cm core depth.

Figure KC151-4. P-wave velocity data from pressure core KC151-3-13R, collected on pristine core and repressurized core, after depressurization. Core starts at about 20 cm logging depth. Note that the high-velocity spike in the center of the core disappeared following depressurization.

Figure KC151-5. Data from pressure core KC151-3-26R, collected from 383.13 mbsf at a pressure of 180 bar. Figure shows gamma density data, collected in the MSCL-V; P-wave velocity and amplitude, collected in the MSCL-P; and linear X-ray scan, collected in the X-ray CT scanner. Low velocity and densities near center of core and low amplitudes may indicate core disturbance by hydrate dissociation during core recovery.

Figure KC151-6. Plot of temperature data from infrared imaging, which takes the temperature of the core liner, and from direct measurement of the center of the core at core section ends for top of Hole KC151-3. Two-dimensional infrared image is shown to the right of the plot.

Figure KC151-7. Plot of temperature data from infrared imaging, which takes the temperature of the core liner, and from direct measurement of the center of the core at core section ends for middle of Hole KC151-3. Two-dimensional infrared image is shown to the right of the plot.

Figure KC151-8. Plot of temperature data from infrared imaging, which takes the temperature of the core liner, and from direct measurement of the center of the core at core section ends for top half of lower portion of Hole KC151-3. Two-dimensional infrared image is shown to the right of the plot.

Figure KC151-3-9. Plot of temperature data from infrared imaging, which takes the temperature of the core liner, and from direct measurement of the center of the core at core section ends for bottom half of lower portion of Hole KC151-3. Two-dimensional infrared image is shown to the right of the plot.

Figure KC151-10. Temperature data for Core KC151-3-15C, including infrared image. The negative thermal anomaly at 253.45 mbsf displayed classic magnitude and morphology for a hydrate generated thermal anomaly. Slight discontinuity at 137.5 cm is a result of joining the adjacent infrared images.

Figure KC151-11. Temperature data from the Seabird CTD cast over Site KC151.

Figure KC151-12. Temperature data from the temperature shoe fitted on the FHPC for core KC151-3-3H.

Figure KC151-13. Temperature and pressure data versus time for Core KC151-3-11P. The retrieval of the tool up the drill pipe is bounded by green dashed lines.

Figure KC151-14. MSCL-S data, including gamma density, P-wave velocity, magnetic susceptibility, and electrical resistivity, for Hole KC151-3. Gamma density and P-wave velocity from pressure cores KC151-3-11P, -13R, and -26R, measured under *in situ* pressure, are included in this composite in orange. High-velocity spike in Core KC151-3-13R of 2074 m/sec is off scale.

Figure KC151-15. Color line scan image of Core KC151-3-20H, 55-65 cm, showing millimeter-thick, sub-horizontal white veins that may be carbonate.

1.0 Introduction

In 2000, Chevron Petroleum Technology Company began a project to learn how to characterize the natural gas hydrate deposits in the deepwater portion of the Gulf of Mexico. Chevron is an active explorer and operator in the Gulf of Mexico, and is aware that natural gas hydrates need to be understood to operate safely in deep water. In August 2000, Chevron working closely with the National Energy Technology Laboratory (NETL) of the United States Department of Energy (DOE) held a workshop in Houston, Texas, to define issues concerning the characterization of natural gas hydrate deposits. Specifically, the workshop was meant to clearly show where research, the development of new technologies, and new information sources would be of benefit to the DOE and to the oil and gas industry in defining issues and solving gas hydrate problems in deep water.

On the basis of the workshop held in August 2000, Chevron formed a Joint Industry Project (JIP) to write a proposal and conduct research concerning natural gas hydrate deposits in the deepwater portion of the Gulf of Mexico. The proposal was submitted to NETL on April 24, 2001, and Chevron was awarded a contract on the basis of the proposal.

The title of the project is

"Characterizing Natural Gas Hydrates in the Deep Water Gulf of Mexico: Applications for Safe Exploration and Production Activities".

1.2 Objectives

The **primary objective** of this project is to develop technology and data to assist in the characterization of naturally occurring gas hydrates in the deep water Gulf of Mexico (GOM). These naturally occurring gas hydrates can cause problems relating to drilling and production of oil and gas, as well as building and operating pipelines. Other objectives of this project are to better understand how natural gas hydrates can affect seafloor stability, to gather data that can be used to study climate change, and to

determine how the results of this project can be used to assess if and how gas hydrates act as a trapping mechanism for shallow oil or gas reservoirs.

1.3 Project Phases

The project is divided into phases. **Phase I** of the project is devoted to gathering existing data, generating new data, and writing protocols that will help the research team determine the location of existing gas hydrate deposits. During **Phase II** of the project, Chevron will drill at least three data collection wells to improve the technologies required to characterize gas hydrate deposits in the deep water GOM using seismic, core and logging data.

1.4 Research Participants

In 2001, Chevron organized a Joint Industry Participation (JIP) group to plan and conduct the tasks necessary for accomplishing the objectives of this research project. As of March 2006 the members of the JIP were Chevron, Schlumberger, ConocoPhillips, Halliburton, the Minerals Management Service (MMS), Total, JOGMEC, and Reliance Industries Limited.

1.5 Research Activities

The research activities began officially on October 1, 2001. However, very little activity occurred during 2001 because of the paperwork involved in getting the JIP formed and the contract between DOE and Chevron in place. Several Semi-Annual and Topical Reports have been written that cover the activity of the JIP through September 2005.

1.6 Purpose of This Report

The purpose of this report is to document the activities of the JIP during October 2005 – March 2006. It is not possible to put everything into this Semi-Annual report. However, many of the important results are included and references to the JIP website are used to point the reader to more detailed information concerning various aspects of the project. The discussion of the work performed during October 2005 – March 2006 is organized by task and subtask for easy reference to the technical proposal and the DOE contract documents.

More detailed information generated by the JIP during October 2005 – March 2006 can be found on the JIP website. The link to the JIP website is as follows:

https://cpln-www1.chevrontexaco.com/cvx/gasjip.nsf

2.0 Executive Summary

Chevron formed a Joint Industry Participation (JIP) group to write a proposal and conduct research concerning natural gas hydrate deposits in the deepwater portion of the Gulf of Mexico. The proposal was submitted to NETL on April 24, 2001, and Chevron was awarded a contract on the basis of the proposal.

The title of the project is

"Characterizing Natural Gas Hydrates in the Deep Water Gulf of Mexico: Applications for Safe Exploration and Production Activities".

The **primary objective** of this project is to develop technology and data to assist in the characterization of naturally occurring gas hydrates in the deep water Gulf of Mexico (GOM). **Other objectives** of this project are to better understand how natural gas hydrates can affect seafloor stability, to gather data that can be used to study climate change, and to determine how the results of this project can be used to assess if and how gas hydrates act as a trapping mechanism for shallow oil or gas reservoirs.

The project is divided into phases. **Phase I** of the project is devoted to gathering existing data, generating new data, and writing protocols that will help the research team determine the location of existing gas hydrate deposits. During **Phase II** of the project, Chevron will drill at least three data collection wells to improve the technologies required to characterize gas hydrate deposits in the deep water GOM using seismic, core and logging data.

A website has been developed to house the data and information that were collected in the Workshop, as well as other items submitted during the course of this research endeavor. The link to the JIP website is as follows:

https://cpln-www1.chevrontexaco.com/cvx/gasjip.nsf.

2.1 Research Plan and Management

A Continuation Application for Phase II was submitted to the DOE on 15 May 2003. Several changes were required to the original plan because of delays due to EPA permitting, and drill ship changes. A revised Phase II work plan and budget was prepared and submitted to the DOE in March 2006.

2.2 Sensors

A pressurized measure vessel performed well and properties on one core were measured. The measurements showed the need for obtaining pressure cores for accurate property data.

2.3 Core Measurements

Measurements were made on the cores collected using the MSCL and X-ray equipment on the ship. Pressure cores were degassed to determine the amount of hydrates in the core. The degas experiments indicated that the cores contained from 1 to 10% hydrates.

3.0 Results and Discussion Phase II

3.1 Task 1.0 – Research Management Plan

The goals of this task are to develop a work breakdown structure and supporting narrative that concisely addresses the overall project as set forth in the agreement. Provide a concise summary of the technical objectives and technical approach for each task and, where appropriate, for each subtask. Provide detailed schedules and planned expenditures for each task including any necessary charts or tables, and all major milestones and decision points.

A Continuation Application for Phase II was submitted to the DOE on 15 May 2003. Additional documentation was supplied to the DOE in November and December of 2003, March, July, and December of 2004, and the research plan was revised again in January 2005 to allow for the additional cost of the drilling vessel. Several changes were

required to the original plan because of delays due to EPA permitting, and drill ship changes. The final Phase II revision was submitted to the DOE in March of 2006 along with a revised budget to complete Phase II and prepare a proposal for Phase III.

3.2 Task 2.0 – Project Management and Oversight

A project manager appointed by the Joint Industry Project (JIP) Recipients will manage the technical teams, contractors, and the day to day operation of the project. Project manager will report, verbally and through required reporting, on the progress of the program to the DOE and the JIP as required.

During the period of the progress report the JIP and DOE project managers were in regular contact discussing changes to the research plan. The DOE project manager also attended the internal JIP review meeting in November of 2005. During the internal review meeting research staff presented a draft of the data analysis work and discussed the way forward for the JIP.

3.3 Task 3.0 – Validation of New Gas Hydrate Sensors

Review and evaluate new hydrate sensor development (Phase I – Task 4, Subtasks 4.1 – 4.4). Prototype sensors, if available, will be field tested in well bores and protocols for use will be developed and distributed to all entities involved in drilling wells in the Gulf of Mexico.

The pressurized core measurement vessel, developed by Georgia Tech, and transfer vessels were tested during the Leg 1 cruise. After some initial adjustment, the equipment worked and one pressure core was transferred into the measurement vessel for testing. Georgia Tech's complete report is attached as Appendix B.

Figure 3.1. Data from the Pressure Core Measurement Vessel

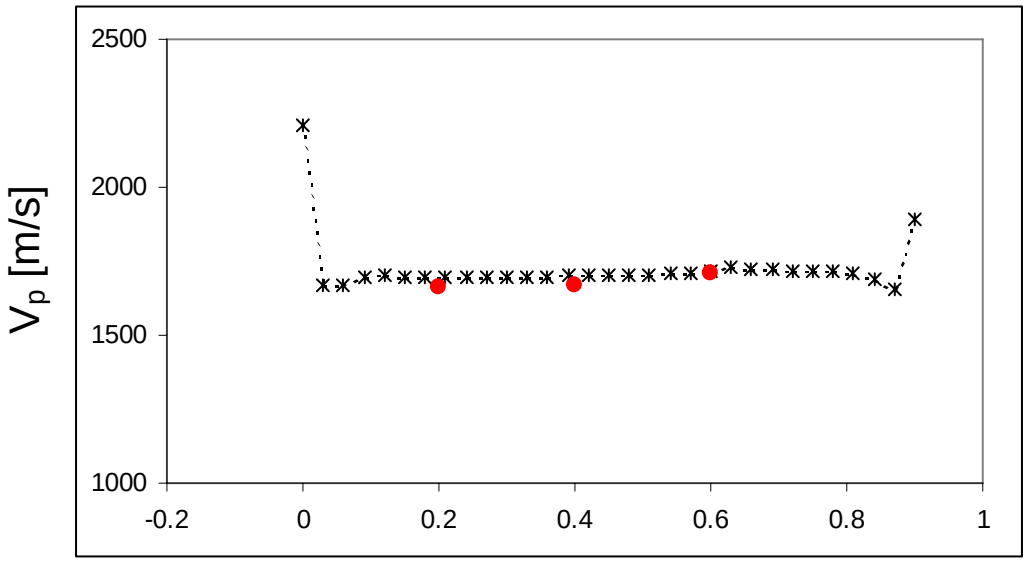

The data presented in Figure 3.1 are from Keathley Canyon at 227 mbsf.

3.4 Task 4.0 – Validation of the Well Bore Stability Model

The goal of this task is to revise the well bore stability model, developed in Phase I – Task 5.0 – Subtasks 5.1 – 5.4, using laboratory data and to validate the model using all available information. Changes or improvements will be made and the model will be distributed for use by organizations drilling wells in the Deep Water Gulf of Mexico.

The well bore model developed in Phase I was used to predict pore pressure and well bore stability before the Leg 1 Cruise. During the cruise one the staff responsible for the well bore model collected data necessary to determine the performance of the model.

Figure 3.2. Well Bore Stability Model Prediction for Atwater Valley 1 Hole

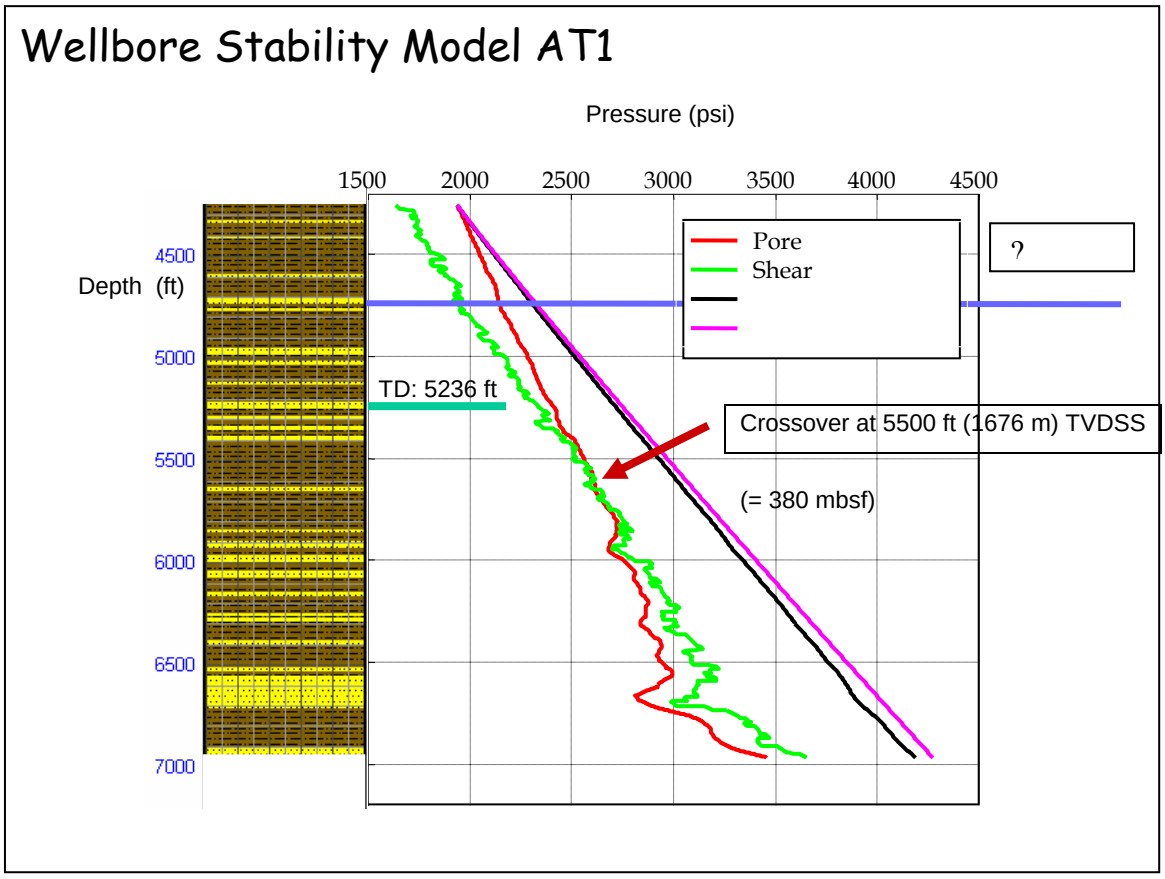

3.5 Task 5.0 – Core and Well Log Data Collection – Area A

In order to develop the necessary ground truth data, twin wells in the most favorable location for gas hydrates identified in Phase I – Tasks 11/12 – Subtasks 11.1 – 11.5 (this will be designated Area A) will be drilled. Well A-1 will be drilled without well control and will gather drilling, MWD and openhole logging information. Well A-2 will be drilled with well control and will gather drilling, MWD, core and openhole logging information. The wells will be surveyed and the core will be sent to laboratories for analyses. An additional well, A-3, will be drilled in the least favorable location for gas hydrates in Area A and appropriate core, logging and drilling data will be obtained.

Leg 1 drilling was conducted at two locations, Atwater Valley and Keathley Canyon in the GOM. In both locations holes were drilled to collect log and core data. In addition to the two primary wells drilled in Atwater Valley two short wells were drilled near the

center of mound. The location of the holes is presented in Appendix A Figures A2 and A3.

Summary of Leg 1 Drilling

Holes Drilled / Footage:

Seven (7) wells, total of 5,540 ft drilled.

AT13 #1 – 809' BML
AT14 #1 – 941' BML
AT13 #2 – 656' BML
ATM1 – 80' BML
ATM2 – 103' BML
KC151 #2 – 1506' BML
KC151 #3 – 1445' BML

Cores Types Used & Recovery:

Fugro Hydraulic Piston Corer (FHPC) – 23 deployments, 570' recovered (95%)
Fugro Corer (FC) – 13 deployments, 90' recovered (59%)

The % recovery for FC and FHPC can be misleading. The % recovered is based on total barrel length. Sometimes due to stiffness of formation, the total penetration was not achieved. Conversely, sometimes more than the penetration can be recovered due to expansion in the formations in the barrel.

Hyace Rotary Corer (HRC) – 9 deployments, 6' recovered (2 cores successfully recovered under pressure) – 20% footage recovery
Fugro Pressure Corer (FPC) – 9 deployments, 10' recovered (3 cores successfully recovered under pressure) – 38% footage recovery
Total – 53 cores taken, 302' recovered (76% of total maximum possible).

Hydrate Recovery (to date):

Two (2) HRC cores were recovered and recovered hydrate
One (1) FC was recovered with a piece of hydrate still evident in the core
One (1) FPC was recovered with evidence of hydrate and is still under pressure.
Other cores had evidence of hydrate but no physical recovery was able to be made due to dissociation.

Log Data:

AT13#1, AT14#1 and KC151 #2

Resistivity, borehole imaging, gamma ray, density, neutron porosity, and magnetic resonance

KC151 #3

Dipole sonic, general inclination & orienting tool, VSP

The quality of the log data was very good for all the wells where log data was obtained especially given the potential conditions for poor logs in the shallow sediments.

Basic Summary of Core Analyses Done:

Infrared scan of all cores
Pore water chemistry
X-ray of cores
CT scans
Controlled degassing of pressurized hydrate cores
Simple strength tests
Gas analysis
P-wave and gamma ray imaging of cores
Density of cores
Re-pressurizing of degassed cores and re-evaluation of characteristics

Test to be Done:

Sediment analysis and description
Extended water analysis
Extended gas analysis
Mechanical and acoustic analysis of cores reconstituted in lab
Analysis of hydrate structure (if enough was preserved)
Background gamma ray on cores
Split cores, image and describe

Other Highlights

Project completed with Zero Health, Environmental or Safety incidents (>48,300 man hours)
First ever attempt at subsurface hydrate recovery in Gulf of Mexico
Tested / utilized emerging technologies with pressurized coring devices
Fugro pushed the FHPC to deeper depths then it previously had.

Plan Forward:

Complete post cruise analysis of cores and logs
Compare results to precruise analysis.
Determine the necessary additional research required.
Conduct a public workshop to report results.

3.6 Task 6.0 – Data Analysis – Initial Cruise

Work under this task will consist of conducting the appropriate analysis of all data obtained during initial field activities (the April—May 2005 activities at the Atwater Valley and Keathley Canyon sites) and provide an initial Scientific Results report that details the following: a) the pre-cruise seismic interpretations and an analysis comparing those interpretations with actual findings; b) the findings of the geochemical surveys; c) the findings of the well logging efforts and analysis; d) the findings of the borehole geophysical surveys; e) the performance of various sampling devices employed; f) as well as any other appropriate results emanating from shipboard or subsequent analysis of data or samples obtained during the cruise.

Data from Drilling Leg 1 was collected both during the cruise and after the cruise at various labs. Appendix A contains hole locations and seismic plots of the drilling targets. Appendix B contains the post cruise report on the data collected using the Georgia Tech Pressure Core Measurement Vessel. Appendix C contains the post cruise report on the work conducted by Geotek. The Geotek work consisted of measurements on cores on the ship as well as lab measurements conducted on split cores at Scripps Institute of Oceanography.

Figure 3.3. Precruise Hydrate Concentrations for KC 151

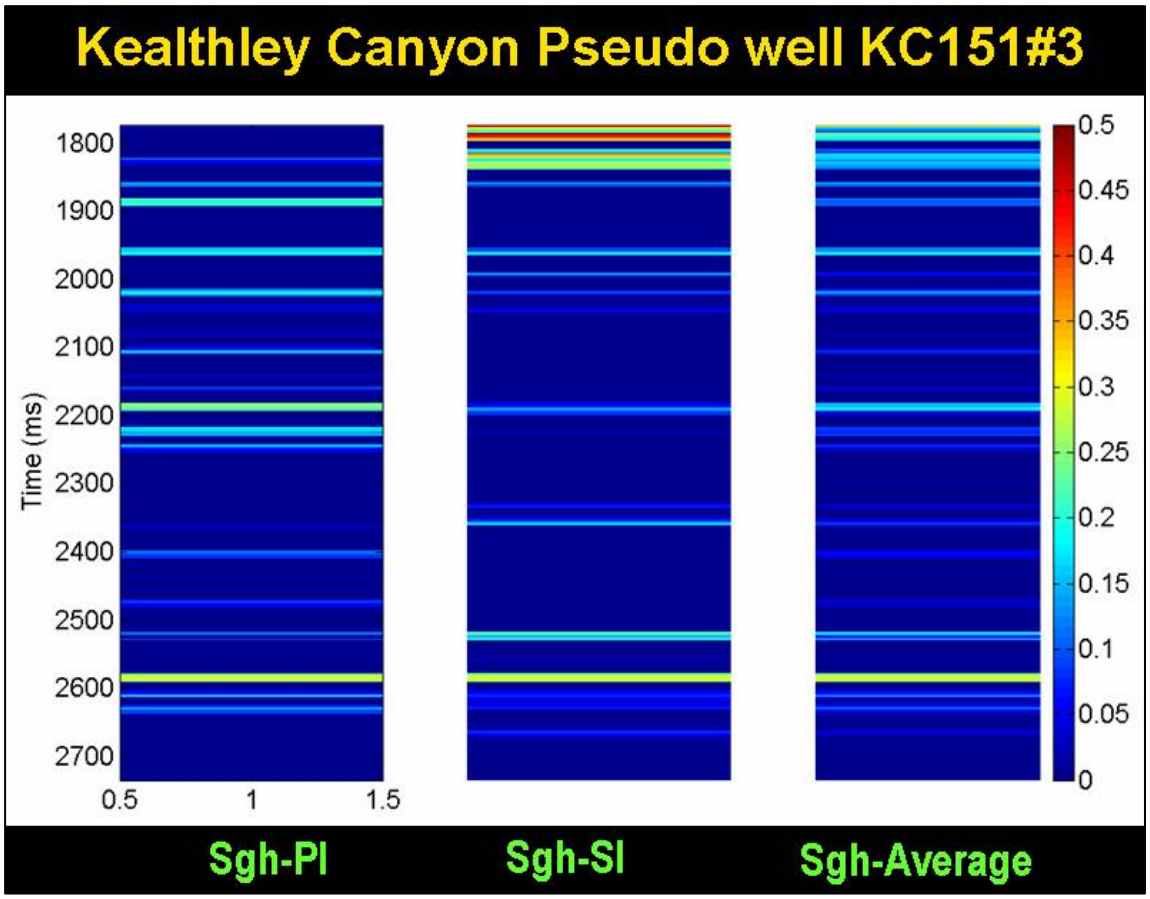

3.7 Task 7.0 – Technical Conference

In order to provide the scientific community with current data from the project, a workshop will be conducted to present all information obtained during the course of the project to industry, academic, government and other interested professionals. This workshop will focus on the opportunities for improving the tools and protocols for effective field investigation of hydrates in the Gulf of Mexico. The output of the workshop will be plans for DOE consideration for acting on specific recommendations arising from this workshop.

Detailed planning for the April Post Cruise Workshop was completed. The workshop will be held in Houston on 13 and 14 April 2006. The workshop draft agenda is presented below.

Draft Agenda

GOM Hydrate JIP/DOE Drilling Data & Hydrate Tool & Protocol Development

13 & 14 April 2006

Hilton Houston Westchase
9999 Westheimer
Houston Texas

Attendees (Presenting)

Brandon Dugan	George Claypool	Miriam Kastner	Emrys Jones
Barry Freifeld	Tom Lorenson	Ben Bloys	Fred Snyder
Sheila Noeth	Tim Collett	Carolyn Ruppel	

Attendees (Breakout Group Leaders)

Tim Collett	Testing protocols and equipment for evaluating hydrates
Deborah Hutchinson	Recommend geologic setting for additional drilling
Randy Utech	Seismic protocols for predicting hydrate occurrence
Ben Bloys	Recommend development of coring tools

Meeting Goals

1. Provide a summary of the data collected in the 2005 GOM Drilling

2. Discuss and recommend geologic setting for additional drilling

3. Discuss and recommend development of coring tools to be used for evaluating hydrates in sediments

4. Discuss and recommend improvements for seismic protocols for predicting hydrate occurrence

5. Discuss and recommend improvements for testing protocols and equipment for evaluating hydrates in the field and lab.

13 April 2006 – Draft

Time	Item	Responsible Person
8:00 AM	Continental Breakfast	All
9:00 AM	Introductions	All
9:05 AM	Agenda Review	Emrys Jones
9:10 AM	Safety Minute	Emrys Jones
9:15 AM	Meeting and JIP Goals	Emrys Jones
9:30 AM	Cruise Operations	Ben Bloys
10:00 AM	LWD and Wireline Logging Results	Timothy Collett
10:30 AM	Break	All
10:45 AM	Core-lab studies and pressure core measurements	Carolyn Ruppel
11:15 AM	Physical Properties	Brandon Dugan
11:45 AM	Pore water chemistry	Miriam Kastner
12:15 PM	Lunch	All
1:15 PM	Gas geochemistry	George Claypool
1:45 PM	Well Bore Modeling	Sheila Noeth
2:15 PM	Cruise Report	George Claypool
2:45 PM	Break	All
3:00 PM	Precruise Seismic Predictions	Fred Snyder
3:30 PM	Breakout Groups	All
5:00 PM	Adjourn for the day	Emrys Jones

14 April 2006 – Draft

Time (min)	Item	Responsible Person
8:00 AM	Continental Breakfast	All
9:00 AM	Breakout Groups	All
10:30 AM	Break	All
10:35 AM	Review Agenda	Emrys Jones
10:40 AM	Safety	Emrys Jones
10:45 AM	Breakout Groups Report	Emrys Jones
11:45 AM	Adjourn and lunch	Emrys Jones
12:45 PM	Meeting Adjourned	Emrys Jones

3.8 Task 8.0 – Field Sampling Device Development

In addition to any specific data/tool needs identified in the Task 7 workshop, the acquisition of improved technologies for the acquisition, retrieval and subsequent analysis of samples under in-situ pressure (and possibly temperature) conditions will be pursued. Pressure coring equipment will be evaluated both from the JIP membership and the development of new devices to accomplish these goals (both sample retrieval and extensive analysis of samples in systems capable of minimizing hydrate dissociation and sample alteration from its natural state).

3.9 Task 9.0 – Recommendation for Further Activities

Analysis of initial cruise findings will be used to determine the need for additional field activities to properly characterize the full range of hydrate occurrences in the Gulf. New locations will be selected and evaluation of existing geophysical and well log data will be conducted to evaluate the existence of sites or the location of favorable transects in the Gulf of Mexico that have the best potential to provide the missing data. Recommendations will be prepared for a second phase of field activities, including a description of the sites and a plan for conducting field operations.

4.0 Discussion and Results PHASE III – Follow on Field Activities and Final Reporting

Tentative tasks are provided for Task III activities, which will include the execution of a second field program as identified in Phase II/Task 9.0, and full reporting to both DOE and the broader scientific community.

4.1 Task 1.0 – Research Management Plan

Develop a work breakdown structure and supporting narrative that concisely addresses Phase III activities and includes a concise summary of activities, schedules and costs for each Phase III Task.

4.2 Task 2.0 – Project Management and Oversight

A project manager appointed by the Joint Industry Project (JIP) Recipients will manage the technical teams, contractors, and the day to day operation of the project. Project manager will report, verbally and through required reporting, on the progress of the program to the DOE and the JIP as required.

4.3 Task 3.0 – Field Activities

Conduct field operations as developed in Phase II Task 9.0 and outlined in Phase III Task 1.0.

4.4 Task 4.0 – Data Analysis

Conduct appropriate analysis of all data obtained during the Phase III cruise, integrate these data with those from the Phase II cruise, and provide a detailed Final Report on the findings and their implications. Recommend and pursue options for providing this report as a Special Volume in a manner similar to that provided from other large-scale hydrate research efforts (for example, the special volumes emanating from the Mallik programs).

4.5 Task 5.0 – Technical Conference

Conduct a technical conference to present all information obtained during the course of the project to industry, academic, government and other interested professionals.

5.0 Experimental

Experimental work was conducted during the period of this report. Photos and drawings of some of the experimental equipment that was used on the cruise were presented in previous semi-annual reports.

6.0 Conclusions

Precruise estimates of hydrate concentrations and degas experiments on the pressure cores collected yielded approximately the same hydrate concentrations.

The first experimental results, from the pressurized measurement vessel developed by Georgia Tech, showed that sediment properties are affected by depressurizing the core.

Post cruise analysis of the split cores showed that the sediment was mostly clay and silts with only minor indications of sands.

7.0 References

No external references were used for this report.

8.0 Appendix

Appendix A. Science Plan

Table A1. Hole Locations and Target Depths

Name	PROPOSED HOLE LOCATION	INLINE	TRACE	X	Y	LAT	LONG	2WT WB	DEPTH WB	2WT TD	DEPTH TD	DEPTH BML TD
KC3L	KC151 #3 Open	5700	20248	1643513.88000	9733112.29000	26° 49' 22.6" N	92° 59' 25.8" W	1.782	4375	2.407	6190	1815
KC1L	KC151 #1 Open	5700	20280	1644827.03010	9733112.40830	26° 49' 22.6" N	92° 59' 11.3" W	1.752	4301	2.435	6300	1999
AT2L	AT13 #2 Shell	2615	6997	901438.18940	10148521.86390	27° 56' 49.4" N	89° 17' 21.6" W	1.712	4203	2.100	5238	1035
AT1L	AT14 #1 BHP	2562	7064	904181.44430	10145035.55470	27° 56' 15.4" N	89° 16' 50.3" W	1.722	4228	2.100	5236	1008
AT1C	AT14 #1 BHP	2562	7064	904181.44430	10145035.55470	27° 56' 15.4" N	89° 16' 50.3" W	1.722	4228	2.100	5236	1008
AT2C	AT13 #2 Shell	2615	6997	901438.18940	10148521.86390	27° 56' 49.4" N	89° 17' 21.6" W	1.712	4203	2.100	5238	1035
KC3C	KC151 #3 Open	5700	20248	1643513.88000	9733112.29000	26° 49' 22.6" N	92° 59' 25.8" W	1.782	4375	2.407	6190	1815
KC1C	KC151 #1 Open	5700	20280	1644827.03010	9733112.40830	26° 49' 22.6" N	92° 59' 11.3" W	1.752	4301	2.435	6300	1999
ATM1	AT14 #1 BHP	2556	7073	904551.77030	10144646.35110	27° 56' 11.62" N	89° 16' 46.09" W		4257			159
ATM2	AT14 #5 BHP	2556	7071	904470.29280	10144646.25410	27° 56' 11.6" N	89° 16' 47.0" W	1.715	4210	1.829	4505	99

Figure A1. Drill Site Location Map

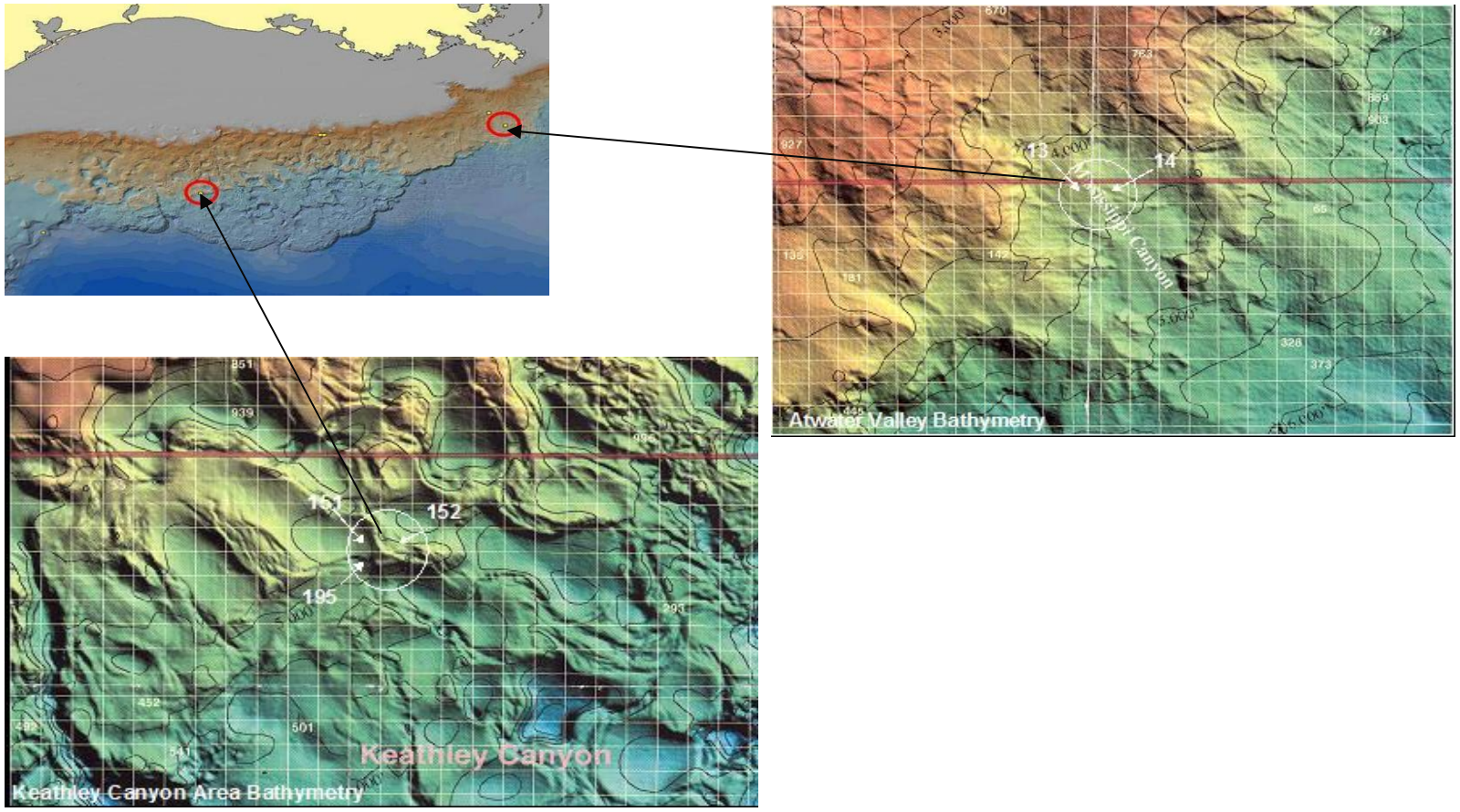

Figure A2. Atwater Valley Seismic Plot

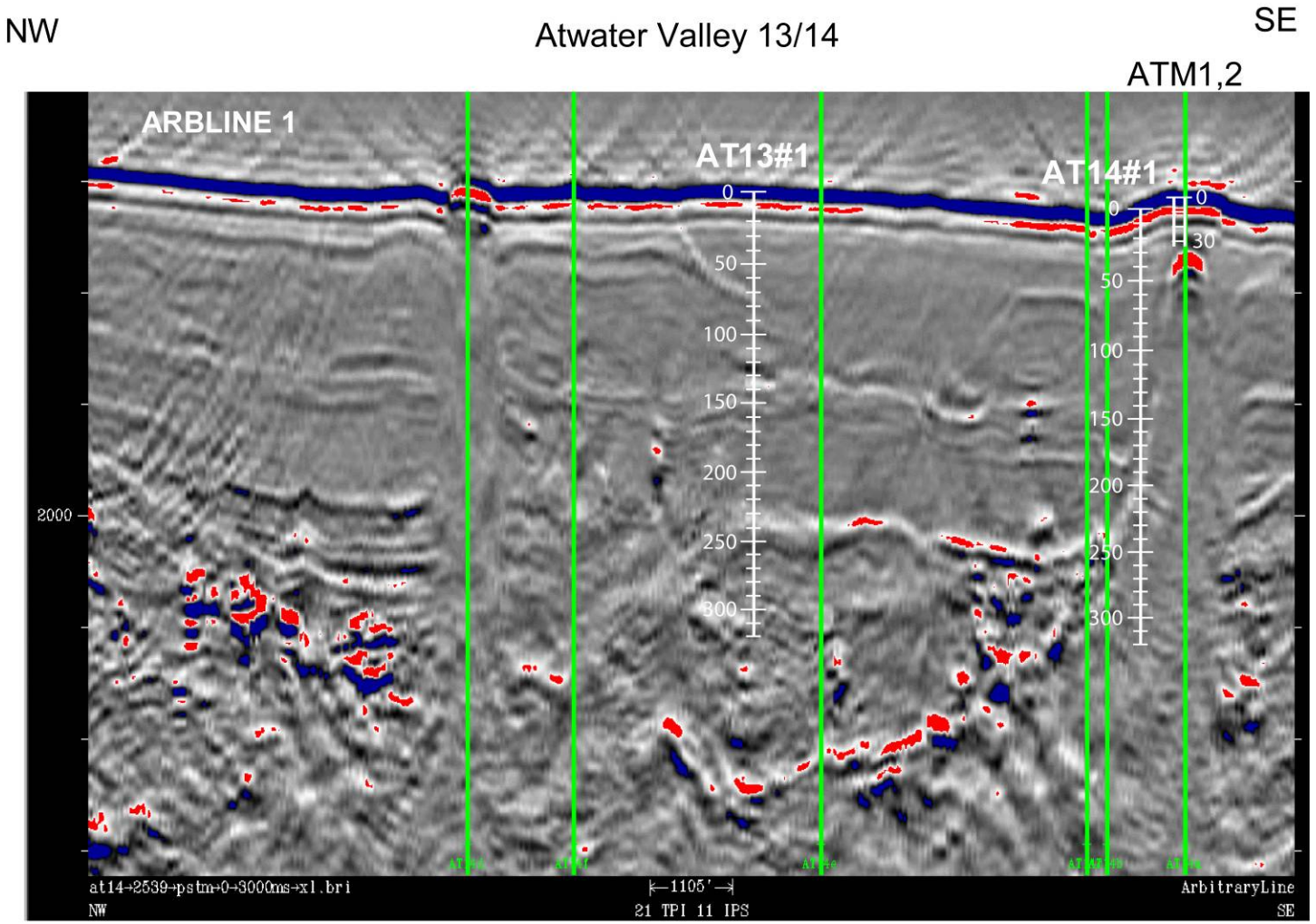

Figure A3. Keathley Canyon Seismic Plot

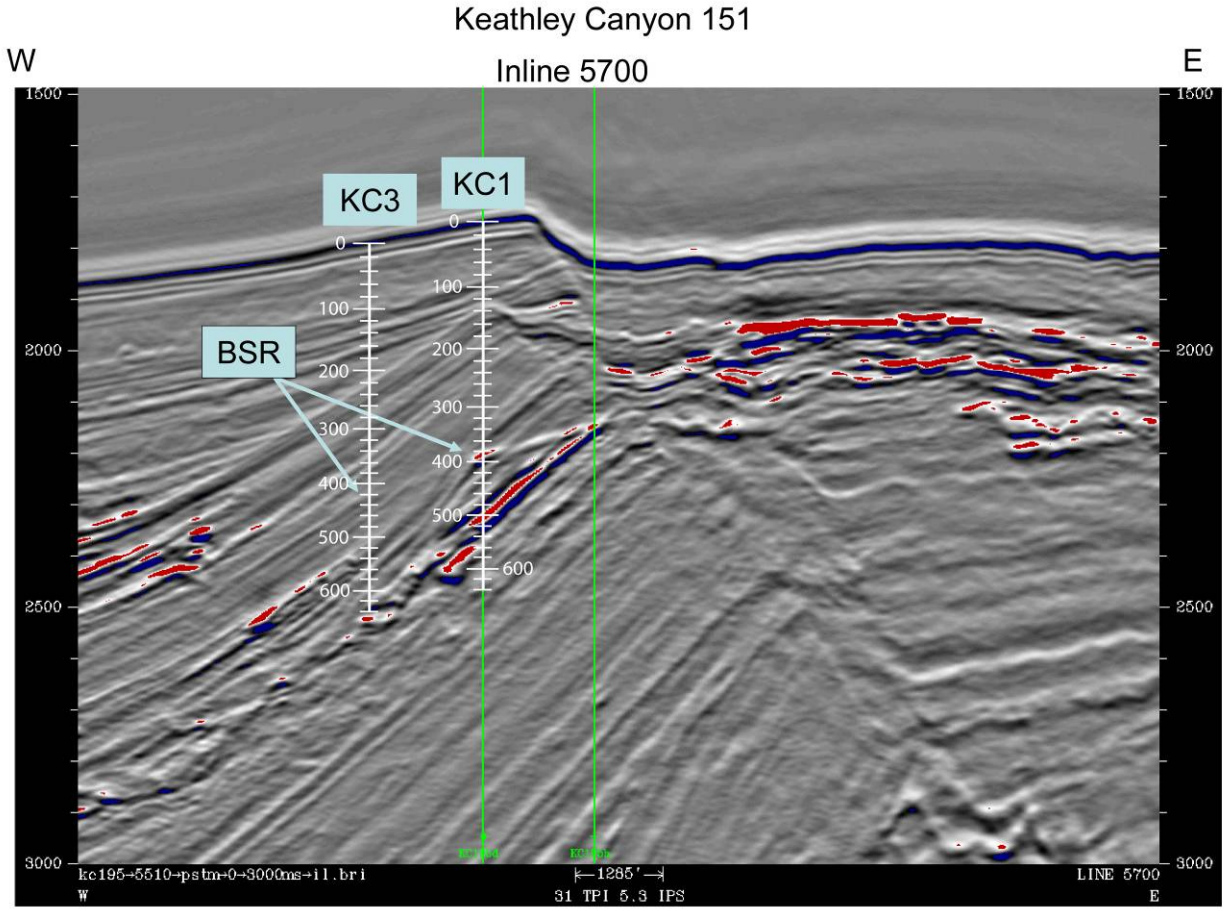

?

APPENDIX B. Georgia Tech Pressure Core Measurements

Georgia Tech – JIP Methane Hydrates Program

Preliminary Results

Georgia Tech Instrumented Pressure Testing Chamber

Deployed on JIP Gas Hydrate Drilling Program in Gulf of Mexico, April to May 2005

Submitted June 5, 2005

PIs: Carolyn Ruppel and J. Carlos Santamarina

Georgia Institute of Technology

Data in this report were collected and analyzed by shipboard scientists Dr. T-S Yun and Ph.D. Candidate G. Narsilio with support from the Georgia Tech JIP contract

Summary

We provide an overview of data collected with the Georgia Tech instrumented pressure testing chamber constructed under contract with the ChevronTexaco JIP. The Georgia Tech instrumented pressure testing chamber for the first time ever in the drilling community measures mechanical properties, strength, and electrical conductivity on pressure cores maintained at pressure. The chamber was used to test cores obtained during drilling in the Gulf of Mexico in April and May 2005. Due to difficulties retrieving pressure cores, the Georgia Tech sampling plan was modified shipboard and measurements were completed on 68 whole rounds from conventional cores, 2 re-pressurized cores, and 2 pressure cores. For conventional cores, Georgia Tech independently measured some parameters being measured by other groups for the purpose of comparison methods and results. The results yield a set of correlative plots that may yield important insights into the behavior of the sediments at the microstructural level. For the re-pressurized and pressure cores, Georgia Tech conducted through liner measurements of Vp and invasive measurements of Vp, Vs, electrical conductivity, and strength. Despite some difficulty with the third-party manipulator, the Georgia Tech data provide proof-of-concept that the vessel operated as planned. A preliminary comparison between Vs data obtained on a pressure core and on conventional core whole rounds at comparable depths demonstrates the potential importance of pressure coring. The Vs data from the conventional cores show wide scatter and have significantly lower velocity than the Vs result measured on a pressure core, probably due to the disturbance of the conventional core's soil structure by gas expansion during retrieval.

Non-Pressure Cores (FHPC and FC)

Due to early difficulties with acquisition of pressure cores, the Georgia Tech sampling plan was altered aboard ship to include tests on conventional cores. A total of 68 5- to 10-cm long whole rounds were obtained near the pore water sampling locations. Specimens are sealed to prevent moisture loss. Most properties were measured shipboard in the Georgia Tech instrumented pressure testing chamber. In some cases, Georgia Tech and others measured the same properties using different techniques, as a means to compare methodologies and results later.

Conventional cores: Measured properties

Properties		Method	Party responsible
Elastic wave velocity (vertical)	P-wave	Pinducer	GeoTek (horizontal) Georgia Tech
	S-wave	Bender element	Georgia Tech
Electrical conductivity		Needle probe	Georgia Tech
Undrained shear strength		Penetrometer / torvane	Fugro
pH		pH strip (resolution: ±0.25)	Scripps
Specific surface (S_a)[1]		Methylene blue method	Georgia Tech
Gravimetric water content[1]		ASTM standard (GT)	Fugro Georgia Tech

1: on-shore measurement (at Georgia Tech)

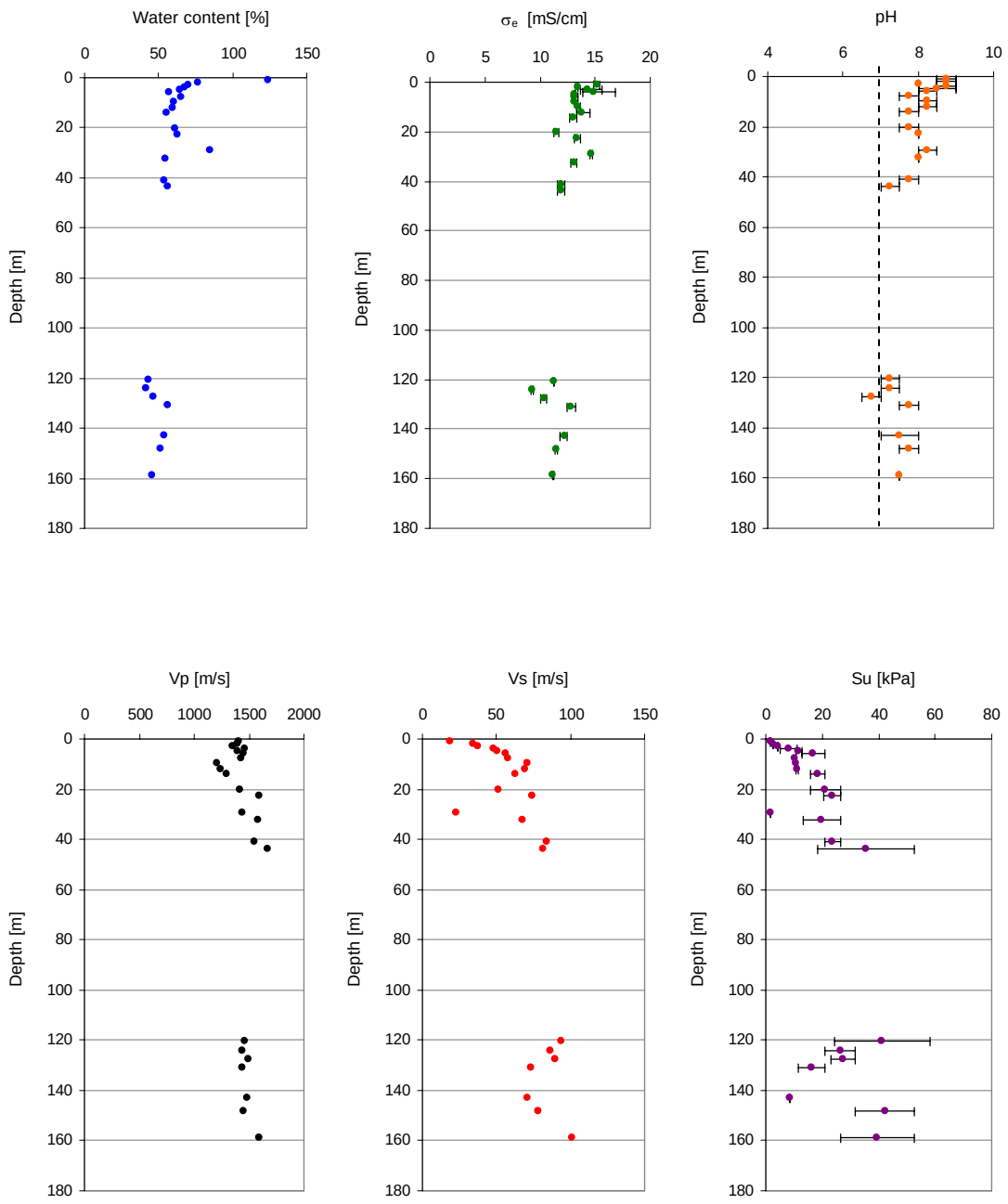

Figure 1. Stacked data from conventional core whole rounds analyzed at AT 13-2 site.

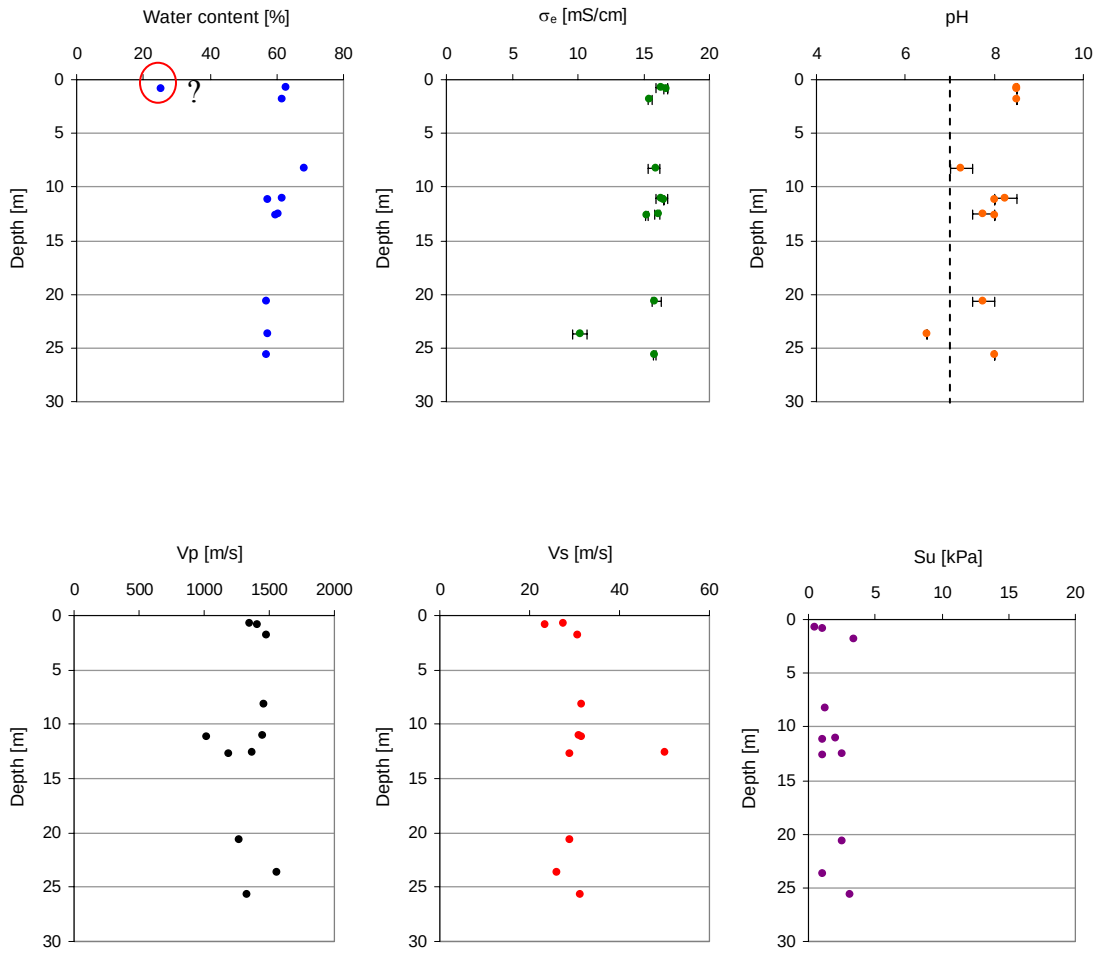

Figure 2. Stacked data measured on whole rounds from conventional cores at the AT Mound sites (ATM 1 and ATM 2).

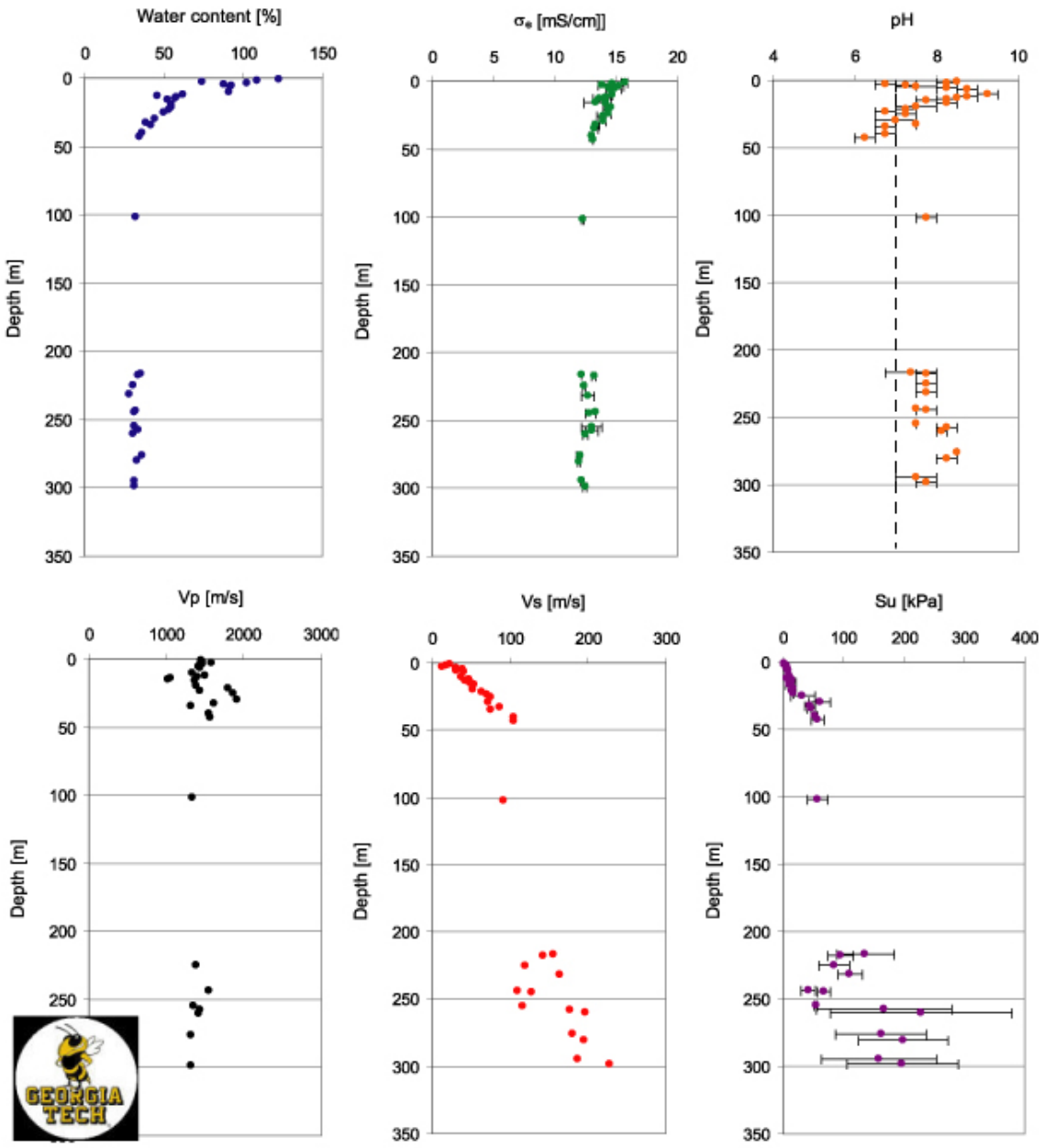

Figure 3. Stacked data from conventional core whole rounds obtained at site KC 151-3.

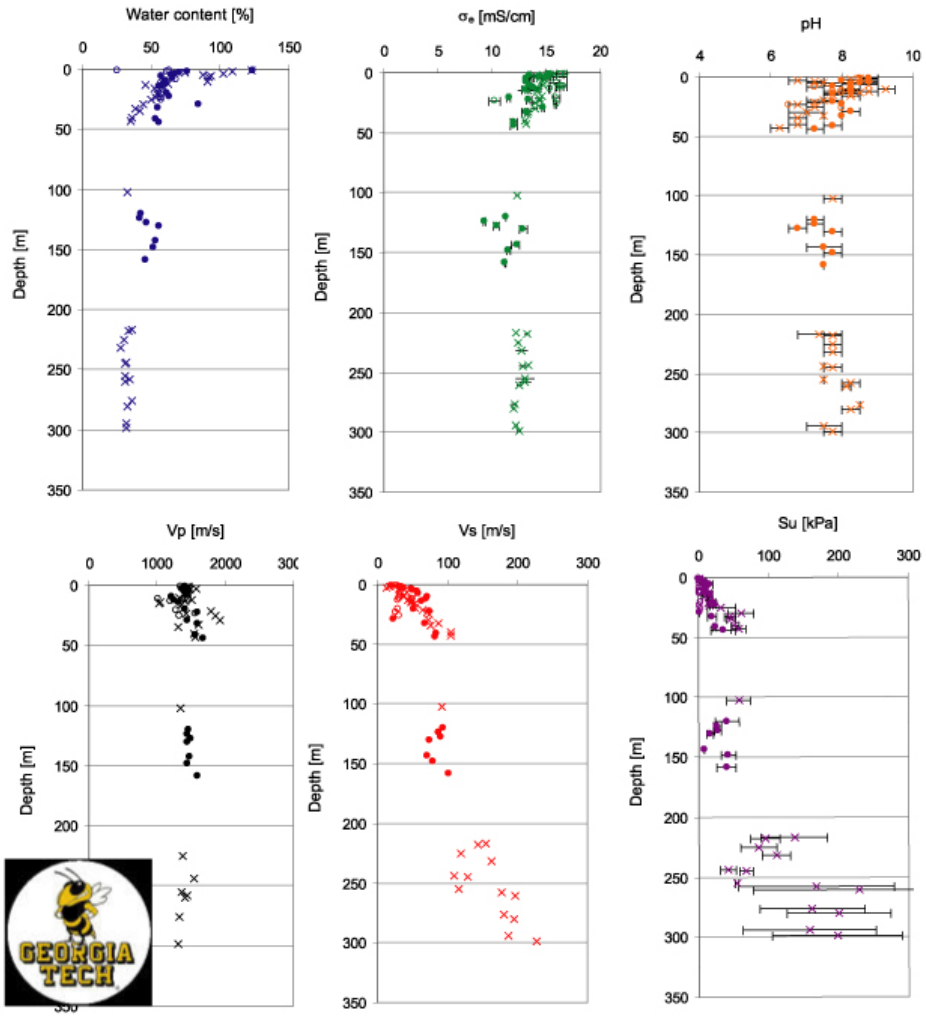

Figure 4. **Compilation of data from measurements on conventional core whole rounds at all sites. Closed circles denote AT 13-2; open circles represent ATM 1 and 2, and crosses show data for KC 151-3.**

Correlations / Observations

Here we present only raw data correlations, without any interpretation. Some of the interpretations in Francisca et al. (revised for EPSL, June 1, 2005) for shallow cores obtained elsewhere in the Gulf of Mexico may provide insight into these results.

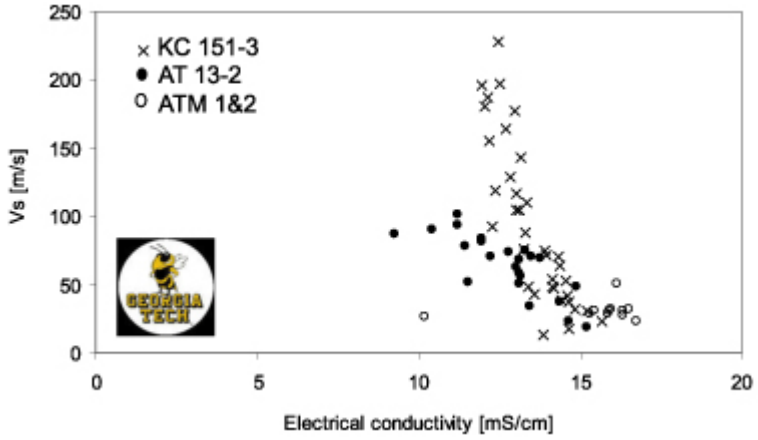

Figure 5. **S-wave velocity vs. electrical conductivity for conventional cores. V_s decreases with increasing electrical conductivity. V_s/σ_e at the different locations have different slopes.**

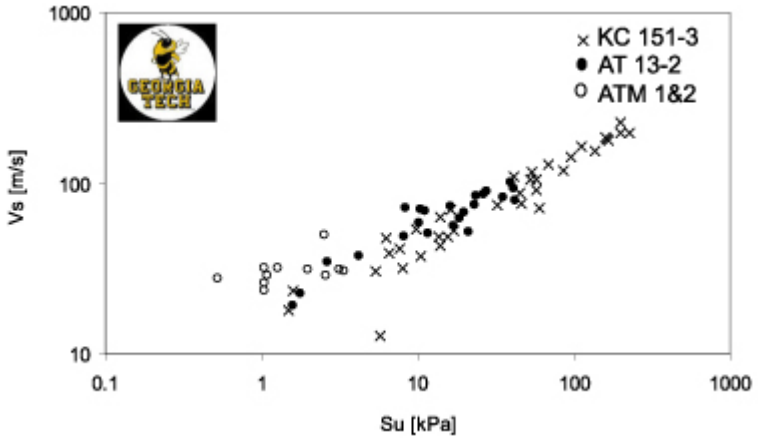

Figure 6. **S-wave velocity vs. undrained shear strength for conventional cores. Best fit line is:** $V_s = 20[m/s] \cdot \left[\frac{S_u}{kPa}\right]^{0.4}$

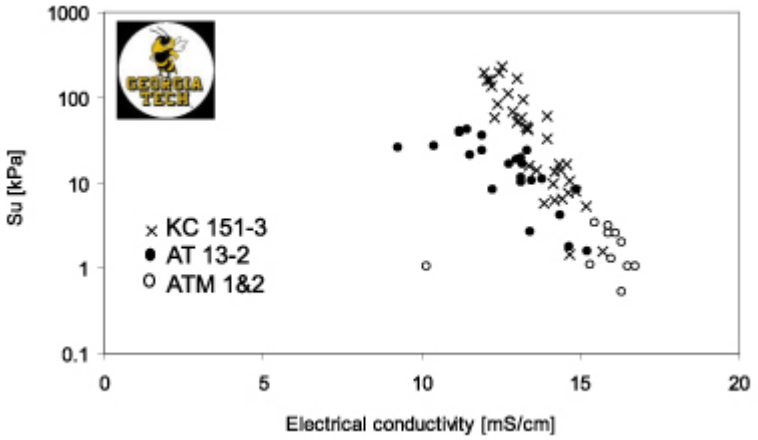

Figure 7. Undrained shear strength vs. electrical conductivity for conventional cores.

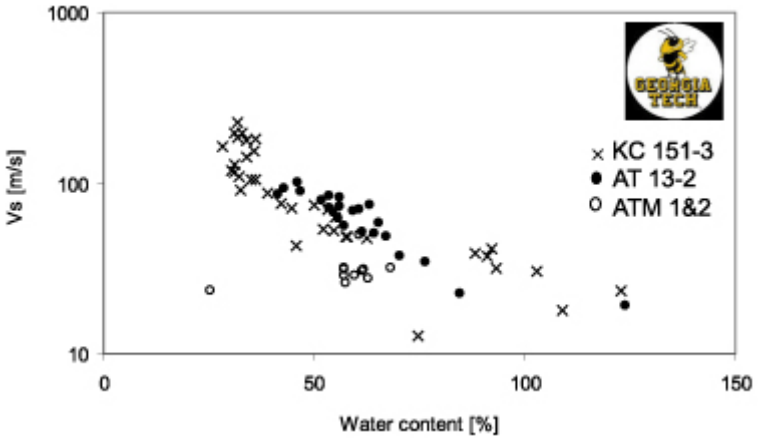

Figure 8. S-wave velocity vs. water content for conventional cores.

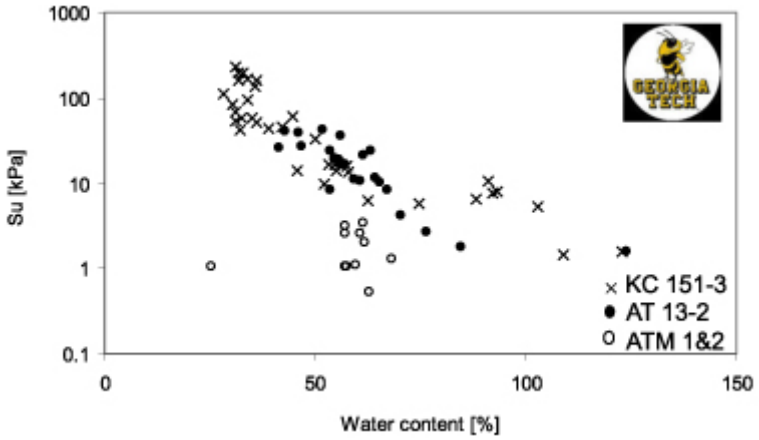

Figure 9. Undrained shear strength vs. water content for conventional cores.

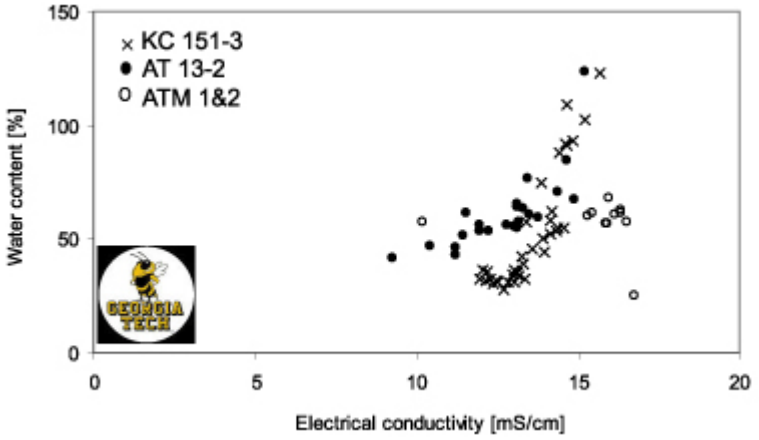

Figure 10. Water content vs. electrical conductivity for conventional cores.

Pressure cores (FPC and HRC)

Georgia Tech originally planned no work on re-pressurized cores since these cores have experienced significant disruption of their mechanical properties. However, the sampling plan was modified aboard ship, and Georgia Tech analyzed two re-pressurized cores and two pressure cores. Measurements are performed after X-ray and CT-scanning in all cases, another modification to the original sampling plan.

Measured properties

	Sites	V_p			V_s	S_u	R	Depth	Applied pressure
		Scan	Non-invasive	Invasive					
Re-pressurized cores	AT13-2-3P	O	O	O	O	O	O	1291.1m water 15.54mbsf	14MPa
	AT13-2-12P	O[1]	O	O		O[2]		1291.1m water 134.1mbsf	14MPa
Pressure cores	KC151-3-11P	O	O	O	O	O	O	1322.5m water 227.1mbsf	14MPa
	KC151-3-13R	O	O	O			O	1322.5m water 235.9mbsf	14MPa

[1]: without and with fluid pressure.

[2]: Penetrometer and vane shear test

Electrical resistance has not been converted to conductivity due to problems with corrosion of the sensor.

Strength measurements are currently being calibrated.

Sample: AT13-2-3P

P-wave scan

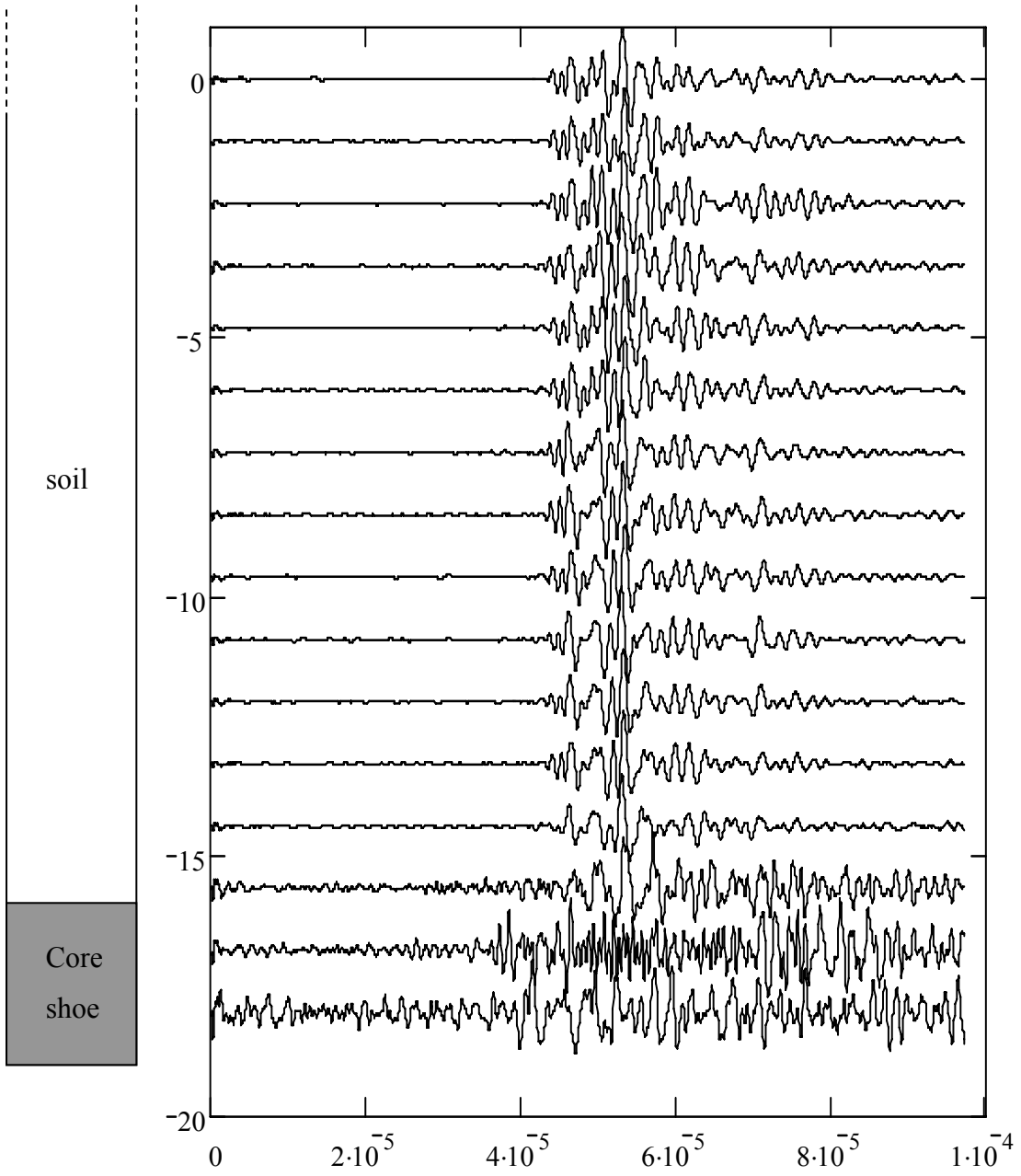

Figure 11. P-wave scan measurements every 3cm with 14MPa (re-pressurized).

Elastic wave velocities

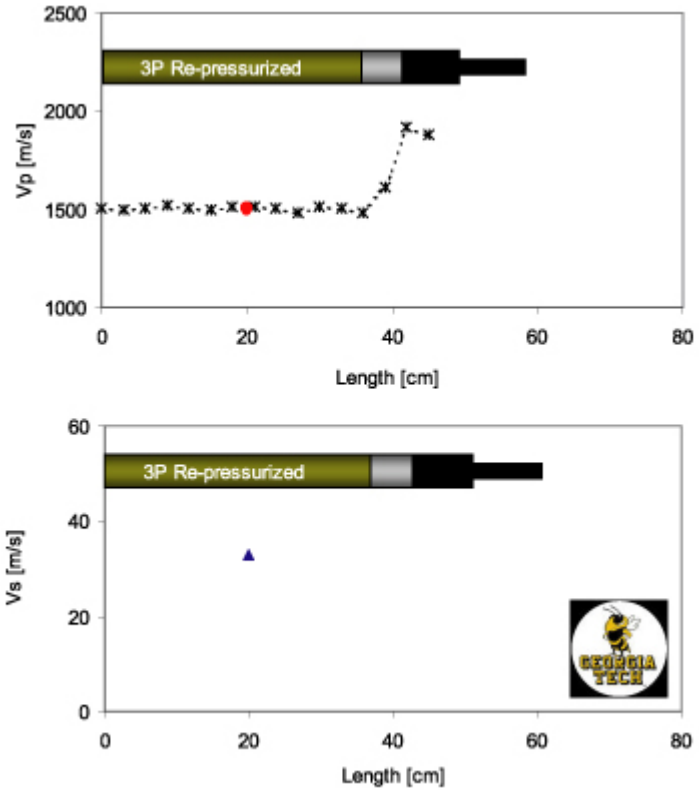

Figure 12. Measured elastic wave velocities. The dotted line with asterisks indicates the P-wave scan while red symbol shows V_p through a liner hole. The triangle (Δ) shows the measured V_s. Symbols are the same in other seismic velocity figures that follow.

Strength

Specimen strength is too low to measure with penetration probe.

Pocket vane shear test confirmed very soft sediment.

Electrical Resistance

Values oscillate between 1135 and 1131 ohms (single wedge needle). This high value results from using iced water to saturate the system.

OBSERVATIONS

- The estimated P-wave velocity by non-invasive P-wave measurement ranges from 1480 to 1510m/s.
- The invasive P-wave measurement shows similar values.
- S-wave velocity ranges from 33 to 45 m/s.
- Strength is appropriate for very soft sediment.
- Electrical conductivity: The resistance is higher than seawater because the system was saturated with an ice water/seawater mixture rather than pure seawater.

Sample: AT13-2-12P

P-wave scan – 0MPa

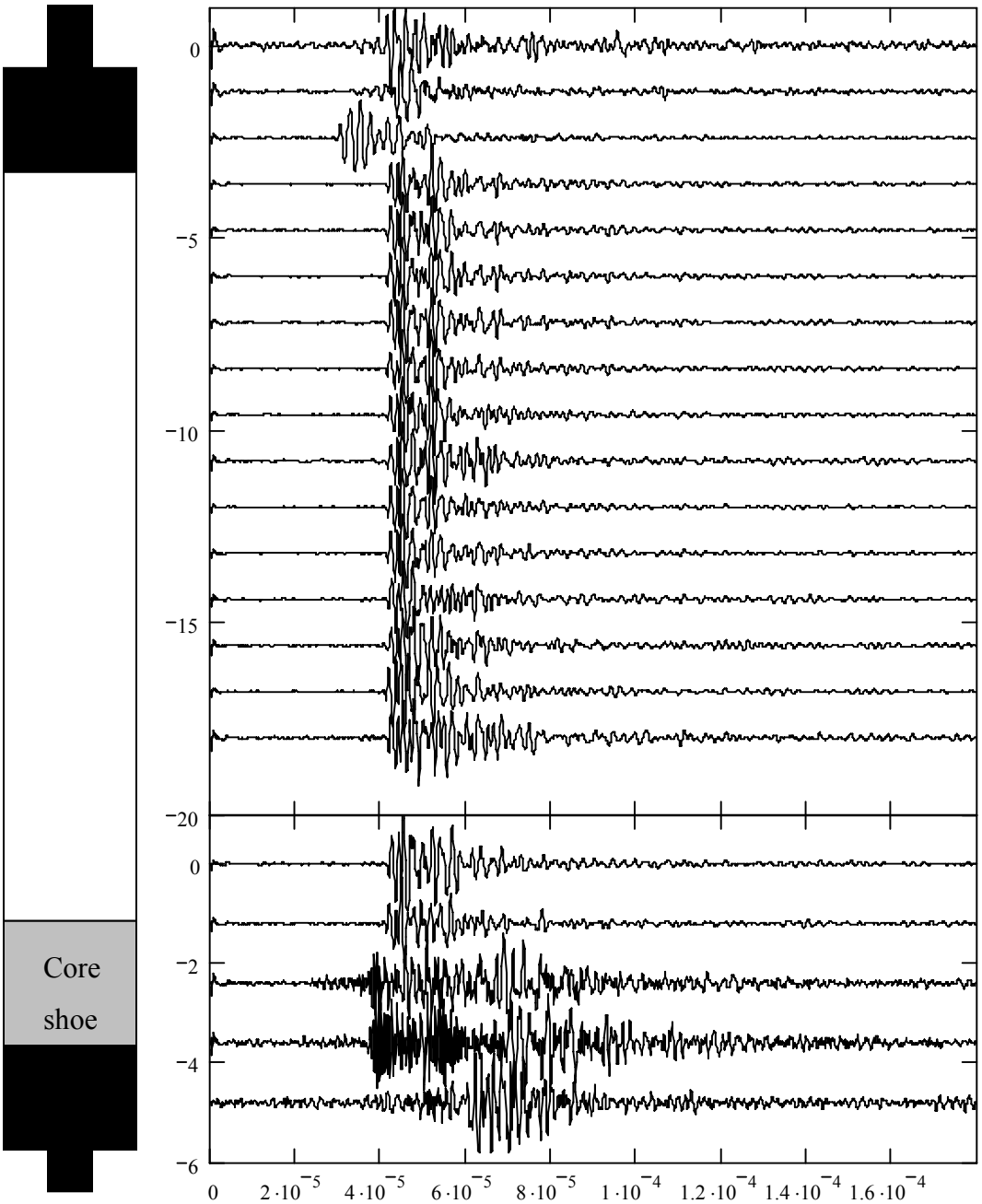

Figure 13. P-wave scan measurements every 3cm without pressure.

P-wave scan – 14MPa

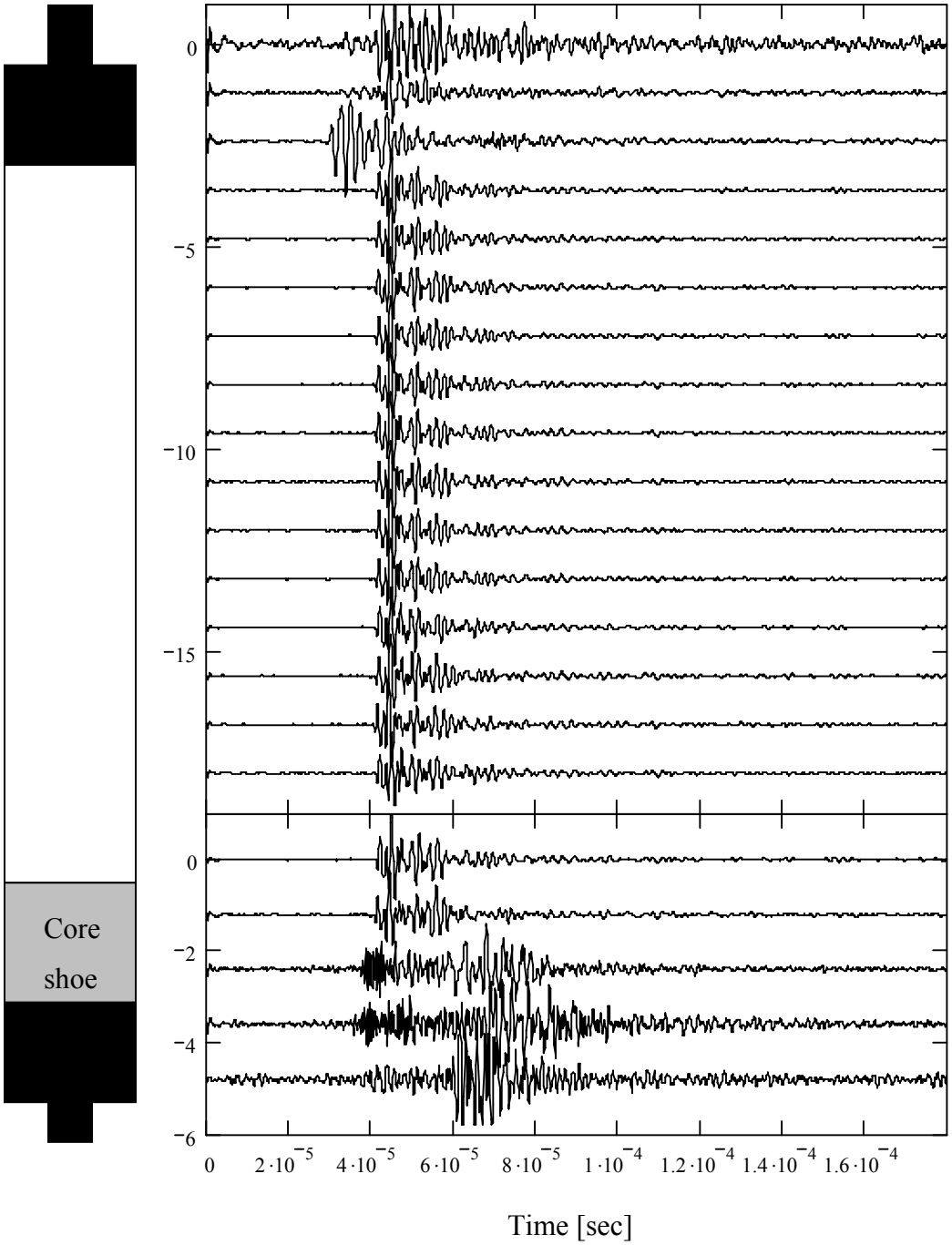

Figure 14. P-wave scan measurements every 3cm (re-pressurized to 14MPa).

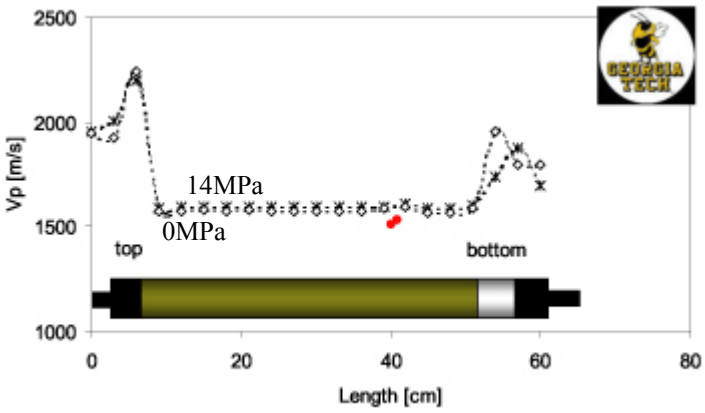

Figure 15. Invasive and non-invasive P-wave measurements under atmospheric pressure (diamonds) and under 14 MPa (asterisks). Red dots indicate invasive P-wave velocities. Higher velocity is measured under pressure, which may reflect gas dissolution into the fluid.

P-wave velocity (without and with pressure / invasive and non-invasive)

	Without pressure (0 MPa)	With pressure (14 MPa)
Invasive	1512 m/sec	1531 m/sec
Non-invasive	1515 m/sec	1529 m/sec

Strength – pocket penetrometer and vane shear test

Penetrometer: 28.7 kPa (at 0 MPa fluid pressure)

Vane shear test: 95.8 to 144 kPa (at 0 MPa fluid pressure)

Sample: KC151-3-11P

P-wave scan

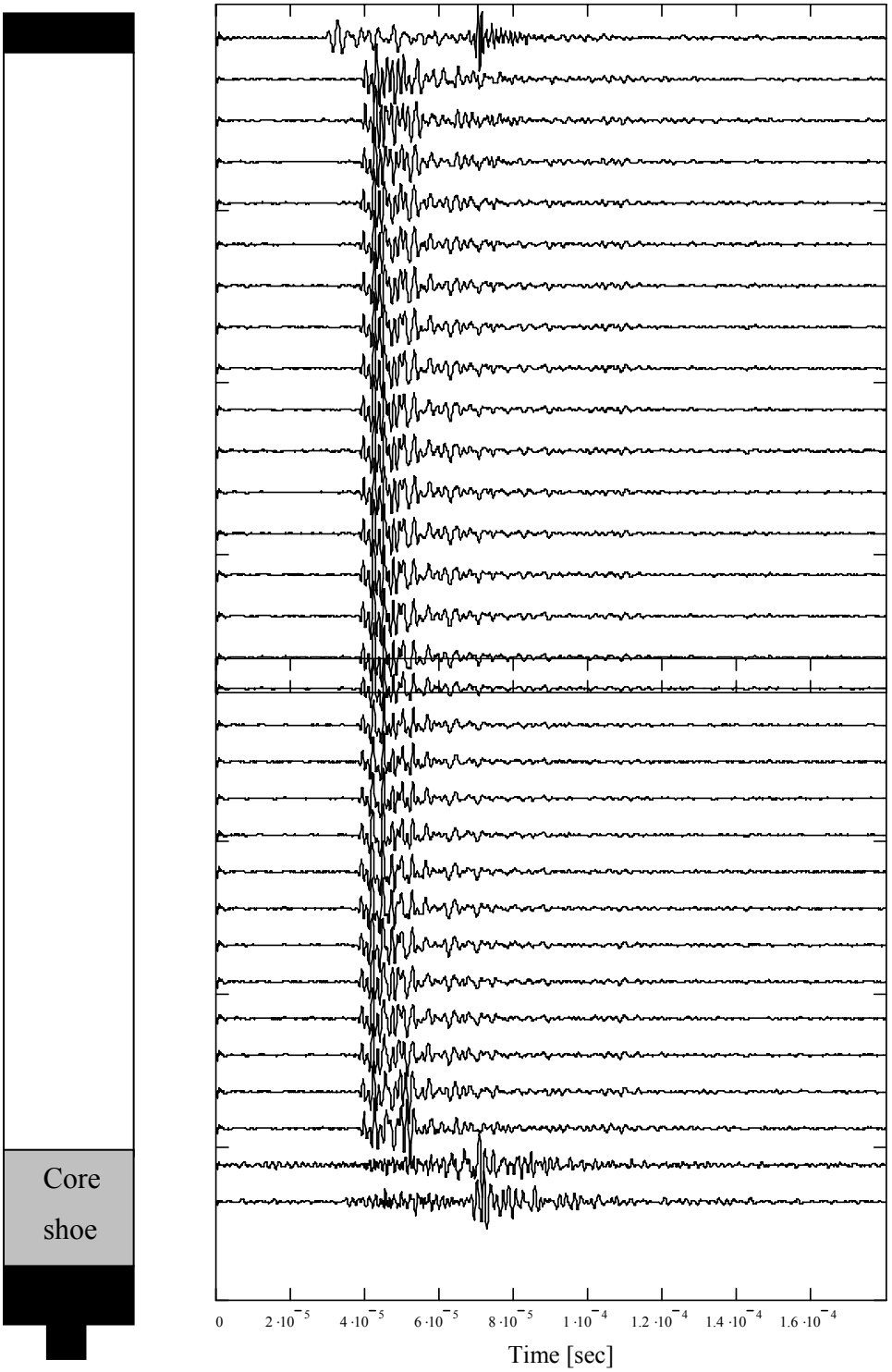

Figure 16. P-wave scan measurements every 3cm (pressure core).

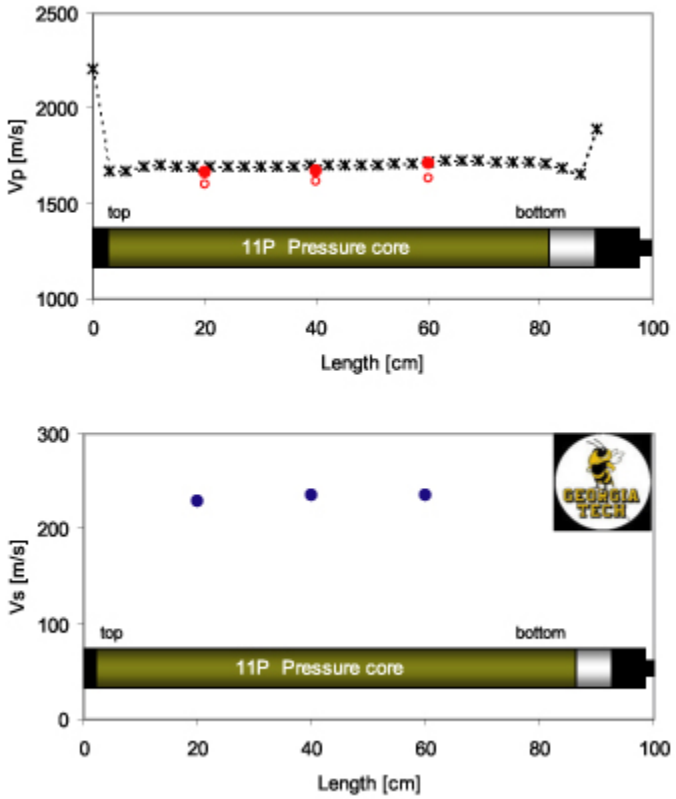

Figure 17. **Elastic wave velocity measurements. Measured P-wave velocity is ~ 1700m/s and S-wave velocity is ~ 230m/s. In this and subsequent diagrams, asterisks marks the results of the 3-cm interval seismic wave scan, filled circles mark the invasive velocity measurement, and open circles are the non-invasive velocity measurement.**

Electrical Resistance

The measured values are: 609 ohm, 555 ohm and 514 ohm.

Strength

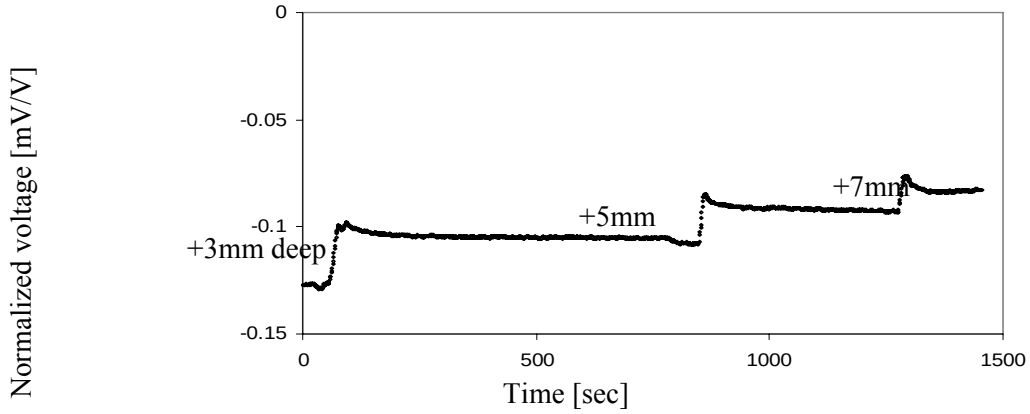

Figure 18. Voltage evolution with time for the strength determination test. Analysis is in progress.

Sample: KC151-3-13R (HRC specimen-chamber with chamber reducer)

P-wave scan

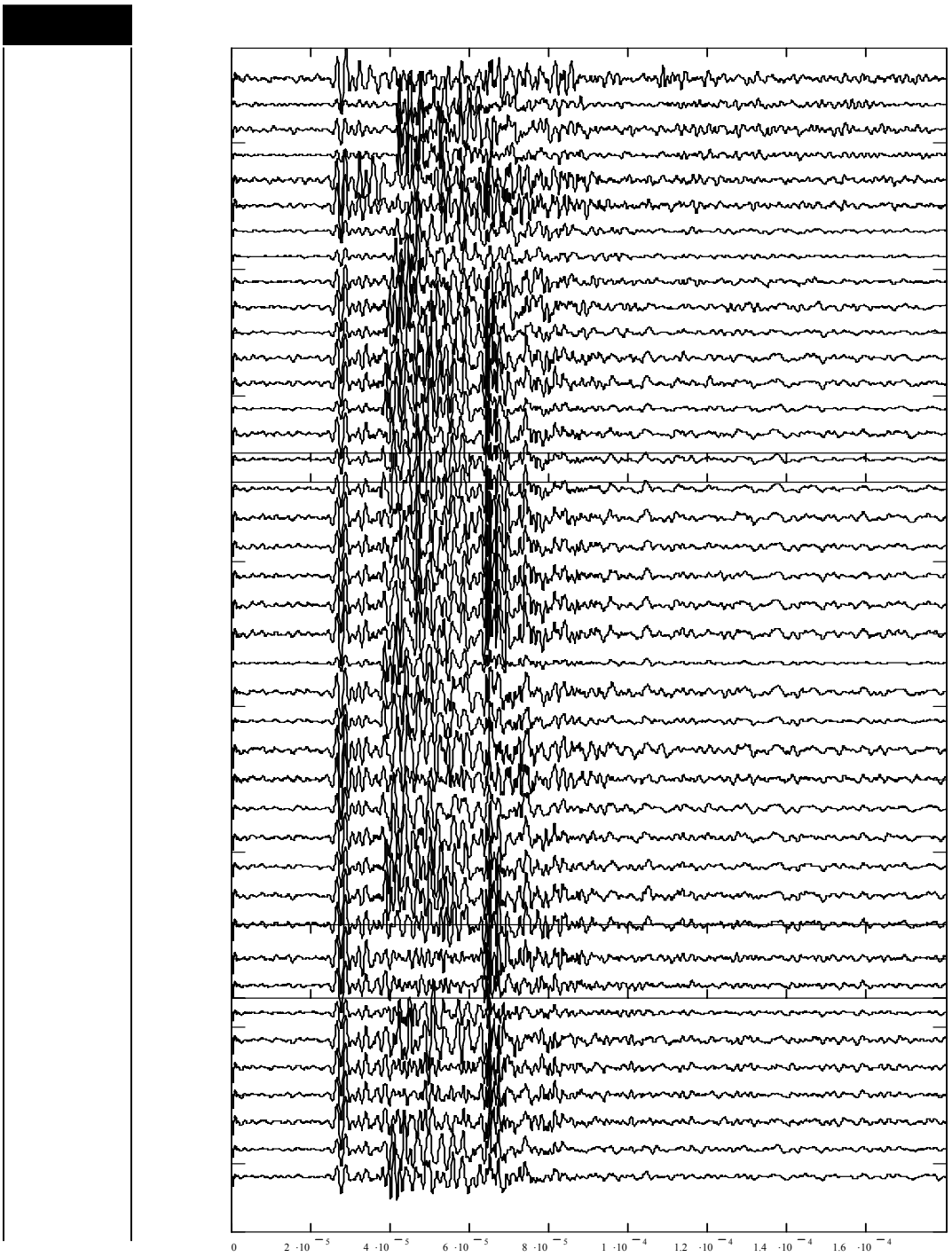

Figure 19. P-wave scan measurements every 2cm (pressure core).

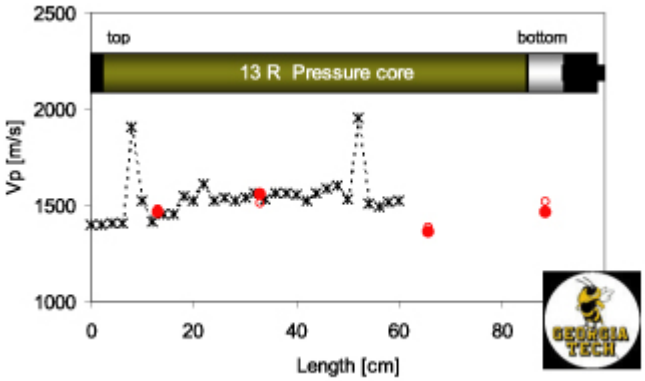

Figure 20. Noninvasive and through liner hole V_p measurements. See caption of Figure 17 for more information.

NOTES: 1. The explanation for the two high velocity peaks in the noninvasive measurements is not yet certain. The first arrival for the peak at ~55cm is not clear, and the received signal at this location is different from the surrounding recorded signals.

2. The third party manipulator had a motor control failure and positioning in the core was lost after the 2nd hole.

Electrical Resistance

The measured values are: 572 ohm, 542 ohm and 593 ohm.

Comparison of conventional cores and pressure cores

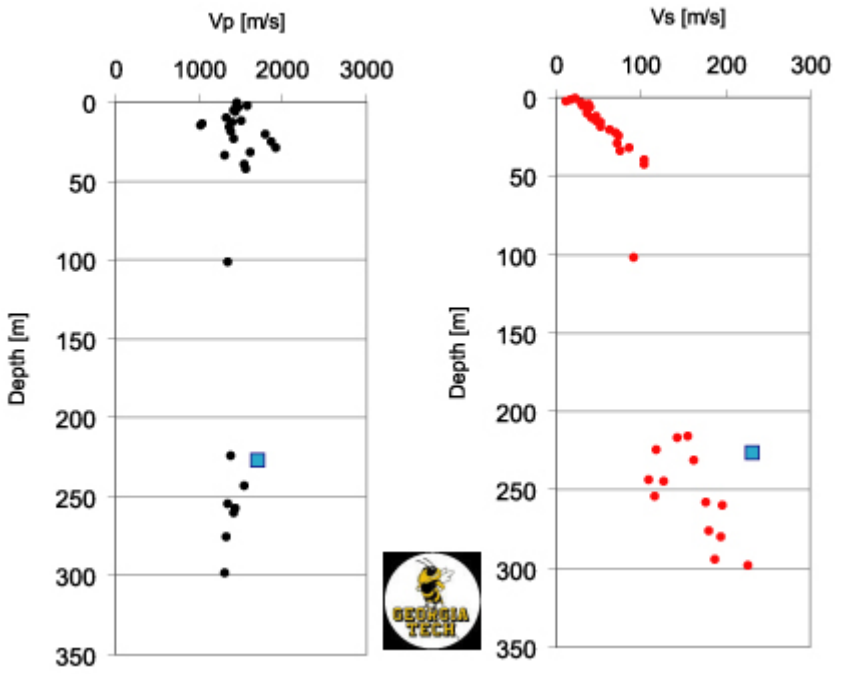

Figure 21. Conventional core P-wave and S-wave velocity data for KC151 with data measured in the pressure core denoted by the blue square. In particular, the S-wave result for the pressure core may have significance for demonstrating the effect of sampling (coring) on the sediments. Although the pressure core apparatus maintains only hydrostatic, not effective, stress, the pressure core prevents gas expansion that disturbs the soil microstructure. Such gas expansion probably contributes to the dramatically lower and much more scattered S-wave velocities measured in conventional cores from the same depth as the pressure core.

Appendix C. Geotek Pressure Coring and Core Logging Report

Gulf of Mexico Gas Hydrates
Joint Industry Project

Characterizing Natural Gas Hydrates in the Deep Water Gulf of Mexico: Applications for Safe Drilling and Production Activities

GOM-JIP Pressure Coring& Core Logging Report Geotek Ltd.

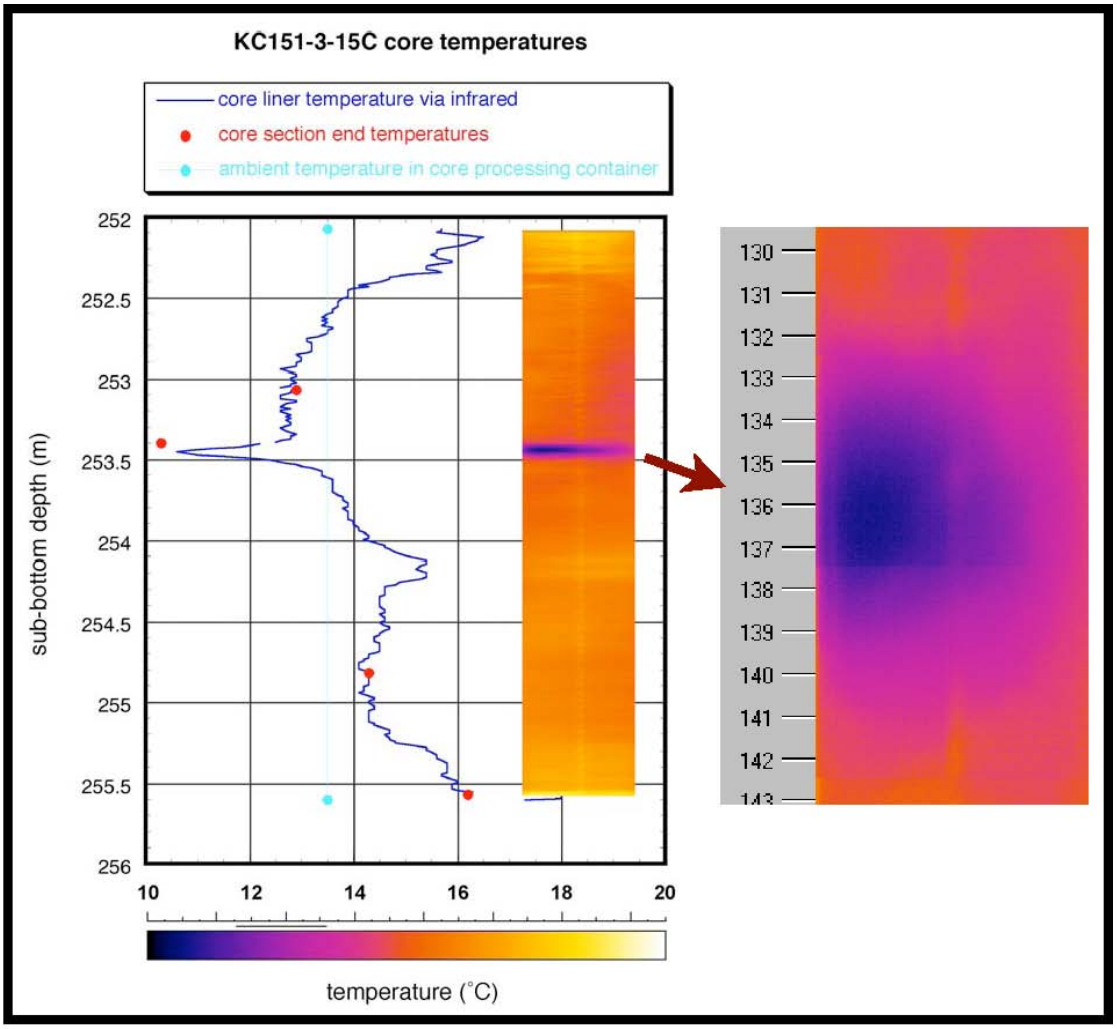

Geotek Ltd., 3 Faraday Close, Drayton Fields, Daventry, NN11 8RD, UK
+44 (1327) 311 666 info@geotek.co.uk

Introduction

One of the goals of the US Department of Energy's Gulf of Mexico Joint Industry Project (GOM-JIP) is to "develop technology & data to assist in the characterization of naturally occurring gas hydrates." To help achieve this goal on the 2005 expedition on the D/V *Uncle John*, Geotek, Ltd., was contracted to mobilize the HYACINTH pressure coring system and to make non-destructive geophysical measurements to determine hydrate presence and sediment properties on all recovered cores, both conventional (non-pressure) cores and pressure cores.

The HYACINTH pressure coring system (Schultheiss et al., 2005) is designed to recover cores under *in situ* pressure and allow measurements to be made (e.g., gamma density, acoustic velocity, radiographs) and sub-samples to be taken from these cores while still maintaining pressure. Without pressure maintenance, sediment cores containing any significant amount of hydrate can suffer dramatic disturbance during core retrieval (Figure INT-1)–if they are retrieved at all! Not only does methane hydrate begin to dissociate during recovery, causing the cores to become soupy, but because methane hydrate only forms when pore waters are saturated with methane, cores also become disturbed by methane exsolution from porewater and subsequent gas expansion. Pressure coring obviates disturbance caused by gas expansion and retards methane hydrate dissociation. Pressure coring is particularly important for hydrate recovery in the warm waters of the Gulf of Mexico where core temperatures rise significantly during retrieval, which can result in the complete dissociation of hydrate in conventional cores before they are extracted from the core barrel.

Infrared thermal imaging was used to detect the existence of hydrate in conventional cores on the GOM-JIP Expedition. Hydrate dissociation within a core creates cold spots. Negative thermal anomalies attributable to methane hydrate were measured on Ocean Drilling Program (ODP) Leg 201 (Ford et al., 2003), and this work was expanded upon during ODP Leg 204, where massive and disseminated methane hydrate was identified by thermal anomalies (Shipboard Scientific Party, 2003). During the GOM-JIP Expedition, the temperatures of the cores were monitored primarily to identify negative thermal anomalies in a qualitative fashion, either for immediate hydrate identification and preservation or documentation of where hydrate may have existed.

Other non-destructive measurements made shipboard on most cores included gamma density, acoustic velocity, magnetic susceptibility, and electrical resistivity, using the Geotek MSCL-S. While most of these measurements are affected by the presence of methane hydrate, their primary purpose is to

characterize the geological formation that hosts the hydrate and to provide a link to the downhole log data. Further measurements were made on shore using the Geotek MSCL-XYZ after the cores were split, which included RGB linescan imaging, color spectrophotometry, high-resolution magnetic susceptibility, and selective measurements of natural gamma activity.

Explanatory Notes

These Explanatory Notes contain descriptions of techniques used on the GOM-JIP Expedition, and also address general issues encountered while performing measurements on cores from this Expedition.

HYACINTH Pressure Coring System

The HYACINTH pressure coring system is designed to recover cores at in situ pressure and transfer those cores, under pressure, into other pressure vessels or analytical equipment. The system consists of pressure coring tools and equipment to move the core from the coring autoclave into secondary pressure equipment. Analytical equipment used with these pressure cores on the GOM-JIP included the MSCL-V, the MSCL-P, and the X-ray computed tomography (CT) scanner.

HYACINTH Downhole Tools

Two types of wireline pressure coring tools have been developed: a percussion corer and a rotary corer, which were designed to cut and recover core in a wide range of lithologies where gas hydrate bearing formations might exist. Although the tools are quite different they include a number of important common features: they recover lined cores and mate to a common transfer system, use 'flapper valve' sealing mechanisms rather than ball valves to maximize the core diameter, and incorporate downhole drive mechanisms to ensure high core quality.

The percussion corer was developed by Fugro Engineers BV and is known as the Fugro Pressure Corer or FPC (Figure EXPL-1). The FPC uses a water hammer, driven by the circulating fluid pumped down the drill pipe, to drive the core barrel into the sediment up to 1 m ahead of the drill bit. The core diameter is 57 mm (liner outer diameter is 63 mm). On completion of coring, the recovery of the corer with the wireline pulls the core barrel into the autoclave, in which the pressure is sealed by a specially designed flapper valve. The FPC is designed to retain a pressure of up to 250 bar (25 MPa).

It is suitable for use with unlithified sediments ranging from stiff clays to sandy or gravelly material. In soft sediments it acts like a push corer prior to the hammer mechanism becoming active.

The rotary corer was developed by the Technical University of Berlin and the Technical University of Clausthal, and is known as the HYACE Rotary Corer or HRC (Figure EXPL-2). The HRC uses an Inverse Moineau Motor driven by the circulating fluid pumped down the drill pipe to rotate the cutting shoe up to 1 m ahead of the roller cone bit. The cutting shoe of the HRC uses a narrow kerf, dry auger design with polycrystalline diamond (PCD) cutting elements. This design allows the core to enter into the inner barrel before any flushing fluid can contaminate the material being cored. The core diameter is 51 mm (liner outer diameter is 56 mm). On completion of coring, the recovery of the corer with the wireline pulls the core barrel into the autoclave in a similar manner to the FPC, and the pressure is sealed by a specially designed flapper valve. The HRC is designed to retain a pressure of up to 250 bar (25 MPa) and is primarily designed for use in sampling lithified sediment or rock. The HRC has also sampled softer formations effectively, though in “sticky” clay the flushing holes can become clogged with cuttings.

Transfer and Chamber Systems

The ability to manipulate cores, take sub-samples, and make measurements, all at *in situ* pressures, are major features of the HYACINTH system. To this end a series of interconnecting chambers and manipulator mechanisms have been developed to enable cores to be transferred, not only initially from the corer autoclaves, but subsequently between different chambers to enable a variety of measurements and sub-sampling tasks to be performed at full pressure. When the core is recovered on deck in the autoclave it is first cooled in an ice bath before being moved into a cold processing container. The autoclave is connected to a shear transfer chamber where the core is withdrawn and the core liner is cut to separate the geological part of the core from the remaining technical components which were inside the autoclave.

The pressure core in the FPC or HRC autoclave is similar to a conventional piston core in that the piston remains within the top of the liner; however, this pressure core piston assembly contains many more technical components than a conventional piston. The core and piston/sensor mechanism (referred to as the Catch Assembly, approx. 1.6 m long) consists of a "technical portion" (approx. 0.6 m long) and a "geological portion" (approx. 1.0 m long). The first transfer is designed to extract the Catch Assembly from the autoclave and to separate it into its 2 components (technical and geological). To achieve this, the autoclave is connected in series to a Shear Transfer Chamber (STC)

and a Manipulator (Figure EXPL-3). After equalizing the pressures, the Manipulator is extended through the STC and mates to the Catch Assembly in the autoclave. The core is withdrawn into the STC where the technical and geologic parts of the Catch Assembly are separated by shearing the liner between them. At this stage the corer autoclave is isolated, removed, and replaced by another chamber (logging or storage). The pressures are again equalized and the Manipulator pushes the geological portion of the core into the logging or storage chamber. The technical portion of the core (still attached to the Manipulator) is pulled back into the STC. The ball valve on the logging or storage chamber is closed and the chamber, containing the geological portion of the core, removed for scientific measurements. The technical portion of the core is recycled for subsequent coring operations. Since the FPC and the HRC cores have slightly different diameters, the STC is supplied with two cutting boxes adapted to the specific core dimensions. The cutting boxes can be quickly interchanged by means of quick-fit flange clamp connections.

To move a core under pressure from one chamber to another, the chambers are connected, a Manipulator is attached to the end of the appropriate chamber (pushing vs. pulling), and the empty chambers are filled with water and pressurized until the pressure is equal to that in the chamber containing the core. The ball valves are opened and the core is moved from one chamber to the other with the Manipulator, which is retracted before closing all valves and depressurizing the empty chambers.

Logging / Storage Chambers

Once the core has been isolated in a sealed chamber, it can be examined by geophysical logging. Detailed structural information is necessary for many types of scientific study, as well as to provide information to guide sub-sampling. The Storage Chamber (Figure EXPL-4) is a simple cylindrical pressure vessel, sealed at one end with a ball valve and at the other with the conical seal fitting to which the Manipulator can be attached for making transfers. The cylindrical part of the Storage Chamber is manufactured from stainless steel or high-strength aluminum alloy. The Storage Chamber is designed to preserve a core under pressure for periods of hours, days, or possibly months. While in either steel or aluminum Storage Chambers, density profiles can be obtained using a gamma attenuation densitometer (see MSCL-V below). The aluminum Storage Chambers are suited to X-ray scanning for either 2-D radiographs or 3-D computed tomography (CT) as well as gamma densitometry, and these chambers can be manufactured at different thicknesses (different maximum working pressures) to maximize the X-ray transmissivity. While still under pressure the core can be

transferred from the storage chamber into the to MSCL-P to make other geophysical measurements (see MSCL-P below), or into the HYACINTH sub-sampling system.

Pressure Core Depressurization Experiments

Pressure cores not only preserve the properties of a sediment/hydrate core under near-*in-situ* conditions, they also seal a volume of porewater, sediment, hydrate, and gas such that mass-balance calculations can be used to determine whether hydrate was present in the sediment. Depressurizing a core, collecting the gas, and analyzing the composition of the gas are integral components of this mass balance process.

Cores recovered under full pressure were subjected to non-destructive measurements to characterize the core and any hydrate potentially captured. After all measurements were made, the cores were incrementally depressurized, sometimes with non-destructive measurements at intervals in the depressurization. When the cores were depressurized in the MSCL-V, the gas rose to the ball valve end of the chamber where it was easily collected. The total volume of evolved gas and the composition of this gas was measured by the on-board gas geochemists. Water forced out of the chamber was also measured; the volume of water corresponded to a volume of gas left at the end of depressurization (at 1 bar) inside the storage chamber. This gas was assigned the composition of the final gas sample for purposes of calculation. Total methane volume is reported as methane from gas (just the measured gas) and methane from gas & liquid, which includes the estimate of gas remaining in the storage chamber.

Hydrate volume was calculated by determining the amount of evolved methane that could have been dissolved *in situ* and assigning the remaining methane as hydrate (see Hydrate Calculation spreadsheet under Data Files, Pressure Cores). *In situ* methane saturations were calculated using the Xu methane saturation calculation spreadsheet. Total evolved methane was divided by the pore volume (from core volume and core porosity) to calculate a total methane "concentration" which was compared to the saturated concentration at *in situ* conditions. If the total concentration was over saturation, the excess methane above saturation was assumed to be hydrate and converted to a volume of hydrate.

Non-Destructive Measurements on Cores

Four different Geotek core logging techniques were used during the field program and a fifth was used when the cores were split and described on shore. An Infrared core logger was used to log the

long FHPC (Fugro Hydraulic Piston Corer) and the shorter FC (Fugro Corer) cores immediately after they were recovered and removed from the core barrel. A standard Multi Sensor Core Logger (MSCL) was used to make a suite of non-destructive measurements on all non-pressure cores (mainly FHPC and FC cores). A vertically-oriented MSCL (MSCL-V) was used to obtain accurate density profiles of pressure cores in aluminum and/or stainless steel storage chambers. A pressure MSCL (MSCL-P) was used to measure P-wave velocity on pressure cores at *in situ* pressures and temperatures. The same mechanical device was used by Georgia Tech to pass the cores through their Central Measurement Chamber (CMC) to make other measurements by drilling through the core liner (see separate Georgia Tech Report). The final core logging system (used on the split cores) was an MSCL-XYZ that acquires images and other data from the split core surface. All the core logging carried out by Geotek was complemented by both linear X-ray scans and X-ray CT scans of both the non-pressure cores and the pressure cores recovered (see separate Lawrence Berkeley X-ray Report).

Infrared Logging: Measurement of Core Temperature

The external temperature of the core liner was measured using two ThermaCam SC2000 infrared cameras (FLIR Systems), one of which was mounted on a motorized, computer-controlled track (Figure EXPL-5) and the other used in a handheld mode. The FLIR Systems cameras detect infrared radiation with wavelengths of 7-13.5 cm and provide temperature-calibrated images over a temperature range from –40° to 1500°C. For shipboard measurements, the cameras were set to Temperature Range 1 to record environmentally relevant temperatures (-40° to 120°C). The motorized camera was mounted and focused 33 cm above the core and this constant distance from the core was maintained by a wheeled "skate" that moved along the core (Figure EXPL-6). To minimize reflections from local infrared sources (Figure EXPL-7), the skate was covered in black felt. The skate wheels were out of the field of view of the camera and had no adverse effect on the infrared image. The camera's field of view at this distance from the core was 14 cm wide (along the core) and images were collected every 5 cm using the Geotek Infrared Imaging software in conjunction with ThermaCam Researcher software (FLIR Sytems). Using the Geotek Infrared Imaging software, 5 cm from the center of every image (Figure EXPL-8) was used to create a composite false-color thermal image of the entire core (Figure EXPL-9) with an accurate length scale in real time, which was valuable in identifying cold spots. The handheld camera was used to follow up on any cold anomalies and aid in marking and cutting these sections.

Infrared images were processed to obtain downcore temperature profiles using the ThermaCam Researcher software (FLIR Systems). All images were corrected for core liner emissivity and ambient temperature. The emissivity of the core liner was measured at 0.95, as was found on ODP Legs 201 & 204 (Ford et al., 2003; Shipboard Scientific Party, 2003). The ambient temperature of the core processing container was monitored with TMC20-HD soil/water temperature probes & HOBO U12 temperature loggers (both from Onset Corp.). The infrared images of the core had a bright streak down the center, which is a reflection off the warm camera. Temperature data was extracted from the sides of the core, away from this reflection. A ThermaCam Researcher session was created with four squares in a line down the side of the core, at 1 cm spacing (Figure EXPL-10). The average temperature of each square was logged to a file; when a set of images from a core was loaded into Researcher, this data was extracted by "playing" the images like a movie. If cores were loaded sequentially into Researcher in time order, all data could be collected in the same text file.

Core section end temperatures were collected as soon as the core was cut using 8 soil/water temperature probes (TMC20-HD, Onset Corp.) and 2 HOBO U12 temperature loggers (Onset Corp.). The manufacturer's documentation says this probe/logger combination has an accuracy of plus or minus 0.25˚C and a resolution of 0.03˚C over the temperature range 0-20˚C. Temperature probes were checked for consistency by placing them together in water over a temperature range of 0-25˚C. All probes were within 0.1˚C of each other. Data was collected continuously every 10 seconds and core section end temperatures were picked from the extrema in the records (Figure EXPL-11).

Thermal Anomalies & the GOM-JIP Core Recovery Protocols

Identification of cold spots or cold cores requires that the core handling be uniform, so that the thermal history between and along cores is similar. To this end, the core handling was monitored by the curators in an attempt to identify and eliminate sources of thermal "contamination." They attempted to record important times on the core log sheet: the time the core was pulled off the bottom, the time the core reached the drill floor, the time the core was brought to the ice trough, and the time the core was pulled into the core processing van. Other than simple warming in the water column and on deck, the three largest sources of thermal insult to the core were ice in the ice trough, frictional heating of stuck liner, and direct handling of the core by people (Figure EXPL-12). Ice in the ice trough was noted by the curators, including the length of the corer that is affected by the ice and whether the ice covers the top surface of the corer. Direct handling of the core with bare hands was discouraged but happened often and was not recorded.

If gas hydrate dissociates within a core, its only signature may be salinity anomalies and fading thermal anomalies. Thermal anomalies from dissociated hydrate could be erased by cooling the core with ice. Therefore there was a dilemma associated with cooling these unpressurized cores: cooling the core would preserve any remaining hydrate but would damp the negative thermal anomalies, making existing hydrate more difficult to find and destroying the record of already-dissociated hydrate. A decision was made partway through the cruise by the science party to place all cores on ice to preserve potential massive hydrate.

Quantification of hydrate from negative thermal anomalies requires extremely consistent core handling operations and was therefore beyond the scope of this work.

Standard Multi Sensor Core Logger (MSCL-S) Measurements

Whole-core Multi Sensor Core Logger measurements using a 'Standard' Geotek system (MSCL-S) are non-destructive to sediment fabric and can be used to provide intrinsic sediment properties and as proxies for other data. These data can facilitate core-to-core correlation between adjacent holes at the same site or among different sites as well as providing base data to help formulate a core sub-sampling program. The MSCL-S (Figure EXPL-13) was configured to measure a suite of non-destructive parameters on whole FHPC or FC core in its plastic liner: gamma density, P-wave velocity, electrical resistivity and magnetic susceptibility. These measurements were also made on push cores taken in fiberglass liner. Each measurement device has an intrinsic down-core spatial resolution determined by its design specification and the physics of operation (see discussion of each measurement below). Data quality is a function of both core quality and sensor precision. Optimal MSCL measurements require a completely filled core liner with minimal drilling disturbance. Precision is a function of measurement time for magnetic susceptibility and gamma density but not for P-wave velocity or resistivity. Generally the spatial interval used for all sensors was set at 2 cm, although some core sections were logged at 1 cm. The rail and pusher system automatically measures the length of each core section using a laser and pushes them through the stationary sensor array.

MSCL-S Sensor Descriptions and Operating Principles

Gamma Density: Gamma density is measured through the center of the core using a 370 MBq 137Cs source and a NaI scintillation detector. The detection energy window is set to measure only primary (unscattered) gamma photons (0.662 MeV), providing raw gamma attenuation data in counts per second. Gamma density is derived from gamma attenuation (see Sensor Calibration), and is reported

as g/cc. The gamma beam is collimated through a 5 mm hole providing a down-core spatial resolution of around 1 cm. The precision is a direct function of total counts and hence is dependent upon the count times used (see Core Logging Protocols) and the core thickness and density. The data is reported as gamma density to differentiate it from bulk density, which is calculated directly from weights and volume measurements. Under most normal circumstances with the calibration protocols used here, the correlation between gamma density and bulk density should be excellent. Although the empirical calibration procedure for gamma density is based on bulk density measurements (i.e., of a known graduated aluminum and water standard), the measurements can vary from true gravimetric bulk density because of variations in mineralogy. Gamma attenuation coefficients for different materials vary as a function of atomic number. Fortuitously, most earth-forming minerals have similar and low atomic numbers (similar to aluminum). Consequently, the correlation of gamma density and bulk density is usually excellent.

Ultrasonic P-Wave Velocity: Ultrasonic P-wave velocity (V_P) is measured using a pair of Acoustic Rolling Contact Transducers. The travel time for pulse propagation through the core is measured with a precision of 50 ns. At the same time, the core diameter is measured using a set of displacement transducers (precision 0.02 mm) that are mechanically coupled to the ultrasonic transducers. Combined with the calibration, this produces an ultrasonic velocity with a precision of +/- 1.5 m/sec and a likely accuracy of around 5 m/sec. Core temperatures are obtained with a platinum resistance temperature probe (precision 0.05˚C) and the measured velocity is corrected to a velocity at a reference temperature (20˚C). Ultrasonic velocity is reported in m/sec has a typical down-core resolution of about 2 cm.

Electrical Resistivity: The Non Contact Resistivity sensor operates by inducing a primary high-frequency magnetic field in the core from a transmitter coil, which in turn induces electrical currents in the core that are inversely proportional to the resistivity. A receiver coil measures very small secondary magnetic fields that are regenerated by the electrical current. To measure these very small magnetic fields accurately, a difference technique has been developed that compares the readings generated from the measuring coils to the readings from an identical set of coils operating in air. This technique provides the accuracy and stability required. Resistivities between 0.1 and 10 Ω•m can be measured at spatial resolutions along the core of about 4 cm. As with other parameters, the measurements are sensitive to core temperature and should be obtained in a stable temperature environment for best results.

Magnetic Susceptibility: Whole core volume magnetic susceptibility was measured with a 80 mm diameter Bartington loop sensor operating at 513 Hz (note this is a slightly lower frequency than a standard Bartington loop sensor, but corrections to the data ensure there is no net effect). The frequency of the low-intensity, alternating magnetic field produced by the sensor is sensitive to changes in the magnetic susceptibility of material within and near the loop. The instrument has two fixed integration periods of ~1 and 10 s. During the GOM-JIP, magnetic susceptibility was normally measured at a spacing of 2 cm, using the 10 s integration time (because the susceptibilities were generally low). The instrument automatically zeroes at the beginning of each core. Magnetic susceptibility integrates over a core length of approximately 5 cm, with exponentially decreasing sensitivity with distance from the sensor. Magnetic susceptibility, a dimensionless number, is reported as corrected volume susceptibility in SI units with an accuracy typically around +/- 4%.

Sensor Calibration

All sensors were calibrated to ensure that measurements were accurate and comparable throughout the GOM-JIP Expedition and to account for the effects of the core liner. Sections of core liner were cut to make calibration and check pieces for all the sensors as described below.

Gamma Density: Calibration of the gamma density measurement is performed by measuring the intensity of the gamma beam through a stepped aluminum bar of varying thickness sitting centrally in a short length of core liner filled with distilled water. This calibration procedure, using aluminum and water, provides a good approximation for a water-saturated sediment (minerals and water) and has proven to be an excellent calibration protocol for determining density from the attenuation of gamma rays.

Ultrasonic P-Wave Velocity: Calibration of the ultrasonic velocity is performed by measuring the total travel time of an ultrasonic pulse through a core liner filled with distilled water at a known temperature. The velocity of water at the calibration temperature is calculated theoretically and the difference between the actual travel time of the pulse and the theoretical time is calculated. This difference is then used to correct subsequent calculations of sediment velocity.

Electrical Resistivity: Calibration of the electrical resistivity was performed using a number of different salt water solutions, made using pure sodium chloride and distilled water, capped in short lengths of core liner. Dilutions corresponding to salinities of 35 ppt (parts per thousand by weight), 17.5 ppt, 3.5 ppt, and 1.75 ppt were used to construct a calibration profile.

Magnetic Susceptibility: The magnetic susceptibility sensor system is pre-calibrated by the manufacturer who provides a check piece to ensure the calibration is accurate.

Core Logging Protocols

Prior to each core being logged, 3 short "check" pieces were logged to ensure that the sensor systems were operating correctly. These check pieces were assigned negative sub-bottom depths and are easy to identify in the raw data. Core sections were logged at 2 cm spatial intervals, with 10 second integration times for the gamma density and magnetic susceptibility. With this sampling regime, each 1 m core section took about 13 minutes to log and a 9 m long core (with 9 core sections and a "check" section at the top) took a total of about 2.5 hours to log. With these logging speeds we easily kept up with the rate at which core was being recovered.

Butt error distance (the distance between one section and the beginning of the next, mainly taken up by end-caps) was automatically removed during data processing. P-wave velocity and gamma density measurements taken within 1 cm of core section ends were removed from the data set.

Gas Expansion Effects & GOM-JIP Cores

Most of the cores recovered during the GOM-JIP expedition suffered significant disturbance caused by gas-expansion effects. Expansion of free gas, exsolution of dissolved gas, and dissociation of hydrate all cause gas expansion effect that will disturb recovered cores. It is worth noting here that a unit volume of free gas at 1000 m below the sea surface will expand by a factor of 100 by the time it reaches the surface (ignoring any temperature expansion or further exsolution). Another way of visualizing the expansion of gas during the core recovery process is to consider that a 0.1-mm-diameter free gas bubble in the sediment matrix at a depth of 1000 m will become a 4.5-mm-diameter gas bubble at the sea surface. If a sediment core (taken from around 1300 m) has pore waters that are saturated in methane, then at the surface the change in temperature and pressure can typically cause the core to expand by at least 1½ times its original volume. When relatively low volumes of gas exsolve from pore fluids during core recovery, small bubbles will form in the sediment matrix with only minor amounts of core volume expansion. As the gas volumes become greater, the sediment structure begins to fracture and a large amount of core expansion occurs, forming a series of large gas voids in the core. This process takes some time but is readily visible in the processing van. When core expansion occurred on GOM-JIP cores (e.g., Figure EXPL-14), the core was not pushed back together prior to sectioning, and hence the voids were curated and logged in the MSCL.

The expansion of gases inside the sediment matrix and the voids had a noticeable effect on all the parameters measured by the MSCL-S. Magnetic susceptibility (loop sensor) measurements were probably the least affected by core expansion, as these measurements depend only on the sediment/mineral volume. However, significant lowering of the magnetic susceptibility value was seen where there were clear gas gaps (greater than ~0.5 cm).

Gamma density measurements can be significantly affected by gas voids and sediment cracks. The downcore spatial resolution is ~1 cm, and hence, all cracks, no matter how minor, will show up in the gamma density profile. With significant gas expansion in many cores, this effect shows up as a very "noisy" data set. These data are, in fact, quite accurately representing the state of the core but of course do not represent the *in situ* condition. The closest representation of the *in situ* condition is achieved by taking the upper values of the gamma density data envelope. However, even these values are often lower than the *in situ* densities because of gas in the matrix.

Electrical resistivity measurements increase as a result of small gas bubbles that have formed in the sediment matrix and increases dramatically around the major gas cracks. The largest excursions caused by the major cracks have been edited from the processed data sets but most remaining data is still affected by the core disturbance.

Gas expansion has the largest effect on the measurement of ultrasonic P-wave velocity (V_P). Even very small amounts of free gas in the sediment matrix (<1%) will cause a significant decrease in velocity. More importantly, the very high attenuation of P-waves at ultrasonic frequencies in sediments with even very low volumes of free gas makes the measurement of velocity all but impossible. During the GOM-JIP expedition, we generally encountered gas-rich sediments, in which P-wave velocity measurements were possible only in the upper few meters. In practice, we observed that P-wave velocity was generally only measurable above the sulfate/methane interface. Below the sulfate-methane interface, the gas exsolved generally prevented the acquisition of any reliable data.

Vertical Multi Sensor Core Logger (MSCL-V) Measurements

The MSCL-V accommodates cores vertically, and the sensor cluster moves up and down along the stationary core. For the GOM-JIP, the MSCL-V was configured to accommodate HYACINTH storage chambers in order to measure gamma density of pressure cores (Figure EXPL-4). The gamma density sensors and detectors are the same as used on the MSCL-S (see above, MSCL-S Sensor Descriptions and Operating Principles), and calibration was performed in a similar fashion (see

Sensor Calibration). The stepped aluminum calibration sample was logged in the two different pressure core liners (FPC and HRC) within a pressure vessel to provide the appropriate calibration.

Pressurised Multi Sensor Core Logger (MSCL-P) Measurements

The MSCL-P (Figure EXPL-15) enables geophysical measurements to be made on HYACINTH pressure cores while maintaining them at *in situ* pressures. As used on the GOM-JIP, the MSCL-P system had 2 different Central Measurement Chambers (CMCs):

a) a Geotek CMC, which, for the GOM-JIP, had a set of P-wave transducers that enabled detailed P-wave profiles to be obtained rapidly and automatically along the core.

b) a Georgia Tech CMC that enabled a suite of measurements to be made manually as the core was moved through the chamber. These measurements generally relied on holes being drilled in the core liner (see separate Georgia Tech Report).

The core transport/manipulation system is based on existing HYACINTH technology and philosophy with modifications and adaptations to suit this particular application. In operation, the CMC was joined to a standard HYACINTH storage chamber (stainless steel or aluminum) which contained the original core to be logged. On the other side of the CMC was an extension chamber that provided enough space for the core to completely pass through the CMC. On both ends of the system, linear manipulators (pressurized, precision push rods) were fitted that allowed the core to be pushed in both directions. The manipulators allowed the core to be securely held between the two ends of the push rods during the manipulation process. Mechanisms were designed to ensure that the core did not rotate during the linear translation and that small end confining pressures could be applied to the core material (if the core liner were full). All the components in the system were coupled together using the HYACINTH quick fit couplings, which fit around the flanged ends of the chambers. To ensure precise motion of the core, the manipulators were driven synchronously using servo motors under computer control. Before opening the storage chamber to begin logging the pressure core, the system was bled and filled with seawater using a compressed-air-driven high pressure water pump.

The system enables pressurized cores to be incrementally moved from a HYACINTH storage chamber through the CMC under computer control to any predetermined position with a precision of about 0.1 mm, enabling multiple probes to enter the same hole in the liner as required by the Georgia Tech measurement devices. The Geotek P-wave velocity profiles were generally collected at a spatial interval of 0.5 cm, using an automated core logging program.

Calibration of the Geotek CMC P-wave velocity measurement system is done as with the MSCL-S over the pressure range of interest using water with a known temperature and salinity. The process is repeated for both types of core liner (FPC and HRC).

Split-Core (multi-section) Multi Sensor Core Logger (MSCL-XYZ) Measurements

The MSCL-XYZ (Figure EXPL-16) contains multiple trays to hold up to nine split core sections. The sensor array, on a robotic arm, moves along each of these trays in turn. The MSCL-XYZ can make contact measurements or non-contact measurements. For the GOM-JIP, the MSCL-XYZ was equipped for color linescan imaging, color spectrophotometry, high-resolution magnetic susceptibility, and measurement of natural gamma radiation.

MSCL-XYZ Sensor Descriptions and Operating Principles

Color Linescan Imaging: Color linescan images were collected with the Geoscan color linescan camera. The Geoscan color line scan camera uses 3 * 1024 pixel CCD arrays: one for each color, red, green and blue (RGB). The light unit uses 2 high frequency 'white' fluorescent tubes that illuminate the core evenly from both sides of the image line. This provides a flooded illumination that minimises some of the shadow effects caused by microtomographic effects. The camera is arranged directly above the light and "looks" through a slot in the top surface of the light unit.

High-Resolution Magnetic Susceptibility: High-resolution magnetic susceptibility was measured with a Bartington point sensor operating at 565 Hz. The frequency of the low-intensity, alternating magnetic field produced by the sensor is sensitive to changes in the magnetic susceptibility of material within and near the sensor. The instrument has two fixed integration periods of ~1 and 10 s. During the GOM-JIP, magnetic susceptibility was normally measured at a spacing of 2 cm, using the 10 s integration time as the susceptibilities were generally low. The instrument automatically zeroes every five measurements to compensate for drift. The magnetic susceptibility point sensor has a field of influence of approximately 5 mm. Magnetic susceptibility, a dimensionless number, is reported in SI units with an accuracy typically around +/- 4%. The user should be aware that because the point sensor has a very high spatial resolution the data can be significantly affected if the sensor happens to be positioned directly on a small crack.

Color Spectrophotometry: The Minolta color spectrophotometer collects light in 10 nm increments from 360 nm to 740 nm, thus providing complete spectral data in the visible wavebands (400-700 nm) with small extensions into the ultraviolet (360-400 nm) and infrared (700-740 nm) regions. The

diffraction grating creates a Gaussian distribution of wavelengths, centered on the reported value with a 10 nm width at half maximum. Therefore, in practice, the reported value at 360 nm contains photons from 355 to 365 nm with a contribution (about 30%) from wavelengths both larger and smaller.

Natural Gamma Radiation: Gamma radiation is measured on split core sections using a single 3 in. x 3 in. NaI(Tl) detector mounted in a heavily-lead-lined shield. The detector is positioned just above the split core surface during the measurements with additional lead shielding surrounding the core and detector. To further reduce background radiation from the concrete floor in the laboratory, and general background from the Earth, additional half-inch-thick lead tiles were used on the floor beneath the complete instrument. Natural gamma measurements have a down-core resolution of approximately 10 cm (detector diameter 7.5 cm). The precision of the measurement is dependent upon the total number of counts; on the GOM-JIP cores, this intrinsic error is approximately plus or minus 5% (95% confidence interval).

Laser Depth Profiler: The laser depth profiler measures the distance to the surface of the core, allowing the sensor array to contact the core without doing damage. This core thickness is also used in volume correction of natural gamma measurements. The laser depth profiler has a working range of 40 mm.

Sensor Calibration

All sensors were calibrated to ensure that measurements were accurate and comparable throughout the GOM-JIP Expedition as described below.

Color Linescan Imaging: The Geotek MSCL-XYZ software saves calibration files containing the black and white calibrations for each element in the CCD. This ensures that all CCD pixels are scaled to the same black (minimum) and white (maximum) values. White calibrations are performed on a special white ceramic tile. The camera travels a short distance to remove the effects of any dust on the tile. Black calibrations are performed with the lens cap on; data is collected for few seconds and then averaged.

High-Resolution Magnetic Susceptibility: The magnetic susceptibility sensor system is pre-calibrated by the manufacturer who provides a check piece to ensure the calibration is accurate.

Color Spectrophotometry: The spectrophotometer is calibrated internally by using a "white" calibration reference spectrum and a "zero" calibration reference spectrum. These calibration spectra must be acquired each time the Minolta color spectrophotometer is turned off, since they reside in the

spectrophotometer memory and cannot be stored elsewhere. The white calibration spectrum is simply acquired by collecting the spectra with the sensor placed on a special white ceramic calibration tile. For convenience, the same white calibration tile can be used for both the Geoscan camera and the Minolta color spectrophotometer. The "zero" calibration spectrum is simply acquired by collecting a spectrum with the sensor in free air, away from any surfaces. In practice, if the sensor is about 20 cm above the empty core trays an accurate "zero" calibration is obtained.

Natural Gamma Radiation: Although the Natural Gamma measurements are only reported as total count rates (across the complete energy spectrum) the raw data does in fact consist of spectral data up to 3MeV. The NaI(Tl) detector is energy calibrated using Cobalt and Barium check sources. In addition, the background radiation levels were measured along all the trays on the XYZ table so that the raw data could be appropriately corrected.

Laser Depth Profiler: The laser depth profiler is automatically calibrated by the Geotek MSCL-XYZ software by keeping the depth profiler stationary while the z-axis motor moves a target by incremental known distances.

Core Logging Protocols

Core sections were imaged with both a down-core and cross core resolution of 0.1 mm. The lens aperture was normally set at either f8 or f11 (this information is stored in the Geotek image files as well as the RGB datafiles). Labels with full section names were imaged at the bottom of each section.

Color spectra and magnetic susceptibility were collected every 2 cm, with 10 second integration times for the magnetic susceptibility.

Measurements of natural gamma radiation were taken every 5 cm for 5 minutes apiece, on selected cores only. Background radiation was subtracted from the data set and the core data was corrected for differences in core volume, as measured by the laser depth profiler.

Data Files & Formats

Data files are organized on the DVDs by site: Atwater Valley AT13 (& AT14 ROV cores), Atwater Valley Mound (ATM1&2), and Keathley Canyon (KC151). For each site, the DVDs include each of the data types below.

Pressure Core Data

MSCL-V data: Data from the MSCL-V is stored in folders, labeled by core number and an indication of conditions (pressure, depressurization). The files inside (,CAL, .DAT) are meant to be read by the Geotek MSCL software, with the exception of the .RAW file, which is fixed-width, tab-delimited plain text. Fields in the .RAW file are Core Depth (m), Section Number, Section Depth (cm), and Gamma Attenuation (cps). Pressure cores only have one section; pressure core files that appear to have multiple sections are actually repetitive logs of the same core.

MSCL-P data: Data from the MSCL-P is stored in folders, labeled by core number and an indication of conditions (pressure, depressurization). The files inside (,CAL, .DAT) are meant to be read by the Geotek MSCL software, with the exception of the .OUT file, which is fixed-width, tab-delimited plain text. Fields in the .OUT file are Core Depth (m), Section Number, Section Depth (cm), P-wave Amplitude (0-100), and P-wave Velocity (m/sec). Pressure cores only have one section; pressure core files that appear to have multiple sections are actually repetitive logs of the same core.

Processed Data: The .RAW & .OUT files from the MSCL-V & MSCL-P have been imported into Excel (.XLS) files with names that indicate when the data was taken (full pressure before depressurization, during depressurization, or post-depressurization). Plots of the data taken at full pressure are in Adobe Illustrator (.AI) format and .PDF files, and include the X-ray images. The Excel spreadsheet "Hydrate Calculations.xls" contains the calculation of hydrate content for the pressure cores.

Fields in the "Hydrate Calculations" spreadsheet are divided into four sections: Pore Volume Calculation, In Situ Methane Concentration from Xu, Calculation of Methane Oversaturation, and Calculated Hydrate Volume. Section "Pore Volume Calculation" contains Core Diameter, in mm (entered); Core Length, in mm (entered); Core Volume (calculated); Sediment Porosity, in percent, estimated from gamma density (entered); and Pore Volume, in liters (calculated). Section "In Situ Methane Concentration from Xu" contains Water Depth (m), Depth Below Mudline (m), Bottom Water Temp (Temperature, ˚C), Temp Gradient (Temperature Gradient, C˚/m), and Salinity (kg salt/kg water). All these values must be entered into the Xu spreadsheet (included) to get the final column, Methane Saturation from Xu (m<u>M</u>), Section "Calculated Methane Oversaturation" contains Total Volume of Methane Released During Degassing (liters, entered); Molar Gas Volume at Degassing Temp (liters, entered), calculated from experimental temperature, generally 10˚C, and PV=nRT; Total Moles Methane (mmol, calculated); Methane Saturation at Degassing T&P (m<u>M</u>), the

concentration of methane remaining in the pore fluids when degassing is complete; Total Methane Concentration, if all dissolved (mM, calculated), calculated by dividing the total moles of methane by the pore volume; and Excess Methane Concentration (Oversaturation), in mM (calculated). Section "Calculated Hydrate Volume" contains Amount Excess Methane (mmol, calculated); Volume of Excess Methane as Gas (STP), liters (calculated); Volume of Excess Methane as Hydrate (ml, calculated), using the conversion 164 volumes of methane at STP can create one volume of methane hydrate; and Hydrate as a Percentage of Pore Volume (%, calculated), the volume of hydrate divided by the pore volume.

Temperature Data

Infrared Raw Data: Each folder contains the sequential images captured by the FLIR infrared camera on the Geotek IR track for a single core. File 01_0000.X is the top of the core. The four digits after the "_" indicate the distance downcore in millimeters of the center of the image. The image is 14 cm wide in the along-core direction. Each image is stored as a .IMG file (FLIR image file) and a .BMP file. The .IMG file can be read by ThermaCam Researcher (FLIR Systems) and quantitative data can be extracted. The .BMP file is just a picture used to create the core bitmap files. The .INI file allows the images to be read back into the Geotek Infrared Imaging Software, where montages can be created or images can be adjusted, in conjunction with ThermaCam Researcher (FLIR Systems). The temperature range for each set of images is in the folder name. There is a temperature scale included in each folder. Cores imaged in two sections (due to difficulty in removal from the core barrel) are labeled "a" & "b".

Infrared Core Images: The core bitmap (.BMP) files are montages created from the center 5 cm of 14 cm long (downcore) infrared images. Each folder of bitmaps has a temperature scale with it. The ruler is generated electronically in the Geotek imaging software.

Core Temperature Data: Data from the core-section-end thermistors and the infrared images were combined to create Excel (.XLS) files for each hole. Cores are contained on individual worksheets. A hole summary worksheet is also included. Columns are sub-bottom depth (m), core depth (m), IR temperature (˚C) from the infrared camera, and HOBO temperature (˚C) from the core-section-end thermistors.

Core Temperature Plots: Summary plots for each hole are included as .PDF files.

MSCL-S (whole-core log) Data

MSCL-S Logsheet: Logsheet in Excel (.XLS) format giving details, lengths, and any problems with core logging.

MSCL-S Calibrations: Processing parameters used by the Geotek MSCL software (.PRO), derived from on-board calibrations, including the gamma calibration piece logged in the folder Gamma Cal. Calibrations are calculated in "FHPC MSCL Cal.xls."

MSCL-S Raw Data: Data from the MSCL-S is stored in folders by core number. The files inside (,CAL, .DAT, .DEL, .SBD) are meant to be read by the Geotek MSCL software, with the exception of the .OUT file, which is fixed-width, tab-delimited plain text. Fields in the .OUT file are explained in MSCL-S Spreadsheets, below.

MSCL-S Spreadsheets: The .OUT files for each core have been imported as worksheets into Excel (.XLS) files for each hole. The columns are SBD (m), sub-bottom depth; Sediment Thickness (cm); P-wave Amplitude (0-100); P-wave Velocity (m/s); Gamma Density (g/cc); Magnetic Susc (SI), magnetic susceptibility in SI units; Acoustic Impedance (m•g/sec•cc, or 10^3 kg/m^2•sec), acoustic velocity multiplied by density, Fractional Porosity (0-1), calculated from gamma density; and Resistivity (ohm•m). A hole summary worksheet is also provided. Sub-bottom depths with numbers less that zero are beginning-of-core check pieces. Magnetic susceptibility data in core worksheets (but not Hole Summary worksheets) may contain extremely low (-200 to -600) erroneous values ("dropouts").

MSCL-S Plots: Summary plots for each core and each hole are included as Adobe Illustrator (.AI) and .PDF files.

MSCL-XYZ (split-core log) Data

RGB Linescan Images

Raw Images and RGB: Each section has a set of files, designated as Hole_Core_Section, contained in folders by hole. The .TIF file is the original raw image collected by the linescan camera. Each pixel is 0.1 mm on a side. The .RGB file is a tab-delimited text file, which starts with the core designation on multiple lines, followed by the lens aperature (f8 or f11 for most GOM-JIP cores), other numbers used by the Geotek imaging software that define the image resolution and cropping, and, just above the word START, the downcore resolution of the data in cm. After the word START, the RGB data,

whose values range from 0-255, begins as tab-delimited columns of Section Depth (cm), Red, Green, and Blue. The .ICO and .XML files are for use with the Geotek Imaging Software.

JPEGS Large: These folders contain, by hole, jpeg files (.JPG) created from the .TIF files mentioned above. Jpegs are near full resolution of the original .TIF files. File sizes range from 2-8 Mb.

JPEGS Small: These folders contain, by hole, jpeg files identical to those above, only at a lower resolution. File sizes are less that half a Mb.

Concatenated Images: Small jpeg images of core sections have been concatenated to re-create the entire core (with missing core intervals in black). Files are named Hole-Core.

Magnetic Susceptibility Point Sensor & Minolta Color Spectrophotometry

Mag Susc-Spec Raw Data: Data from each core is stored in an .XML file, titled with the core name, meant to be read by the Geotek MSCL-XYZ software. These files are stored in folders named for the cores, and the cores are grouped into folders by hole.

Mag Susc-Spec CSV Files: Data from each core has been exported as comma-separated value files (.CSV) that can be read into most spreadsheet programs. Fields in the .CSV files are explained in Mag Susc-Spec Spreadsheets, below.

Mag Susc-Spec Spreadsheets: The .CSV files from each core have been imported as worksheets in Excel (.XLS) files for each hole. Columns are Sub-Bottom Depth (m), or Core Depth (m) for single-core worksheets; Core, GOM-JIP core number; Section; Laser Profiler (mm), the height of the core relative to a full half-core; Magnetic Susceptibility (SI); Munsell Color, the Munsell value of the color measured by the Minolta color spectrophotometer; and Reflectance (Xnm), where X varies from 360 to 740, and the values range from 0 to 100, calibrated across all GOM-JIP cores.

Natural Gamma Measurements

Natural gamma measurements were only made on Keathley Canyon cores.

Nat Gam Raw Data: Data from each core is stored in an .XML file, titled with the core name, meant to be read by the Geotek MSCL-XYZ software. These files are stored in folders named for the cores, and the cores are grouped into folders by hole.

Nat Gam CSV Files: Data from each core has been exported as comma-separated value files (.CSV) that can be read into most spreadsheet programs. Fields in the .CSV files are explained in Nat Gam Spreadsheets, below.

Nat Gam Spreadsheets: The .CSV files from each core have been imported as worksheets in Excel (.XLS) files for each hole. Columns are Sub-bottom Depth (m); Core; Section; Laser Profiler (mm), the height of the split core surface relative to a full half core; Corrected Natural Gamma (cps), the natural gamma data corrected for background and volume effects; Corrected Natural Gamma Smoothed (cps), the corrected natural gamma data averaged over four or five consecutive data points, where they exist; and Natural Gamma from LWD (API), the downhole natural gamma data from the Schlumberger Logging While Drilling tool. The worksheets representing single cores have Natural Gamma (Raw) (cps); these data have not been corrected for volume or background effects.

Atwater Valley, Hole AT13-2

HYACINTH Tool Operations

Fugro Pressure Corer (FPC)

The FPC recovered Core AT13-2-7P at full *in situ* pressure from Atwater Valley Hole AT13-2. AT13-2-7P was from 35.7 mbsf and contained 53.5 cm of core (Table 1). Unfortunately, the latching mechanism jammed in the shear transfer chamber and the core had to be depressurized, precluding any measurements at *in situ* pressure. Other FPC deployments were hampered by problems associated with over-penetration (Table 1): the tool was coring but extending too far, which meant that it could not retract the core into the autoclave. For instance, Core AT13-2-12P overshot, broke the central rod, and could only be recovered with the use of an improvised fishing tool. This over-penetration was occurring because a) the sediments were generally very soft and b) because there was no landing ring at the bit to prevent excessive movement of the core barrel. Bottom-hole assembly compromises to accommodate all the different tools meant that the smaller bit with the landing ring could not be used.

HYACE Rotary Corer (HRC)

Two HRC deployments were made at Atwater Valley Hole AT13-2 (Table 2). A good core (AT13-2-5R) was recovered from 27.1 mbsf, which demonstrated that the more recent modifications to the HRC enabled it to core in softer formations than its original design. However, this core did not retract into the autoclave and hence the *in situ* pressure was not retained. A shear pin failed on the next coring run (AT13-2-10R) and hence the motor and coring stroke did not take place. In addition, the inner rod broke and it was tentatively concluded that the shock load on the landing ring may have been too severe. It was noted that there was little fine control on the *Uncle John*'s sand line when trying to lower gently, and hence the shock load at the time of contact would vary for each deployment.

Pressure Cores

Pressure Core AT13-2-7P

Core AT13-2-7P was recovered under full pressure, but it became stuck in the shear transfer mechanism and had to be depressurized to remove it from the equipment. No measurements were made on core AT13-2-7P in its initial pressurized state. When it was depressurized, very little gas was observed.

FHPC & FC Cores

Temperature Measurement via Infrared Logging

The temperatures of each of the cores from Hole AT13-2 were monitored in order to detect any signs of hydrate dissociation, in the form of localized, centimeter-scale thermal anomalies or large cold zones that might span multiple cores. The infrared camera track provided a continuous record of the liner temperature, and temperature probes placed in the center of section ends recorded the actual core temperatures. However, no thermal anomalies were found in this hole that could be linked to gas hydrate.

Figures AT-1 & -2 summarize the temperature data collected for Hole AT13-2. Cores AT13-2-6H & 8H were 3-6 C˚ colder than other cores from this hole (Figure AT-1). These two cores were very expansive, containing many gas voids. Gas expansion can cool cores (Shipboard Scientific Party,

2003) and could explain the cooling seen in these cores. If there had been very low levels of disseminated hydrate within these cores, it would be impossible to differentiate between the cooling effects from gas expansion and/or hydrate dissociation.

These two cores had many local thermal anomalies, most of which are definitely associated with gas voids. The gamma density logs (Figure AT-3) and the X-ray scans that were taken after the core was cut into sections were examined as void detectors . From Figure AT-3, it is evident that the very cold spots with sharp boundaries are gas voids. Unfortunately, in gas sampling, cutting, and general handling, voids and sediment move within the liner, causing the infrared record to be decoupled from the gamma and X-ray scans, making this analysis qualitative rather than quantitative. In future, a visual image of the uncut core would be very helpful in later distinguishing voids from sediment. If there were small amounts of disseminated hydrate in these cores, on meter or centimeter scales, it would be extremely difficult to detect against the background of core variably cooled by gas expansion.

Nonuniform handling explains much of the remaining temperature variations within and between cores. For instance, Core AT13-2-11H had extended handling time and was then placed in ice; the internal core temperatures no longer reflect the *in situ* temperatures to any extent. The core processing container was cooler than the core but with a strong thermal gradient, causing a strong gradient in liner temperature that was not reflected in the internal temperature of the core (Figures AT-2 & -4). These variations make the thermal baseline for cores difficult to determine, and subtle anomalies hard to identify.

The temperature data indicate that actual recovery of small amounts or concentrations of hydrate under these conditions was very difficult. Average cores reached the rig floor with temperatures of 18-22˚C, having warmed during the trip up the drill pipe. The data from the Seabird CTD (Figure AT-5) showed that the thermocline was extremely extended at this site and that over half of the water column was warmer than the cores were *in situ*. Data from the Fugro Pressure Corer temperature and pressure logger shows the temperature of the corer as it was recovered at AT13-2 (Figure AT-6); the corer warms quickly during its 17 minute trip up the drillpipe. This temperature profile is likely to be similar to what was experienced by the Fugro Hydraulic Piston Corer, accounting for the very warm FHPC cores.

MSCL-S Measurements

Cores from Hole AT13-2 were logged with the MSCL-S, using the gamma density, P-wave velocity, electrical resistivity, and magnetic susceptibility sensors. All cores and hence data were adversely affected by gas expansion below the sulfate-methane interface (around 7 mbsf). Figure AT-7 shows a summary plot of all the data along with data envelopes bounding the data least affected by gas expansion. The P-wave data were almost non-existent below the sulfate-methane interface, and while resistivity values are shown, they are not representative of *in situ* conditions (see "Gas Expansion Effects & GOM-JIP Core" under Explanatory Notes). The gamma density data correlated well with the LWD data from the Hole AT13-1 (including the drop in density around 130 mbsf). The magnetic susceptibilty data does show some significant variations, especially in the zone 120-130 mbsf. Variations in magnetic susceptibility indicate changes in the source of the material, which may be useful when developing a sedimentological unit classification or sampling program.

MSCL-XYZ Measurements

Cores from Hole AT13-2 were imaged in the MSCL-XYZ. An example section is shown in Figure AT-8. A summary plot of the Minolta Spectra and Color spectra and magnetic susceptibility measurements are shown in Figure AT-9. The magnetic susceptibilty data shows the same overall trends as the loop sensor but contains another level of detail in the high resolution data that could prove useful when examining the sedimentology.

ROV Push Cores (from AT13 & AT14)

MSCL-S Measurements

An ROV push core, Core AT14-7PC, collected from Atwater Valley in short fiberglass liners was logged with the MSCL-S (Figures AT-10 & -11). This core was taken specifically for measurements of physical properties (see separate Fugro Physical Properties Report), and the MSCL-S data was meant to complement these measurements. The resistivity data is adversely affected by the core end effects and is not calibrated, however, all other data is calibrated and valid.

MSCL-XYZ Measurements

The ROV push cores taken in plastic liners from Atwater Valley (AT13-2PC, AT14-5PC, AT14-6PC, AT14-8PC, AT14-10PC) were imaged in the MSCL-XYZ. Color spectra and magnetic susceptibility point sensor measurements were also made.

Atwater Valley, Holes ATM1 & 2

HYACINTH Tool Operations

Fugro Pressure Corer (FPC)

The FPC recovered one core at full *in situ* pressure from the Mound sites at Atwater Valley (Table 1). Core ATM2-5P was recovered at full pressure from 26.82 mbsf. This core was sheared with some difficulty in the shear transfer chamber and ended up in the storage chamber with the piston assembly and some broken bits of core liner. A portion of the core had been extruded during the transfer process but the rest of the core, containing gas hydrate, did have measurements made at *in situ* conditions. The other 2 pressure coring attempts were unsuccessful.

HYACE Rotary Corer (HRC)

All 3 HRC pressure coring attempts at the mounds sites failed because of jamming issues inside the tool during activation (Table 2). It was concluded that these deployments functioned correctly on the bottom but failed to fully retract because the top of the core cutter was not engaging correctly as it retracted into a sleeve in the autoclave.

Pressure Cores

Pressure Core ATM2-5P

Pressure core ATM2-5P (Figure ATM-1), recovered with the FPC from 26.82 mbsf at 130 bar, was imaged with the X-ray CT scanner, logged for gamma density in the MSCL-V, logged in the MSCL-P using the Geotek P-wave system in a manual mode, and finally depressurized.

After a difficult transfer process (see FPC operations) it was known that the FPC corer/piston mechanism (technical portion of core) was inside the aluminum storage chamber together with the

recovered core material. The complete storage chamber was X-ray CT scanned, which revealed that there was a coherent core 52 cm long surrounded by an intact liner. Within the core there was a zone of lower density material that contained some very interesting and unusual structural features (see separate Lawrence Berkeley X-ray Report). However, the liner was broken around the piston assembly, which was to impede further core manipulations.

The storage chamber was loaded into the MSCL-V, where a detailed density profile was obtained (Figure ATM-1) indicating a low density zone that correlated with the zone revealed by the X-ray scan. After connecting the storage chamber to the MSCL-P and balancing the pressures, the core was moved carefully through the system using the manipulators. However, the resistance (caused by the broken liner) was such that we decided against automated logging and collected the P-wave information manually as the core passed the transducers. This data is also shown in Figure ATM-1 and reveals a high velocity interval that correlates with the low density interval as shown by both the gamma density profiles and the X-ray profiles.

Further movement of the core in the system became more difficult and it was concluded that we had extruded some more core inside the apparatus. This was confirmed when the MSCL-P system was opened (sediment around the transducers) and the chamber (still under full pressure) was X-rayed again. Because of the jamming issues we could not use the core with the Georgia Tech central measurement chamber.

The final core was only 30 cm long. This remaining length of core (which, fortuitously, contained the low density/high velocity anomaly) was depressurized. The MSCL-V could not be used during the depressurization due to the presence of the technical portion of the core. The total volume of methane released was 1015.7 ml (lower estimate; some gas remaining in the corer at 1 bar could not be measured). Over a liter of air was also released; this gas presumably came from the technical portion of the FPC core, which is not normally transferred into the logging chambers.

The final core was sub-sampled and squeezed for pore water analysis that showed significant porewater freshening around the low density zone (see separate Scripps Porewater Chemistry Report). The retrieval of this core and the experiments conducted were far from ideal, but the combination of information retrieved indicated that the core did contain some gas hydrate. Our calculations show that this was about 0.3% of the total pore volume in the core.

It is likely that the gas hydrate was concentrated in the 10-cm-long high velocity interval, which would indicate that this layer had a hydrate concentration of about 3% of total pore volume. While

the velocity anomaly shown in Figure ATM-1 could have been due to hydrate within this zone, the density anomaly cannot be explained simply by the presence of 3% hydrate. This layer has a low density independent of hydrate presence and the low density of the layer may have provided space for preferential hydrate growth.

FHPC & FC Cores

Temperature Measurement via Infrared Logging

The temperatures of each of the cores from Holes ATM1&2 were monitored in order to detect any signs of hydrate dissociation, in the form of localized, centimeter-scale thermal anomalies or large cold zones that might span multiple cores. The infrared camera track provided a continuous record of the liner temperature, and temperature probes placed in the center of section ends recorded the actual core temperatures (Figures ATM-2 & -3).

The moussy texture of all six of the cores from the Atwater Mound site (Figure INT-1), which was first observed while cutting the core into sections and inserting temperature probes, indicates that there may have been gas hydrate in these cores. The mudline core from each hole was colder than the deeper cores, though the rest of the cores were similar in temperature to the cores from AT13-2. However, some of the cores may have been cooled in the ice trough or processing van, as their centers, as measured by the temperature probes, were warmer than the outside, as measured by the infrared camera.

Plenty of small thermal anomalies existed in these cores, many of which are likely due to gas expansion effects. The moussy, frothy expansion of the cores would have chilled the cores in a qualitatively different fashion than the dry gas expansion cracks seen in Hole AT13-2. This small-scale gassy nature can be seen in the split-core images (see ATM MSCL-XYZ) and in the gamma density logs (see ATM MSCL-S). Gas expansion cracks were also present. Attempts to remove these two gas expansion effects using the density data from either the gamma attenuation (Figure ATM-4) or the X-ray images proved complex and beyond the scope of this report.

Comparison of the thermal anomalies with the salinity data provided by the geochemists showed that most thermal anomalies directly associated with gas hydrates at this site were probably lost in recovery and handling. There is a large, low-salinity zone that encompasses the center of Core ATM1-2H that might be due to hydrate dissociation, but there is no corresponding thermal anomaly at

the center of this core (Figure ATM-5). Core ATM2-3H may have retained some thermal anomalies due to hydrate dissociation, based on the salinity anomalies (Figure ATM-6).

The Atwater Mound site was very close to AT13-2, so the water column temperature profile is likely very similar (Figure AT-5), where the thermocline was quite extended. The Adara temperature shoe attached to the FHPC on Cores ATM1-5H and ATM2-3H (Figure ATM-7) as well as the temperature logger on Core ATM2-5P (Figure ATM-8) show that the core would warm substantially during the trip up the pipe and any remaining thermal anomalies from hydrate dissociation were likely to be subtle.

MSCL-S Measurements

Cores from Holes ATM1&2 were logged using the MSCL-S, using the gamma density, P-wave velocity, electrical resistivity, and magnetic susceptibility sensors (Figures ATM-9 & -10). The cores exhibited moussy textures and contained much gas, potentially from dissociated hydrate. No P-wave velocity measurements were possible at any depth and all the other parameters are significantly affected by the core disturbance. Even the gamma density is likely to be significantly low; the density measured in the MSCL-S in ATM1 at full depth (27 mbsf) is around 1.5 g/cc, whereas the density measured from the pressure core just beneath it is 1.6 g/cc. Note the significant differences in the magnetic susceptibility data, taking into account the density, for both holes below 15-20 mbsf, indicating rapid horizontal variation at the Mound site.

MSCL-XYZ Measurements

Cores from Holes ATM1&2 were imaged in the MSCL-XYZ. Even after transport, storage for over a month, and splitting, the moussy texture of the cores was still evident (Figure INT-1). Color spectra and magnetic susceptibility measurements, made with a point sensor, were also taken (Figure ATM-11). The quality of the data in these cores is compromised because of the very moussy texture. Care should be used when interpreting the data.

Keathley Canyon, Hole KC151-3

HYACINTH Tool Operations

Fugro Pressure Corer (FPC)

The first attempted pressure core at Keathley Canyon (KC151-3-6P; Table 1) was thwarted by a backwash of sand in the BHA (bottom hole assembly). The deployment went smoothly but there was no pressure drop indicating the tool had fired. The tool had become stuck in the BHA and the sand line could not free the tool. After many hours of attempting to free the tool from the BHA, the sand line was finally cut and the pipe tripped. It was discovered that the tool had never landed on the landing shoulder because of fine sand that had filled the BHA.

After this deployment it was thought that a number of the pressure corer failures may have been caused by some sediment "sticking up" in the BHA, which might have prevented the tools landing properly. Consequently, it was decided to run the center bit prior to all remaining pressure cores to ensure the BHA was clear of any obstructions. The subsequent 3 resulting successes (FPC and HRC; Tables 1 & 2) may have been partially due to this new procedure. The second FPC deployment (KC151-3-11P) at 227.08 mbsf was a total success and recovered 88.5 cm of core at full *in situ* pressure. This core was logged in the X-ray CT scanner, the MSCL-V, and the MSCL-P (see Keathley Pressure Cores).

The last 2 deployments with the FPC at Keathley Canyon were deep in the hole and did not recover cores under pressure essentially because the sediments were stiffer than the tool was designed for (Table 1). In the case of KC151-3-18P at 265.18 mbsf, the pull-out forces broke the liner and the top half of the liner (which was empty) was recovered under full pressure. The 59 cm core was recovered in the unpressurized outer barrel. During the final FPC deployment at 384.96 mbsf (probably below the depth of gas hydrate stability), the sediment completely jammed the liner in the outer barrel and prevented it being retracted into the autoclave. Excessive pull-out forces on this deployment showed that we had gone beneath the level at which the corer could operate.

HYACE Rotary Corer (HRC)

The HRC operations at Keathley Canyon provided 2 good pressure cores recovered from the 4 deployments in what were difficult coring conditions (Table 2). KC151-3-13R was recovered from a depth of 235.92 mbsf, which was just into the region predicted (from the LWD data) to contain

significant amounts of gas hydrate. The second core retrieved under pressure came from a depth of 383.13 mbsf and was thought to lie just above the base of the gas hydrate stability zone. Both cores were logged in the X-ray CT scanner, the MSCL-V, and MSCL-P before being subjected to depressurization experiments (see Keathley Pressure Cores). The other 2 HRC deployments suffered technical difficulties, as at Atwater Valley, caused by the retraction of the sleeve when the inner core barrel enters the autoclave.

Pressure Cores

Pressure Core KC151-3-11P

Pressure core KC151-3-11P (Figure KC151-1), recovered with the FPC from 227.08 mbsf at 160 bar, was imaged with the X-ray CT scanner, logged for gamma density in the MSCL-V, and logged in the MSCL-P using both the Geotek P-wave system and the Georgia Tech sensors (see separate Georgia Tech Report). The gamma density log showed a relatively uniform core, with slightly higher densities in the lower third of the core (Figure KC151-1). The P-wave velocity log showed somewhat higher velocities (1625 vs 1600 m/sec) in the same interval (Figure KC151-1). P-wave amplitudes were high throughout the core.

The core was stored under pressure in the cold for sub-sampling on shore. Prior to sub-sampling, the water surrounding the core was replaced by nitrogen. The core was sub-sampled under pressure. The top 5 cm of the core was trimmed off and archived. The interval 8.5-34.5 cm was transferred under pressure into a modified Parr vessel for transport to USGS Woods Hole for physical properties studies using the GHASTLI system. The Parr vessel was flushed with methane and reduced to 100 bar pressure before transport. The intervals 5-8.5 cm and 34.5-42.5 cm were depressurized and sent to Woods Hole so the investigators could examine the surrounding core material before opening the pressure vessel.

The interval 42.5-51 cm of the core was cut, depressurized, and archived. The interval 51-54 cm was transferred into a microbiological sub-sampling apparatus for microbiological studies at Cardiff University. The nitrogen surrounding the remaining core (54-90 cm, 46 cm total length) was replaced with water and the core was depressurized. Gas sub-samples were sent to USGS Menlo Park for analysis (see separate USGS Gas Report).

None of the rapidly depressurized core portions showed any evidence of hydrate or increased gas content. The hydrate content of this core is not yet known, but the log and visual evidence points to little or no hydrate.

Pressure Core KC151-3-13R

Pressure core KC151-3-13R, recovered with the HRC from 235.92 mbsf at 160 bar, was imaged with the X-ray CT scanner, logged for gamma density in the MSCL-V, and logged in the MSCL-P using both the Geotek P-wave system and the Georgia Tech sensors (see separate Georgia Tech Report). The gamma density log showed that the upper part of the core is more uniform than the lower part of the core which has some lower density intervals (Figure KC151-2). The P-wave velocity log showed a prominent high velocity spike (2074 m/s) at the midpoint in the core (Figure KC151-2), which may correspond to a thin vein of hydrate. There is no density evidence for a hydrate layer, either from the gamma density or an initial examination of the X-ray scans; if this velocity spike was caused by a hydrate vein, it must have been extremely thin.

The P-wave amplitude was distinctly lower below the velocity spike (Figure KC151-2) and may indicate the presence of microbubbles from partially dissociated dispersed hydrate. Bubble size and density would have been small, as good P-wave signals were still recorded in this interval. P-wave velocity was slightly lower in the bottom half of the core and is also consistent with small amounts of gas in the core. Destabilization of disseminated hydrate due to warming during core recovery could account for these results.

Following the logging, the core was depressurized and gas collected while being repetitively logged in the MSCL-V (Figure KC151-3). Gas was evolved from a point in the core corresponding to the high velocity spike and throughout the core below that point; very little gas was generated from the upper half of the core. Once the core was completely depressurized, it was repressurized to *in situ* pressure (140 bar) and re-logged in the MSCL-P (Figure KC151-4). The high velocity spike had disappeared and the lower portion of the core was completely disturbed, showing velocities near that of water. In contrast, the upper half of the core was relatively unchanged in velocity, with preservation of the basic characteristics.

The core was then cut into subsections for subsequent pore water analysis, which is ongoing (see separate Scripps Porewater Chemistry Report). A total volume of 7,894 ml of gas and 557 ml of liquid was given off during the depressurization process, corresponding to about 6.2 liters (gas only)

to 6.7 (gas and liquid) of methane. The 6.2 liters of methane is equivalent to about 30 cc of methane hydrate, or a hydrate content of approximately 4-5% by pore volume throughout the core.

The interpretation of Core KC151-3-13R was that the core had two distinct halves. There was little if any hydrate in the top half of the core: the top of the core had high P-wave amplitudes and generated very little gas during depressurization. In the bottom half of the core, hydrate was disseminated in the pore space: the lower half had low P-wave amplitudes, possibly from gas produced by hydrate dissociation during core recovery; generated gas during depressurization; and appeared significantly disturbed in the P-wave log taken after depressurization. Hydrate presence within this layer may have been influenced by the lower densities within the sediment. If the hydrate was confined to the low-P-wave-amplitude region of the core, the hydrate content would have been over 10% hydrate by pore volume.

It is possible that a thin, horizontal hydrate vein, no more than a millimeter thick, divided this core in two: this location in the core exhibited a spike in the P-wave velocity, could be seen generating gas during the depressurization, and had disappeared from the P-wave profile after depressurization. Because there is no conclusive evidence from the density data, however, this interpretation is tentative.

Pressure Core KC151-3-26R

Pressure core KC151-3-26R, recovered with the HRC from 383.13 mbsf at 180 bar, was imaged with the X-Ray CT scanner, logged for gamma density in the MSCL-V, and logged in the MSCL-P using the Geotek P-wave system. Variability in the gamma density and P-wave velocity mirrored one another (Figure KC151-5), and low velocity and density zones were also visible on the X-ray image. The variability in the core logs is a reflection of variations in the sediment, which may have been caused by coring disturbance of the rotary corer in the clay substrate. The low P-wave amplitudes seen in the upper and lower portions of the core may be due to microbubbles of gas formed by partial dissociation of disseminated hydrate (see Core KC151-3-13R).

Following the core logging, the core was depressurized while being repetitively logged in the X-Ray scanner (see separate Lawrence Berkeley X-ray Report). A total volume of 2491 cc of gas and 566 cc of liquid was given off during the depressurization process, corresponding to about 1.4 liters (gas only) to 1.7 liters (gas and liquid) of methane. This is equivalent to 1-2 cc of methane hydrate, or a hydrate content of about 0.5% by pore volume.

FHPC & FC Cores

Temperature Measurement via Infrared Logging

The temperatures of each of the cores from Hole KC151-3 were monitored in order to detect any signs of hydrate dissociation, in the form of localized, centimeter-scale thermal anomalies or large cold zones that might span multiple cores. The infrared camera track provided a continuous record of the liner temperature, and temperature probes placed in the center of section ends recorded the actual core temperatures (Figures KC151-6, -7, -8, -9).

Hole KC151-3 contained the only obvious thermal anomaly likely to be associated with gas hydrate on the entire expedition. Core KC151-3-15C (Figure KC151-10), taken with the Fugro Corer, contained a 2.2 C° thermal anomaly centered 136.5 cm below the top of the core. This anomaly was similar in morphology and magnitude to nodular or vein hydrate seen on ODP Leg 204 (Shipboard Scientific Party, 2003).

No other cores showed thermal anomalies likely to be hydrate, either centimeter-scale or whole-core scale. Periodic thermal variation in the top three cores was of unknown origin but was potentially an artifact of data collection. Core KC151-3-19H (Figure KC151-9) was relatively cool, but also was extremely expansive. FHPC and FC cores were distinctly different in this respect. FHPC cores tended to have a dry contact between the core and the liner, while the FC core-liner contact tended to be quite wet. Because the FHPC cores were dry, they created a seal against the liner, which allowed cores to be pushed aside by gas expansion, forming voids within the core. FC cores may have experienced the same amount of gas expansion (and cooling) but the gas could escape along the sides of the core. FC cores therefore had a much more uniform infrared thermal profile. This uniform background was one reason that the thermal anomaly in Core KC151-3-KC could be identified and differentiated from thermal anomalies associated purely with gas expansion.

The Keathley Canyon site had a steeper thermocline than that at Atwater Valley (Figure KC151-11). The Adara temperature shoe attached to the FHPC on Core KC151-3-3H (Figure KC151-12) and the temperature logger on Core KC151-3-11P (Figure KC151-13) showed that the warming for Keathley Canyon cores, while possibly less drastic than that at Atwater Valley, was still substantial and probably enough to mask all but the most intense thermal anomalies. Thermal anomalies, like hydrate itself, are ephemeral beasts: the absence of thermal anomalies does not indicate absence of gas hydrate! The pressure cores taken at Keathley Canyon indicated that there was gas hydrate in the

sediment column, but at levels of hydrate at 1-5% of pore volume, the thermal anomaly created by the dissociation of this amount of hydrate could easily be erased during the pipe trip.

MSCL-S Measurements

Cores from Hole KC151-3 were logged with the MSCL-S, using the gamma density, P-wave velocity, electrical resistivity, and magnetic susceptibility sensors (Figure KC151-14). As at the previous sites, all data are affected by gas expansion below the sulfate-methane interface at about 7 mbsf, the P-wave and resistivity data especially so. The density and magnetic susceptibility data show a number of distinct features that might be used, in conjunction with sedimentological observations, to describe sedimentary units. The density maximum near 230 mbsf was also seen on the LWD logs for Hole KC151-2.

The composite plot for this hole also incorporates the measurements made on the pressure cores at full *in situ* pressure in the MSCL-V and MSCL-P. The densities are slightly higher in the pressure cores, as expected, as there is no gas expansion and therefore these are truer indications of *in situ* densities. The only P-wave velocities below the sulfate-methane interface are from the pressure cores, and a very high velocity peak that is tentatively interpreted as hydrate is not shown on Figure KC151-14.

MSCL-XYZ Measurements

Cores from Hole KC151-3 were imaged in the MSCL-XYZ. Most notable in the images were generally subhorizontal millimeter-thick white horizons (e.g., Figure KC151-15), which are presumably carbonate layers. Color spectra and magnetic susceptibility measurements, made with a point sensor, were also taken (Figure KC151-16). High frequency variations in the magnetic susceptibility may aid in the sedimentological description of the cores.

Measurement of naturally-occurring gamma radiation was made to aid in correlation with the LWD logs from nearby Hole KC151-2. Because the natural gamma measurements collected on the split core were collected at a much higher spatial resolution than the downhole measurements, the core data were smoothed for comparison (Figure KC151-17). The vertical offset in the strata between the two holes appears to be between 0-7 meters and varies downhole; some of the variation may be due to curatorial issues with short cores. However, this does not mean that all features in the two holes should be assumed to be similar. One of the most notable features of the LWD logs from KC151-2 was the high resistivity layers, which were dipping at extremely high angles and are likely to cross strata.

ROV Push Cores

MSCL-S Measurements

An ROV push core, Core KC151-2PC, collected from Atwater Valley in short fiberglass liners was logged with the MSCL-S (Figure KC151-18). This core was taken specifically for measurements of physical properties (see separate Fugro Physical Properties Report), and the MSCL-S data was meant to complement these measurements. The resistivity data is adversely affected by the core end effects and is not calibrated, however, all other data is calibrated and valid.

References

Ford, K.H., Naehr, T.H., Skilbeck, C.G., and the Leg 201 Scientific Party, 2003. The use of infrared thermal imaging to identify gas hydrate in sediment cores. In D'Hondt, S.L., Jørgensen, B.B., Miller, D.J., et al., Proc. ODP, Init. Repts., 201, 1-20 [CD-ROM]. Available from: Ocean Drilling Program, Texas A&M University, College Station TX 77845-9547, USA.

Schultheiss, P.J., Francis, T.J.G., Holland, M., Roberts, J.A., Amann, H., Thjunjoto, Parkes, R. J., Martin, D., Rothfuss, M., Tyunder, F., & P.D. Jackson, 2005. Pressure Coring, Logging and Sub-Sampling with the HYACINTH System, in "New ways of looking at sediment cores and core data", Geological Society Special Publication, in press.

Shipboard Scientific Party, 2003. Explanatory notes. In Tréhu, A.M, Bohrmann, G., Rack, F.R., Torres, M.E., et al., Proc. ODP, Init. Repts., 204, 1-102 [CD-ROM]. Available from: Ocean Drilling Program, Texas A&M University, College Station TX 77845-9547, USA.

Figure INT-1. Moussy core, showing frothy, wet texture indicative of hydrate dissociation. Core at top, containing massive hydrate as well, is from ODP Leg 204. Core at bottom is from the GOM-JIP, ATM1-5H-2, 70-75cm.

Figure EXPL-1. Fugro Pressure Corer (FPC) being deployed on the *Uncle John* during the GOM-JIP Expedition.

Figure EXPL-2. HYACE Rotary Corer (HRC) being deployed on the *Uncle John* during the GOM-JIP Expedition.

Figure EXPL-3. HYACINTH Storage Chamber, connected to the Shear Transfer Chamber & Manipulator (top) and MSCL-P (bottom) in the 40-foot refrigerated core processing container on the *Uncle John* during the GOM-JIP Expedition.

Figure EXPL-4. HYACINTH Storage Chamber in place and ready to be logged in the MSCL-V, inside the 20-foot refrigerated logging container on the *Uncle John* during the GOM-JIP Expedition.

Figure EXPL-5. The infrared imaging track (red arrows) set up along the length of the 40-footcore processing container, above the core rack. The track was driven and the data acquired and displayed by the Geotek Infrared Imaging software.

Figure EXPL-6. The FLIR ThermaCam SC2000 camera, mounted on its wheeled skate and covered with black felt to cut out reflected infrared radiation.

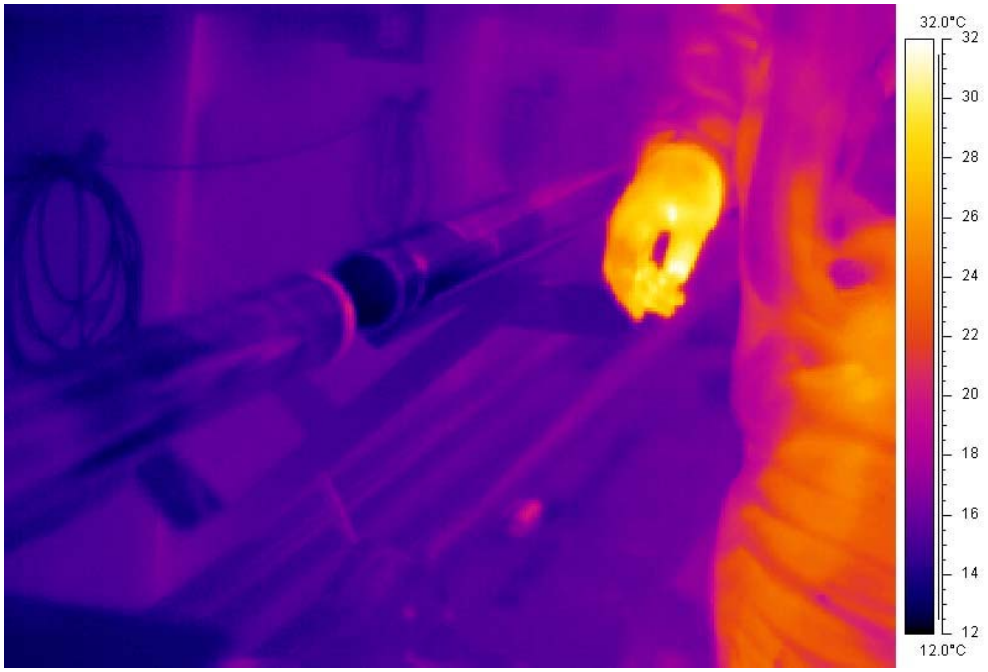

Figure EXPL-7. Scientists were the largest source of extraneous thermal radiation in the core processing container.

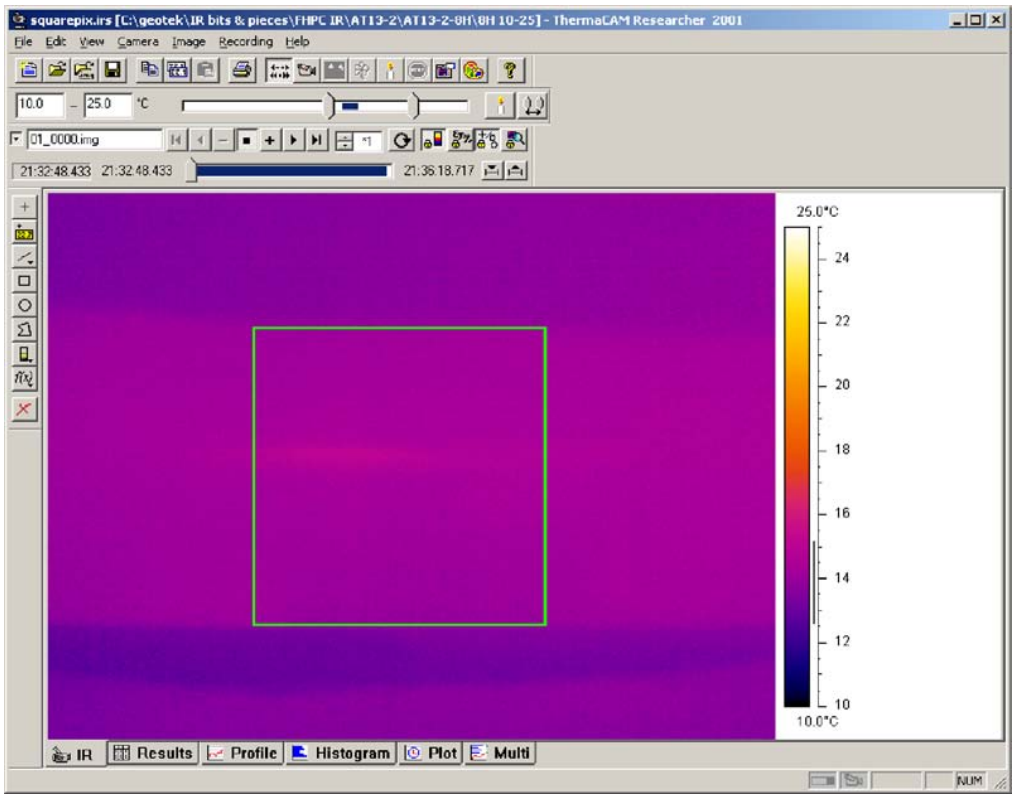

Figure EXPL-8. Sample infrared image, viewed in ThermaCam Researcher, collected automatically by the Geotek Infrared Imaging Software in conjunction with ThermaCam Researcher Software (FLIR Systems). The portion of the image in the central box was used to generate the composite image.

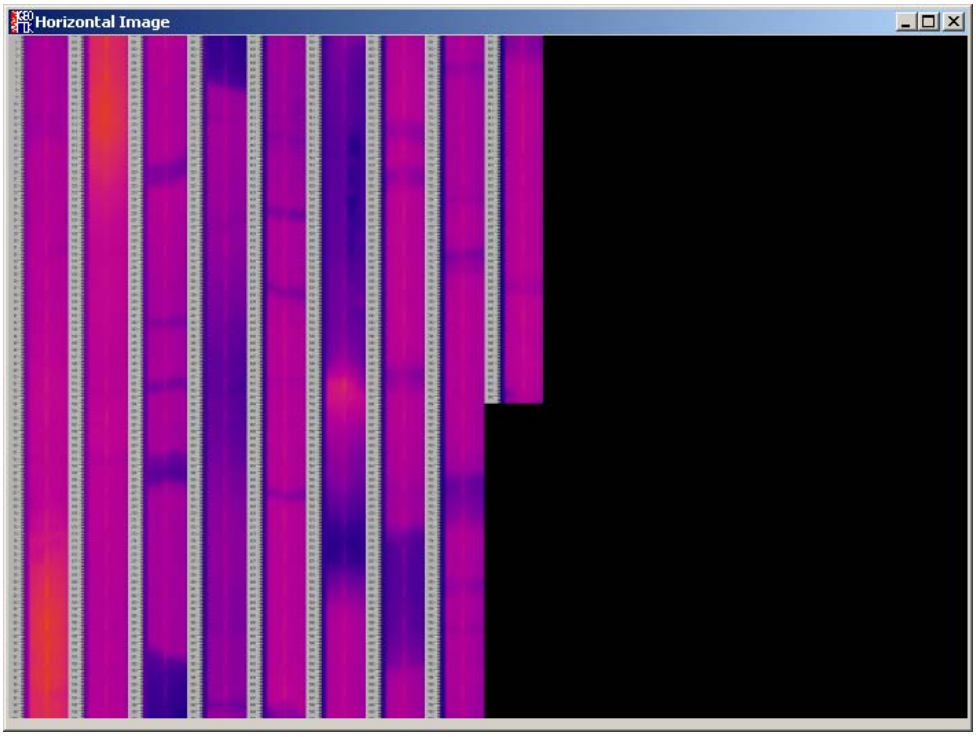

Figure EXPL-9. Composite infrared image of entire core, with ruler, generated by the Geotek Infrared Imaging system in real time.

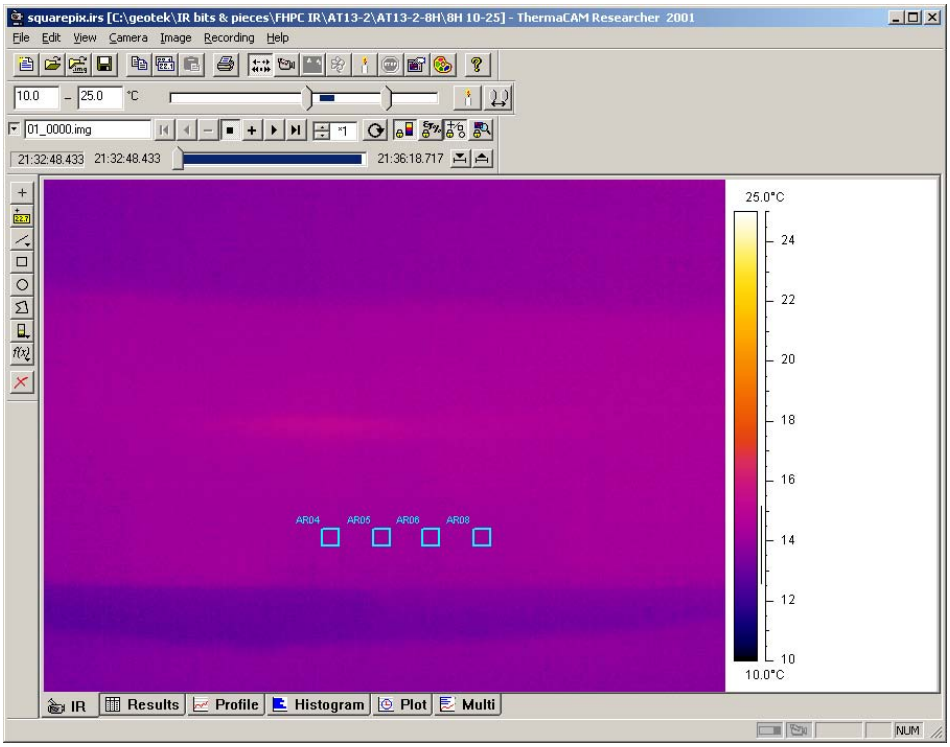

Figure EXPL-10. Screenshot of ThermaCam Researcher session used to extract data from the core image. The location of the squares is offset from the center of the core to avoid the reflection directly beneath the camera, which raises the apparent temperature by approximately 0.5˚C.

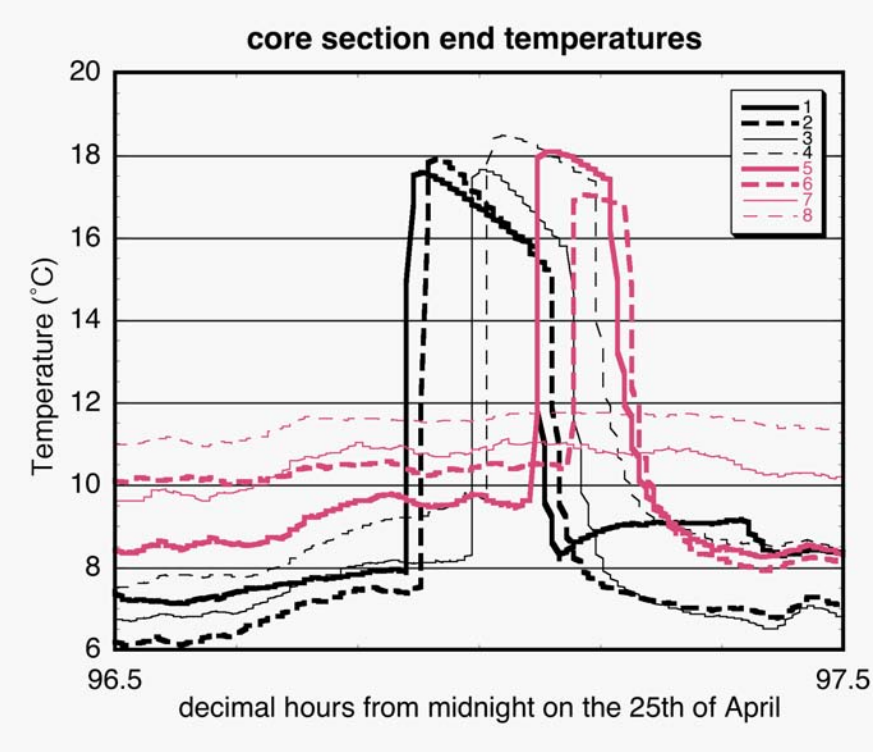

Figure EXPL-11. Sample data from temperature probes inserted routinely into core section ends. Temperatures were picked from maxima in data.

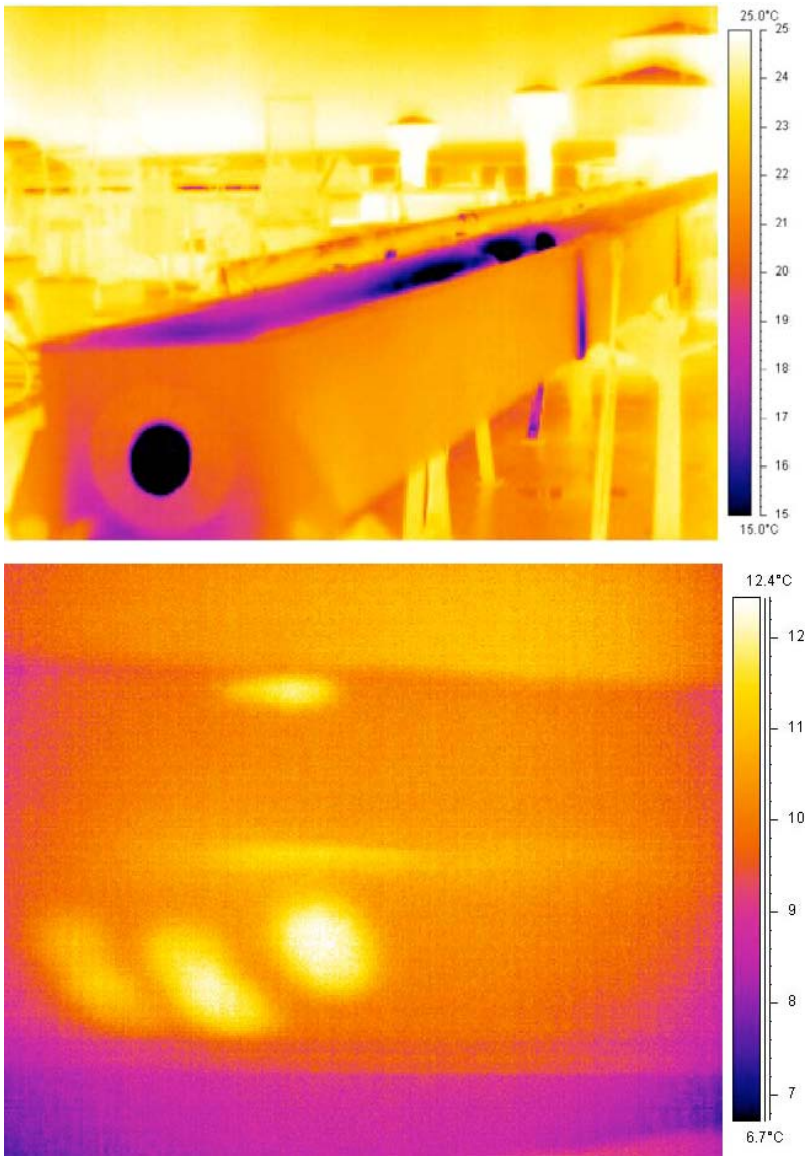

Figure EXPL-12. Infrared thermal images of (at top) the ice trough, half-filled with ice and (at bottom) a core that was recently handled by a gloveless individual. Both ice and people can change the temperature of cores and potentially disturb remnant thermal anomalies from gas hydrate dissociation.

Figure EXPL-13. MSCL-S inside the 20-foot unrefrigerated logging container on the *Uncle John* during the GOM-JIP Expedition.

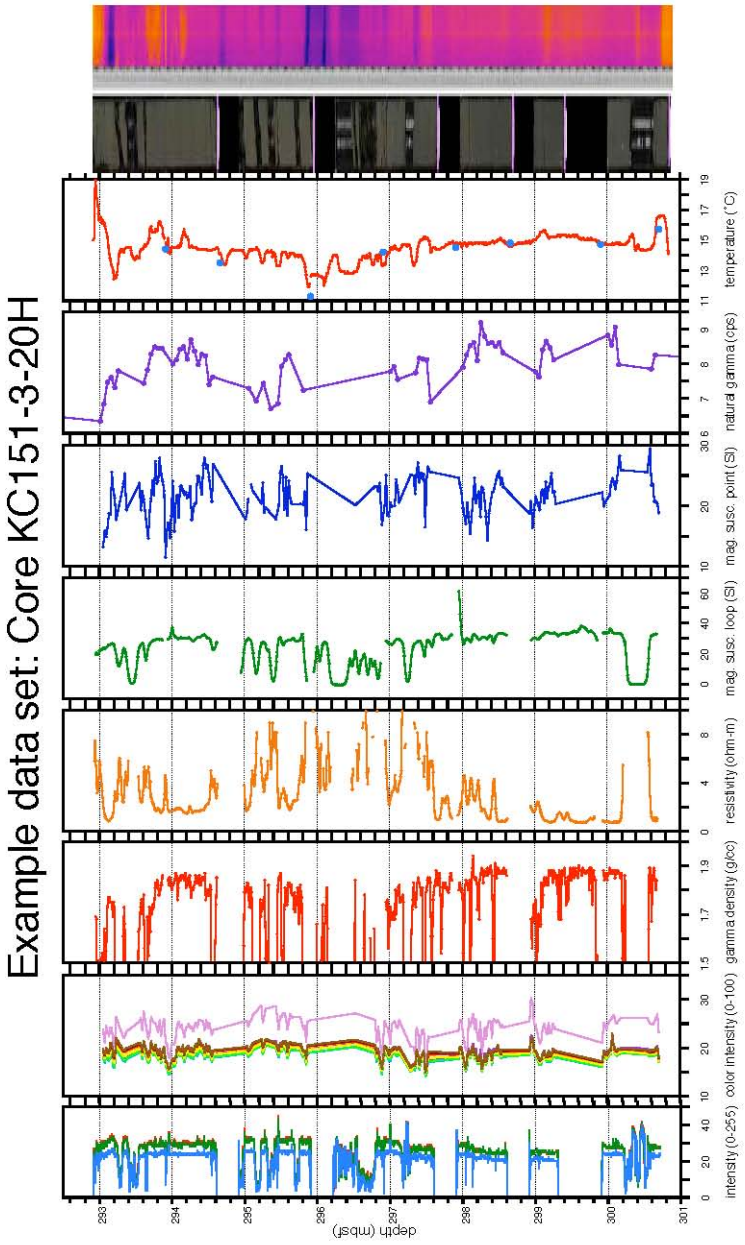

Figure EXPL-14. Complete data set for Core KC151-3-20H, showing influence of gas expansion on data. From left, RGB data from line scan image, spectral color data from Minolta color spectrophotometer, gamma density, resistivity, magnetic susceptibility (loop sensor), magnetic susceptibility (point sensor), natural gamma radioactivity, temperature, line scan image, and infrared image.

Figure EXPL-15. MSCL-P with Geotek P-wave Central Measurement Chamber in place (yellow arrow). The Georgia Tech measurement chamber (not in use) is sitting behind the Geotek CMC.

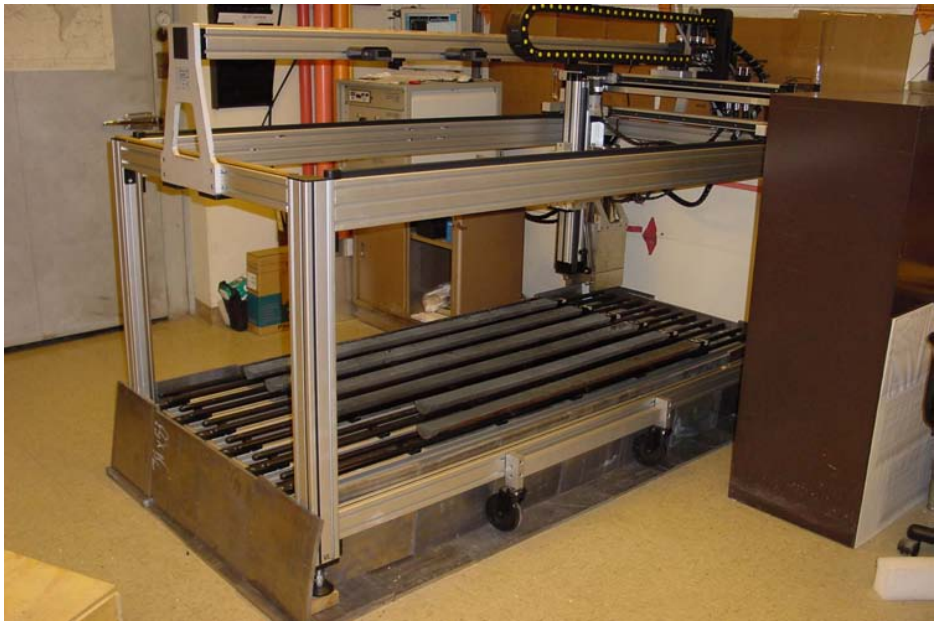

Figure EXPL-16. MSCL-XYZ installed in the DSDP West Coast Repository at the Scripps Institution of Oceanography, where the split cores from the GOM-JIP were logged. The MSCL-XYZ is configured for natural gamma measurements in this photo.

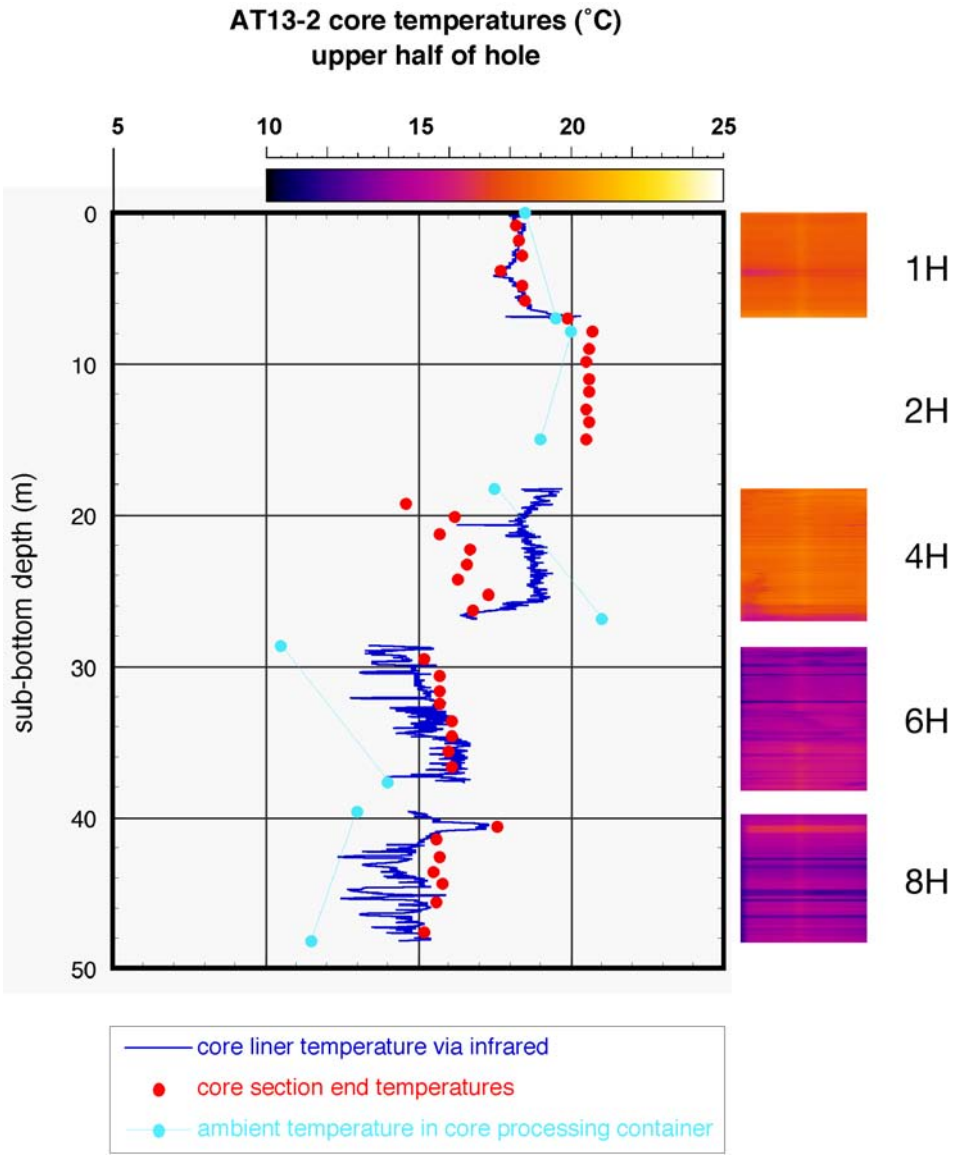

Figure AT-1. Plot of temperature data from infrared imaging, which takes the temperature of the core liner, and from direct measurement of the center of the core at core section ends for the top of Hole AT13-2. Two-dimensional infrared image is shown to the right of the plot.

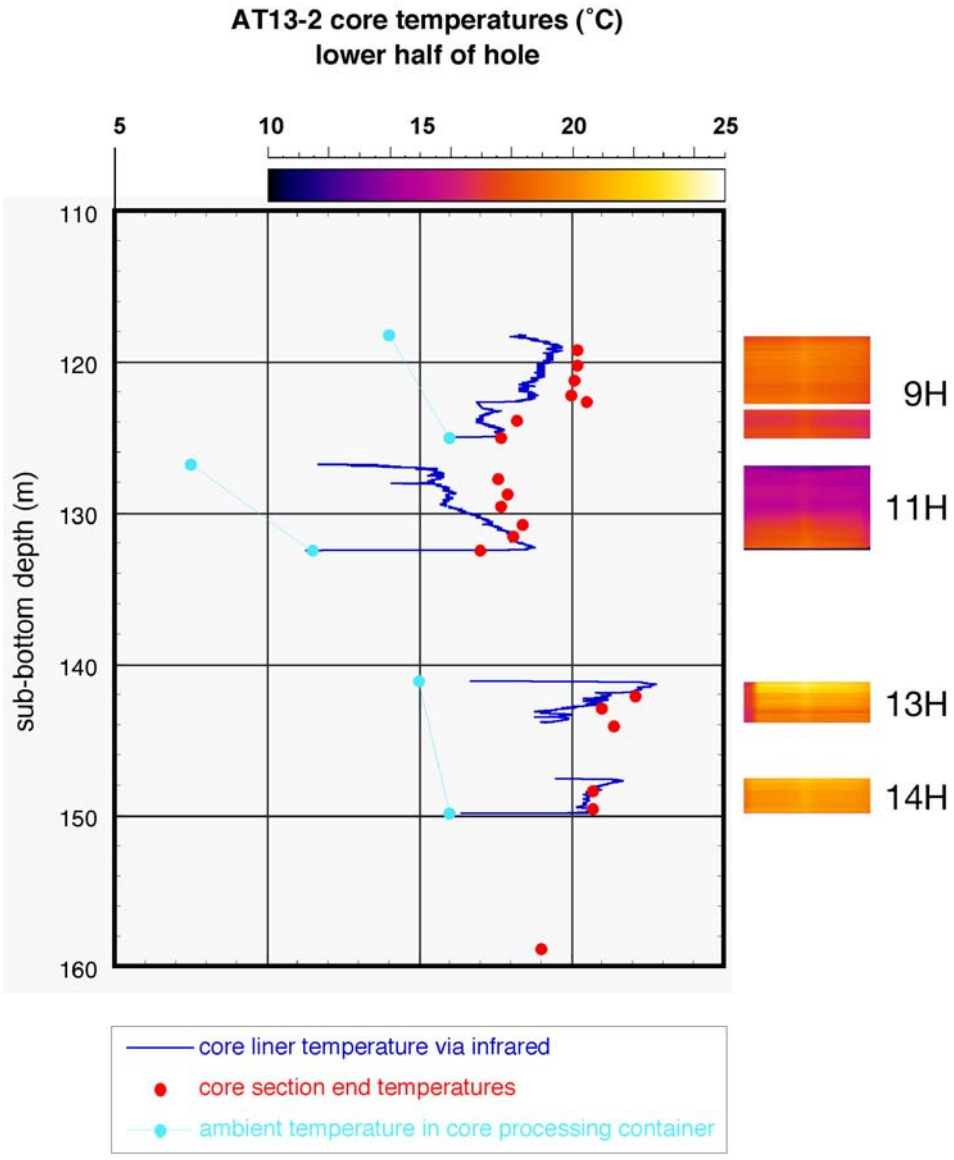

Figure AT-2. Plot of temperature data from infrared imaging, which takes the temperature of the core liner, and from direct measurement of the center of the core at core section ends for the bottom of Hole AT13-2. Two-dimensional infrared image is shown to the right of the plot.

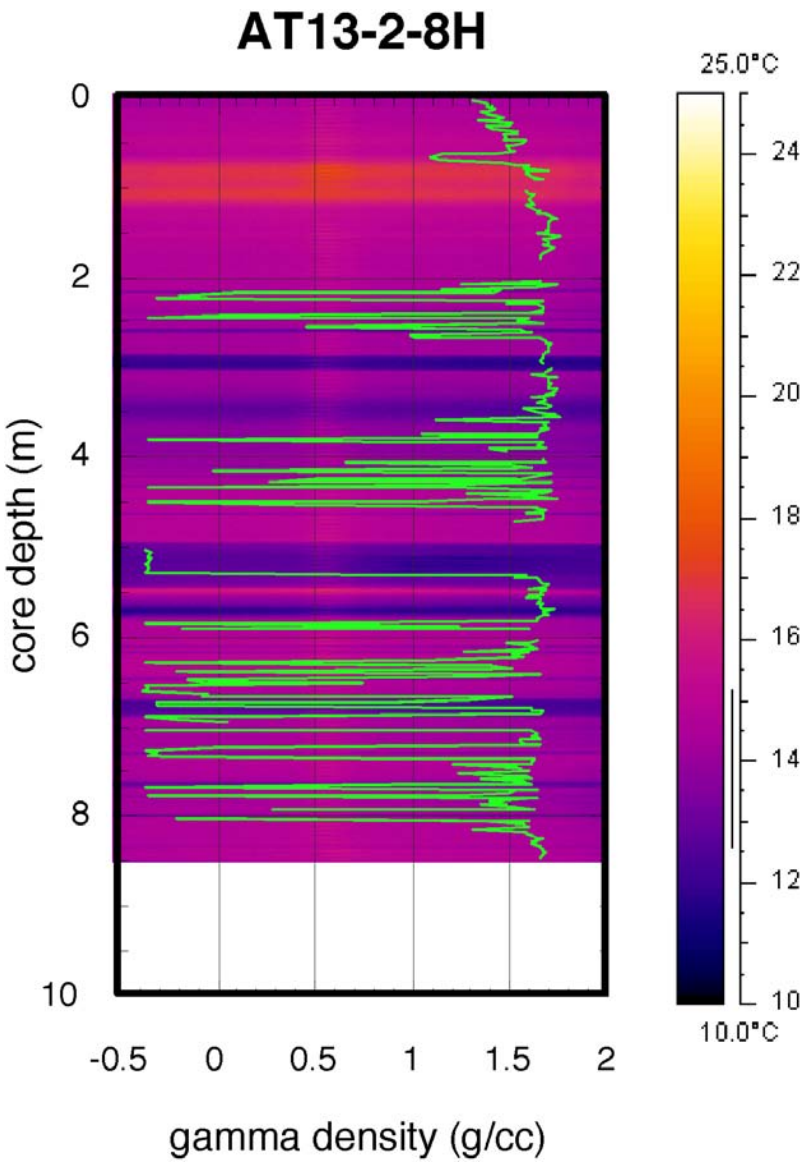

Figure AT-3. Gamma density (green line) and infrared image for Core AT13-2-8H. Sharply bounded cold regions are voids, but the voids had shifted by the time the gamma density is measured. Gamma density was not calibrated for air, so empty liner appears to have negative densities.

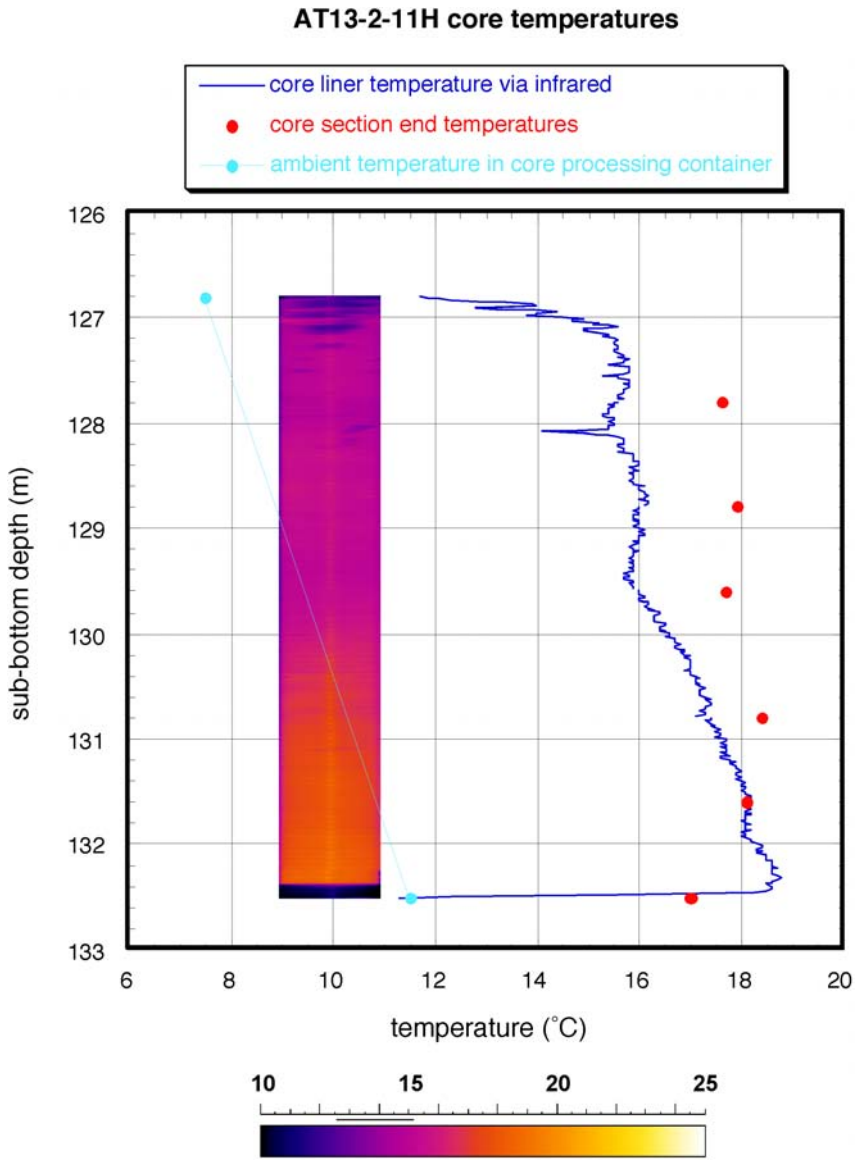

Figure AT-4. Temperature data for Core AT13-2-11H, including infrared image. Internal temperatures and core liner temperatures from infrared scanning did not match due to handling of the core.

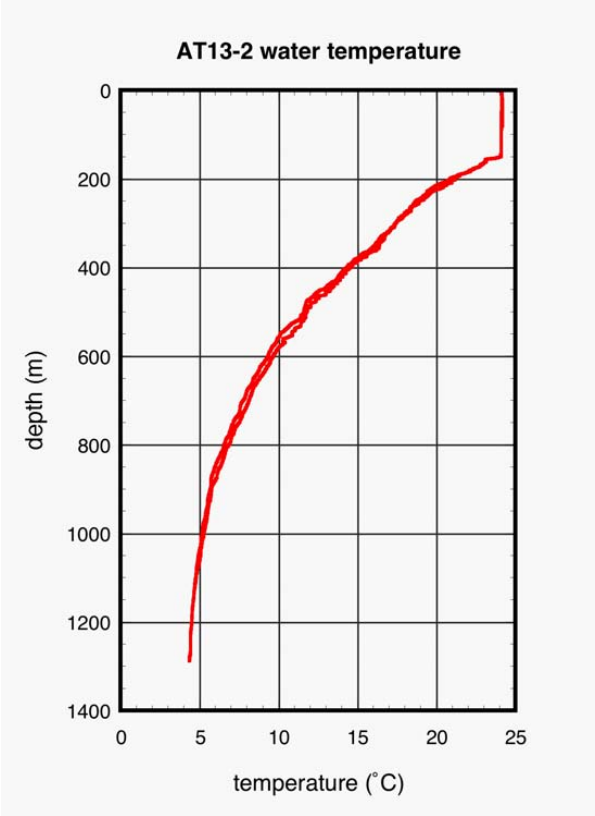

Figure AT-5. Temperature data from the Seabird CTD cast over Site AT13.

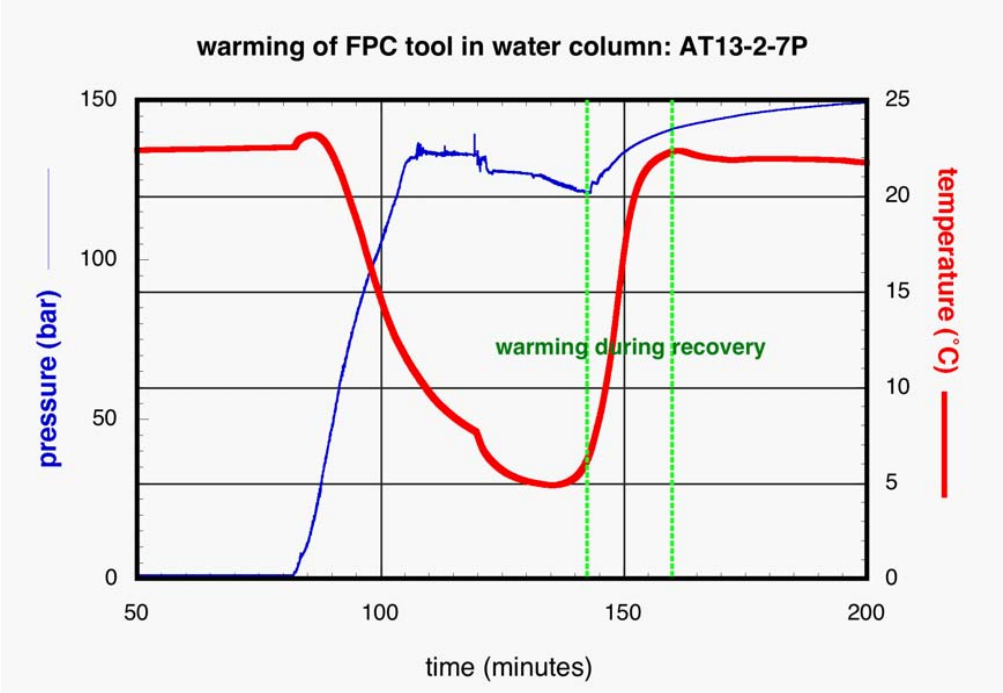

Figure AT-6. Temperature and pressure data versus time for Core AT13-2-7P. The retrieval of the tool up the drill pipe is bounded by green dashed lines.

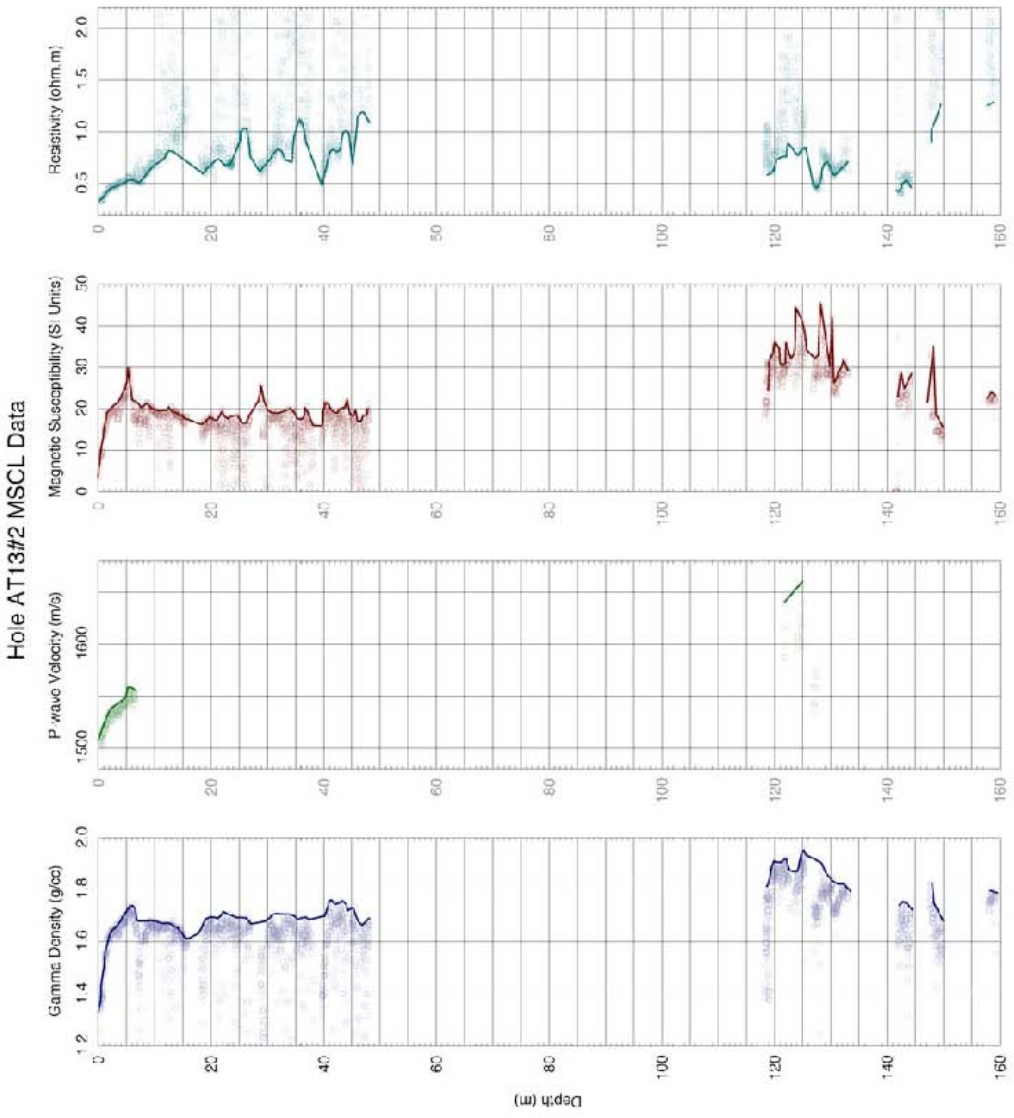

Figure AT-7. MSCL-S data, including gamma density, P-wave velocity, magnetic susceptibility, and electrical resistivity, for Hole AT13-2.

Figure AT-8. Line scan color image taken with the MSCL-XYZ using the Geoscan camera of a typical core section seen during the GOM-JIP Expedition (Section AT13-2-4H-5): clay with gas expansion voids. Pixels are 100 microns on a side. Color fringing on edges of image results from registration of camera CCDs.

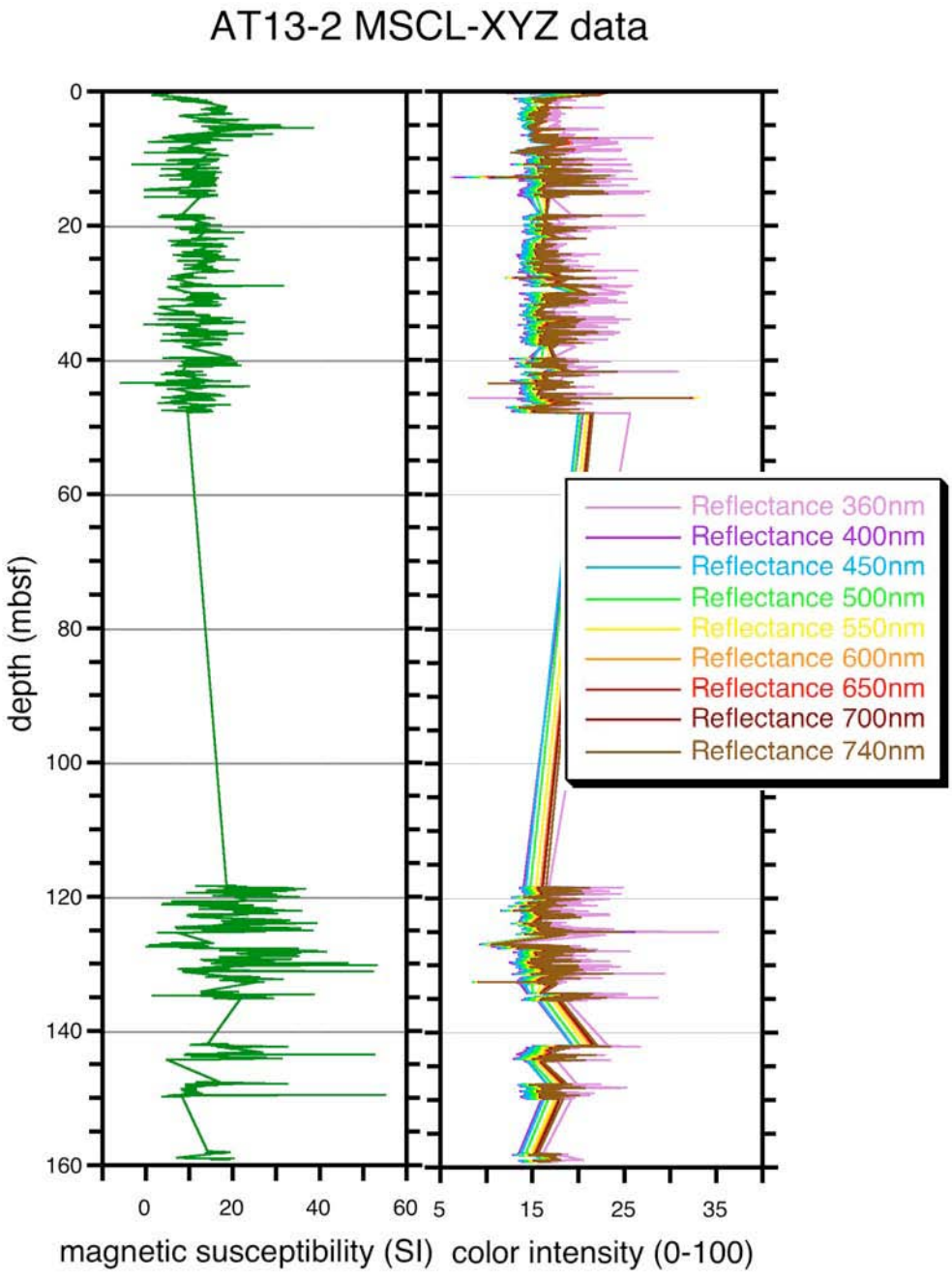

Figure AT-9. MSCL-XYZ data summary plot, including magnetic susceptibility and color spectrophotometry, for Hole AT13-2.

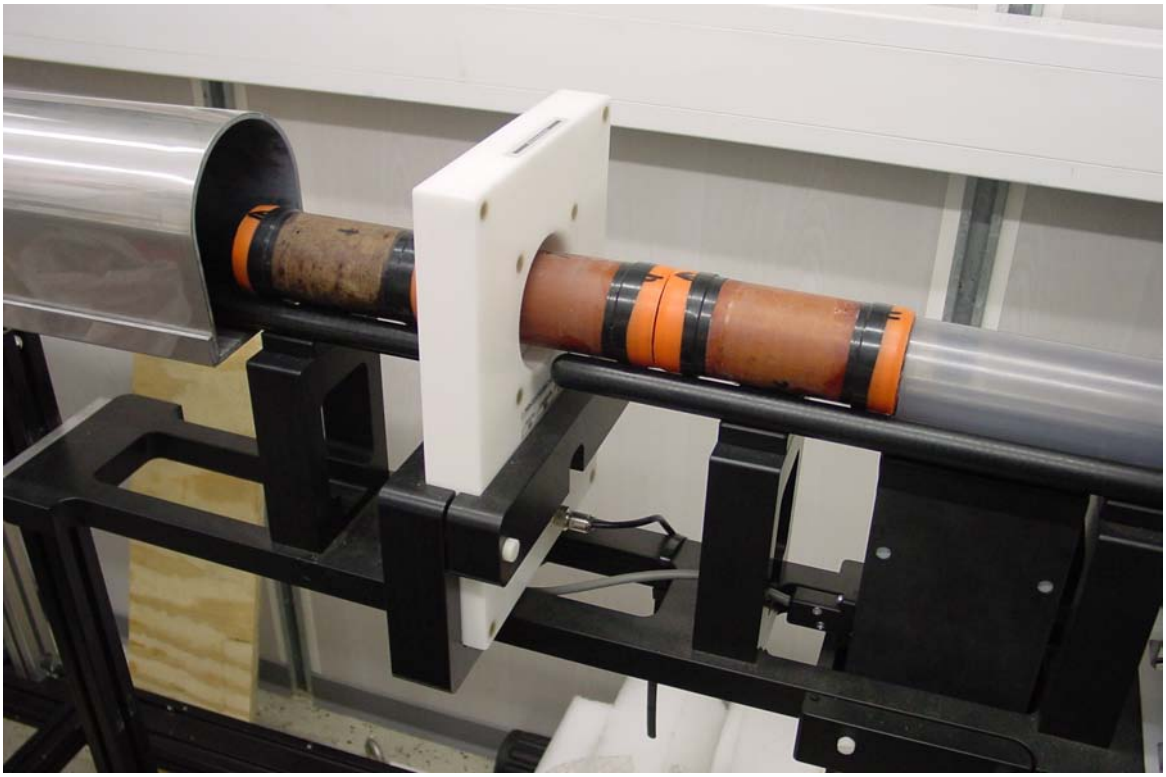

Figure AT-10. ROV push core AT14-7PC, collected in fiberglass liner, in the MSCL-S. Small fiberglass core sections had end-caps taped on for logging to prevent the core from oozing out of the liner.

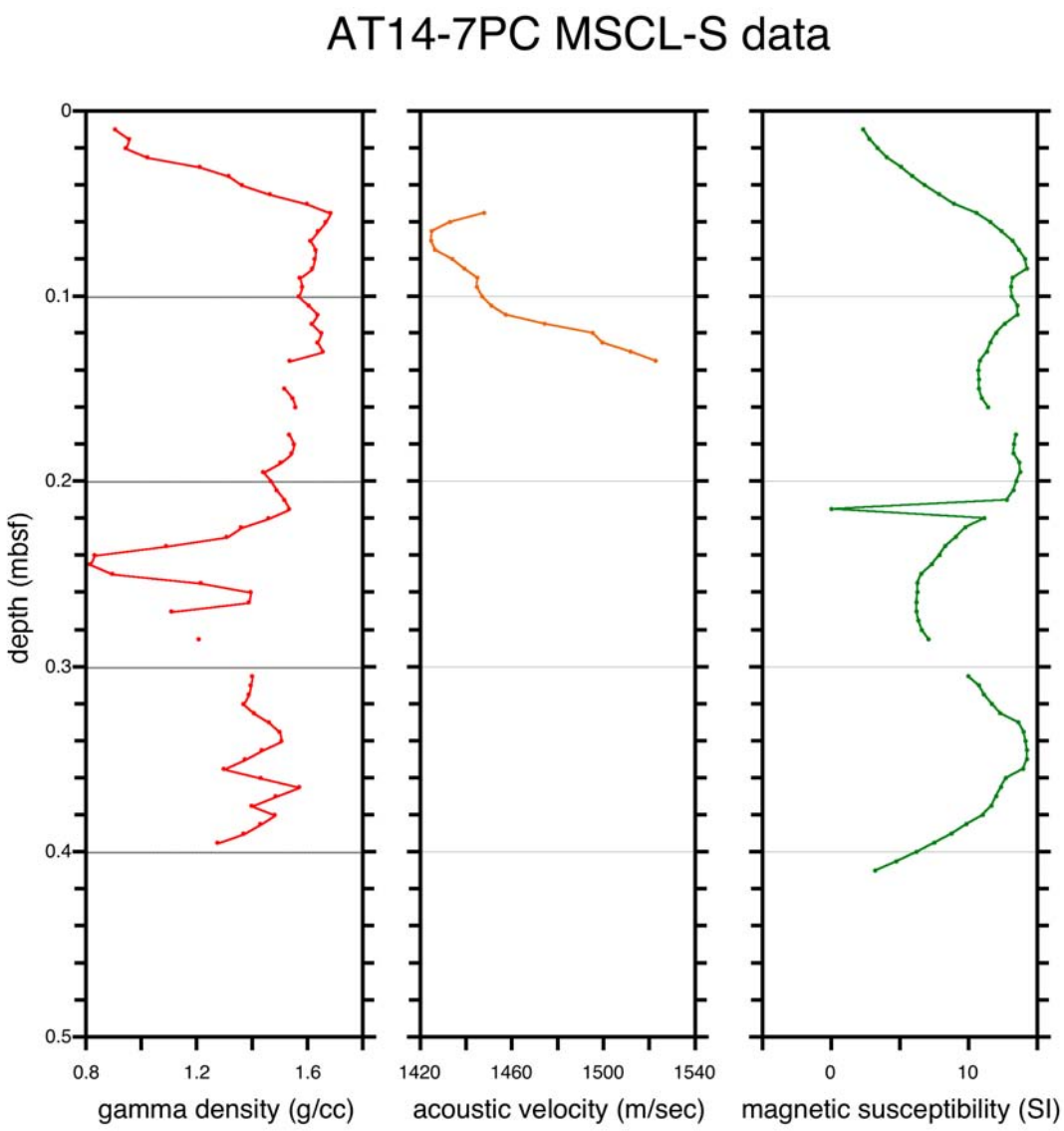

Figure AT-11. MSCL-S data summary plot, including gamma density, P-wave velocity, and magnetic susceptibility, for push core AT14-7PC.

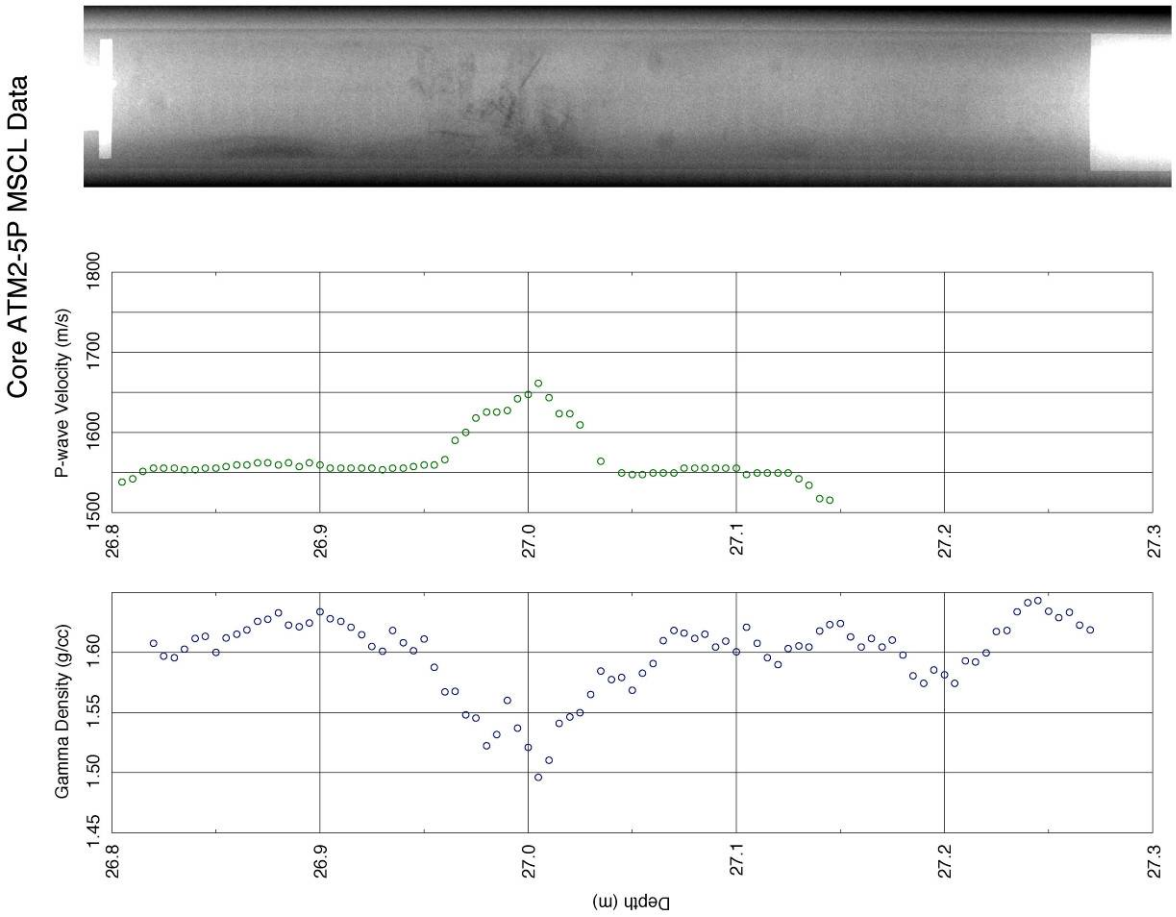

Figure ATM-1. Data from pressure core ATM2-5P, collected from 26.82 mbsf at a pressure of 130 bar. Figure shows gamma density data, collected in the MSCL-V; P-wave velocity, collected in the MSCL-P; and linear X-ray scan, collected in the X-ray CT scanner. Low density/high velocity zone at 27 cm core depth, corresponding to odd X-ray texture, may be a hydrate-bearing layer.

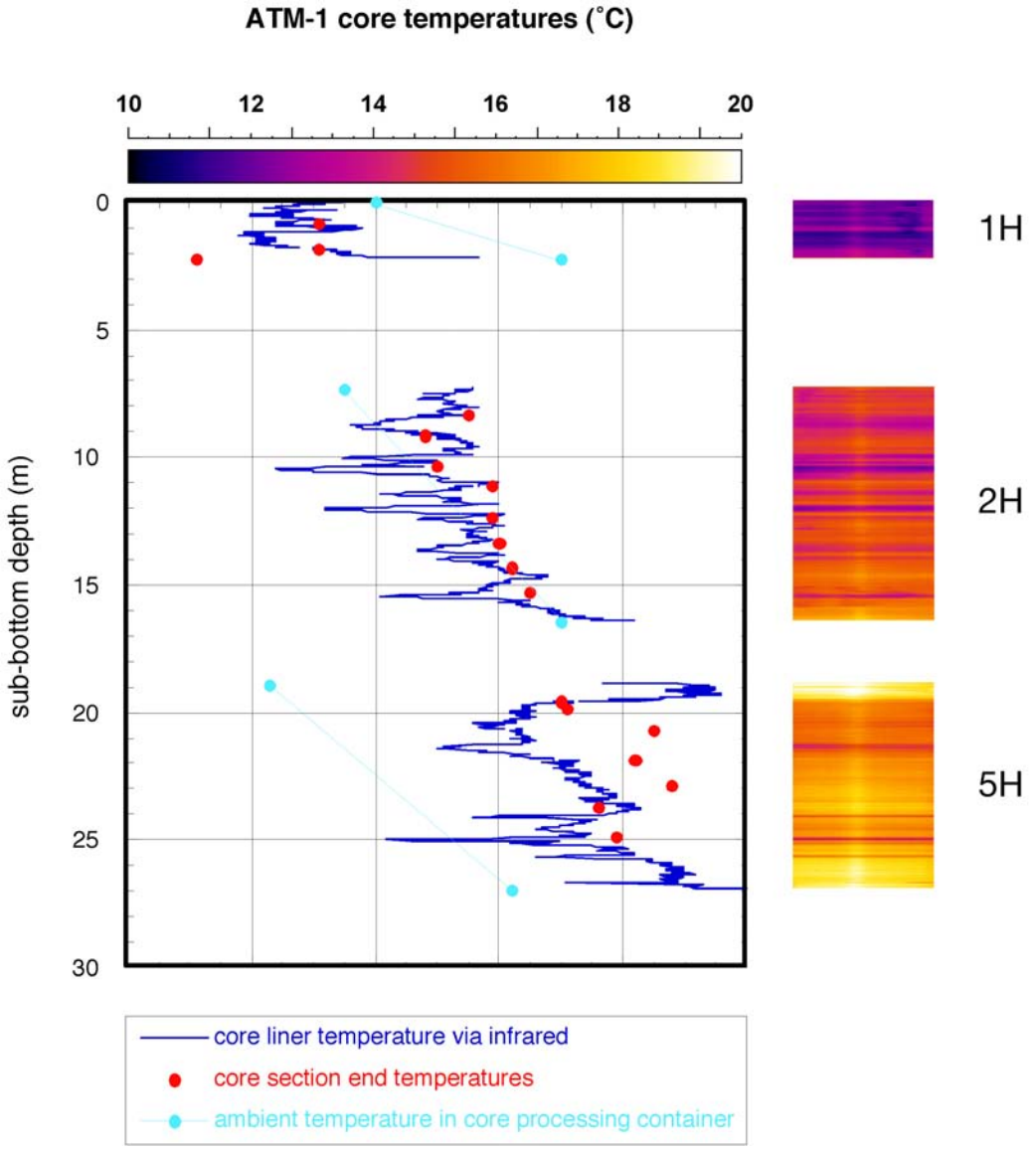

Figure ATM-2. Plot of temperature data from infrared imaging, which takes the temperature of the core liner, and from direct measurement of the center of the core at core section ends for the top of Hole ATM1. Two-dimensional infrared image is shown to the right of the plot.

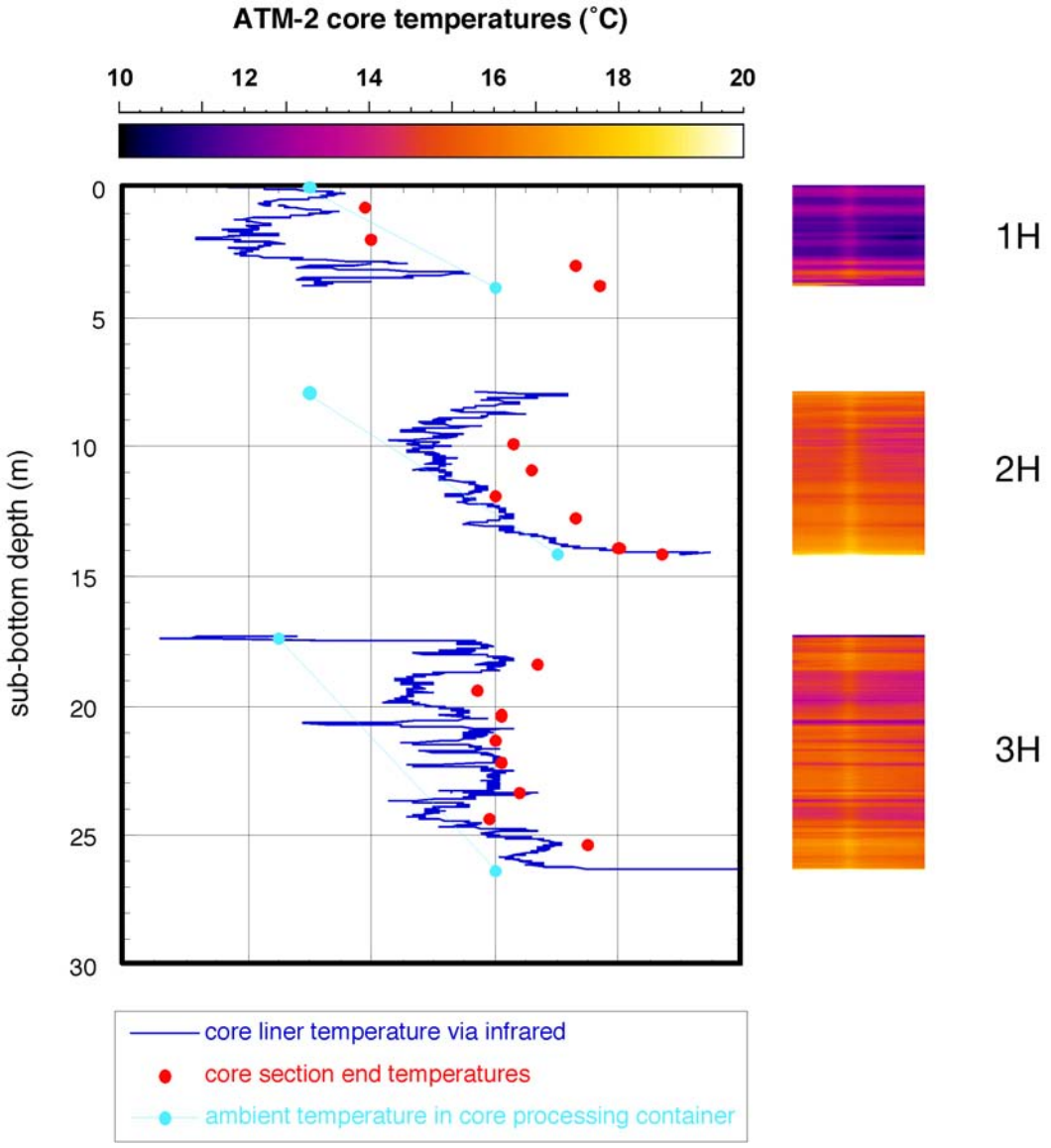

Figure ATM-3. Plot of temperature data from infrared imaging, which takes the temperature of the core liner, and from direct measurement of the center of the core at core section ends for the top of Hole ATM2. Two-dimensional infrared image is shown to the right of the plot.

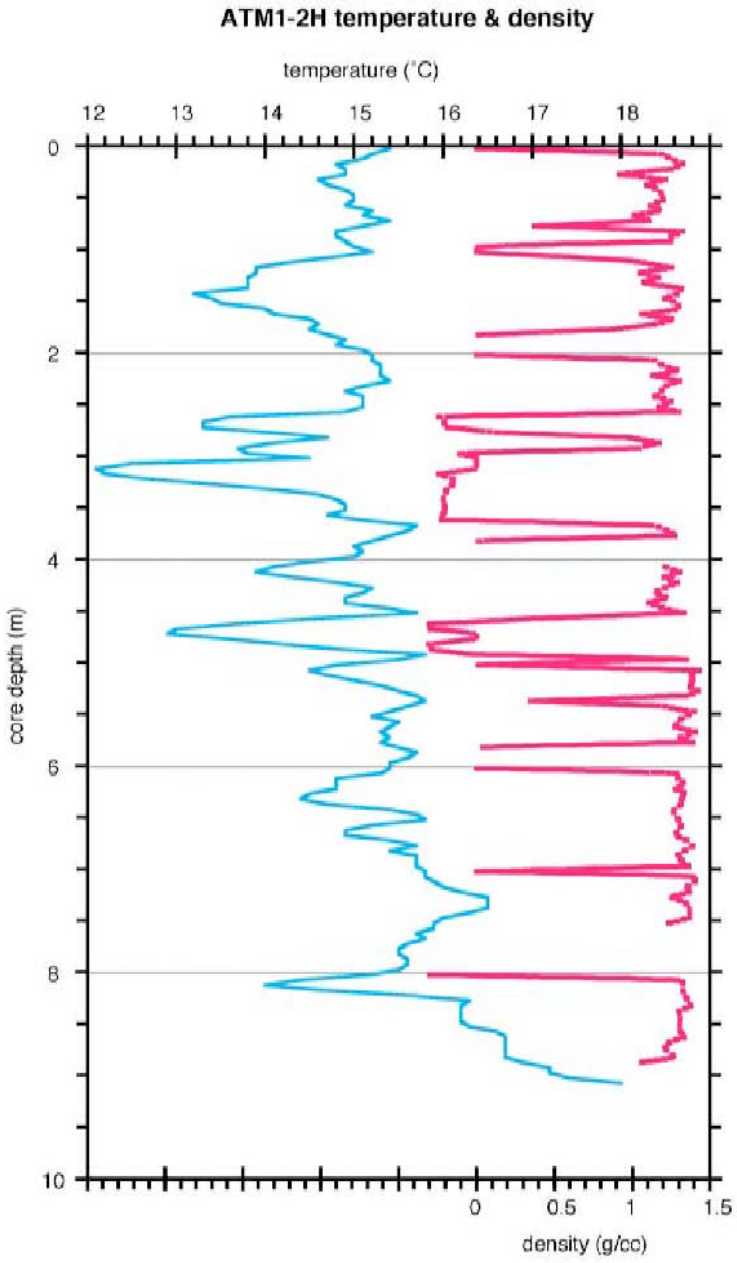

Figure ATM-4. Plot of gamma density and infrared-derived temperature for core ATM1-2H, showing difficulty in distinguishing cold regions that correspond to voids from cold regions that correspond to hydrate. Voids had shifted an unknown distance between the two measurements.

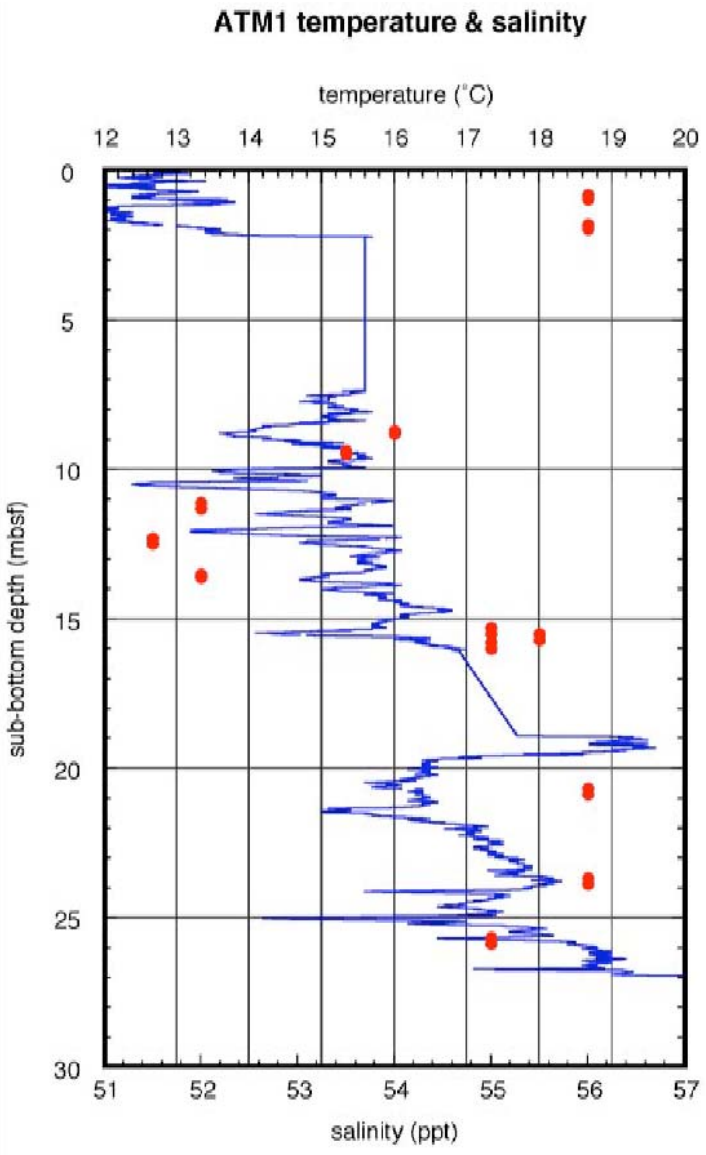

Figure ATM-5. Temperature from infrared track (blue) and pore water salinity (red) for Hole ATM1. Freshening trend from 8-15 mbsf is not reflected in the recorded thermal anomalies.

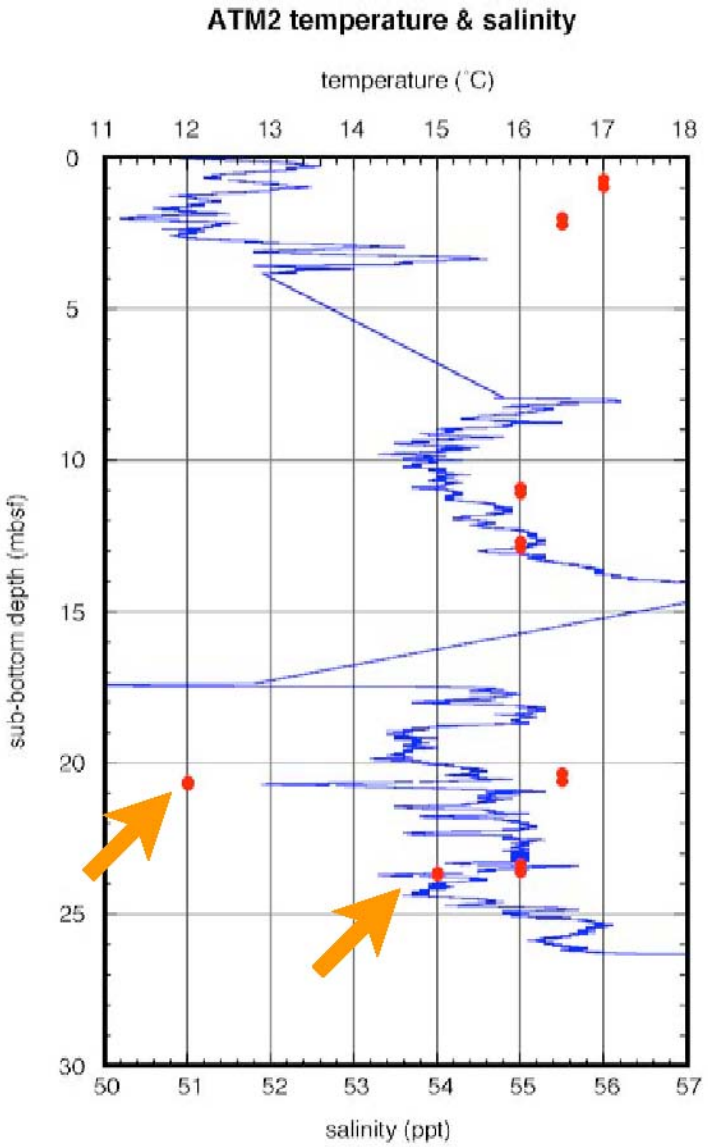

Figure ATM-6. Temperature from infrared track (blue) and pore water salinity (red) for Hole ATM2. The two pore water freshening anomalies in bottom core (arrows; ATM2-3H) may correspond to negative thermal anomalies.

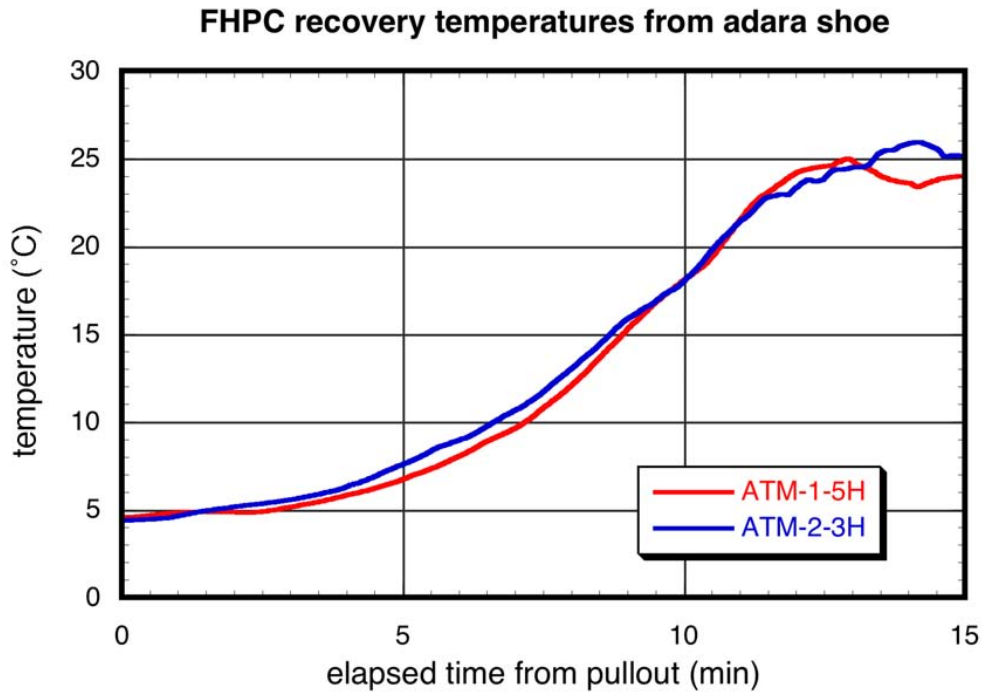

Figure ATM-7. Temperature data from the temperature shoe fitted on the FHPC for cores ATM1-5H and ATM2-3H.

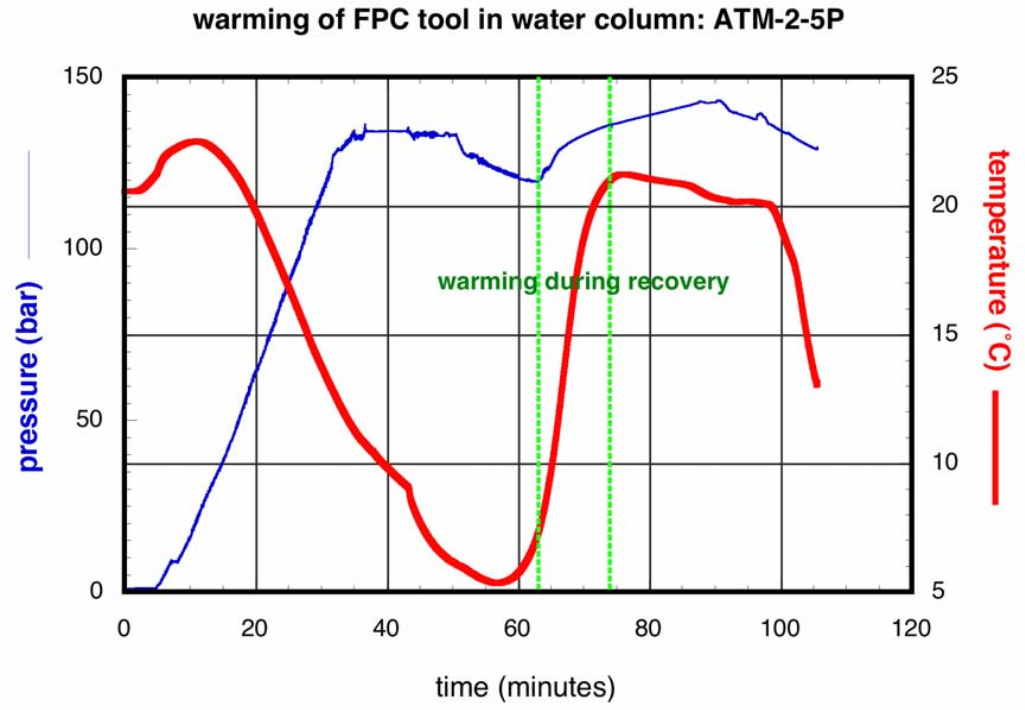

Figure ATM-8. Temperature and pressure data versus time for Core ATM2-5P. The retrieval of the tool up the drill pipe is bounded by green dashed lines.

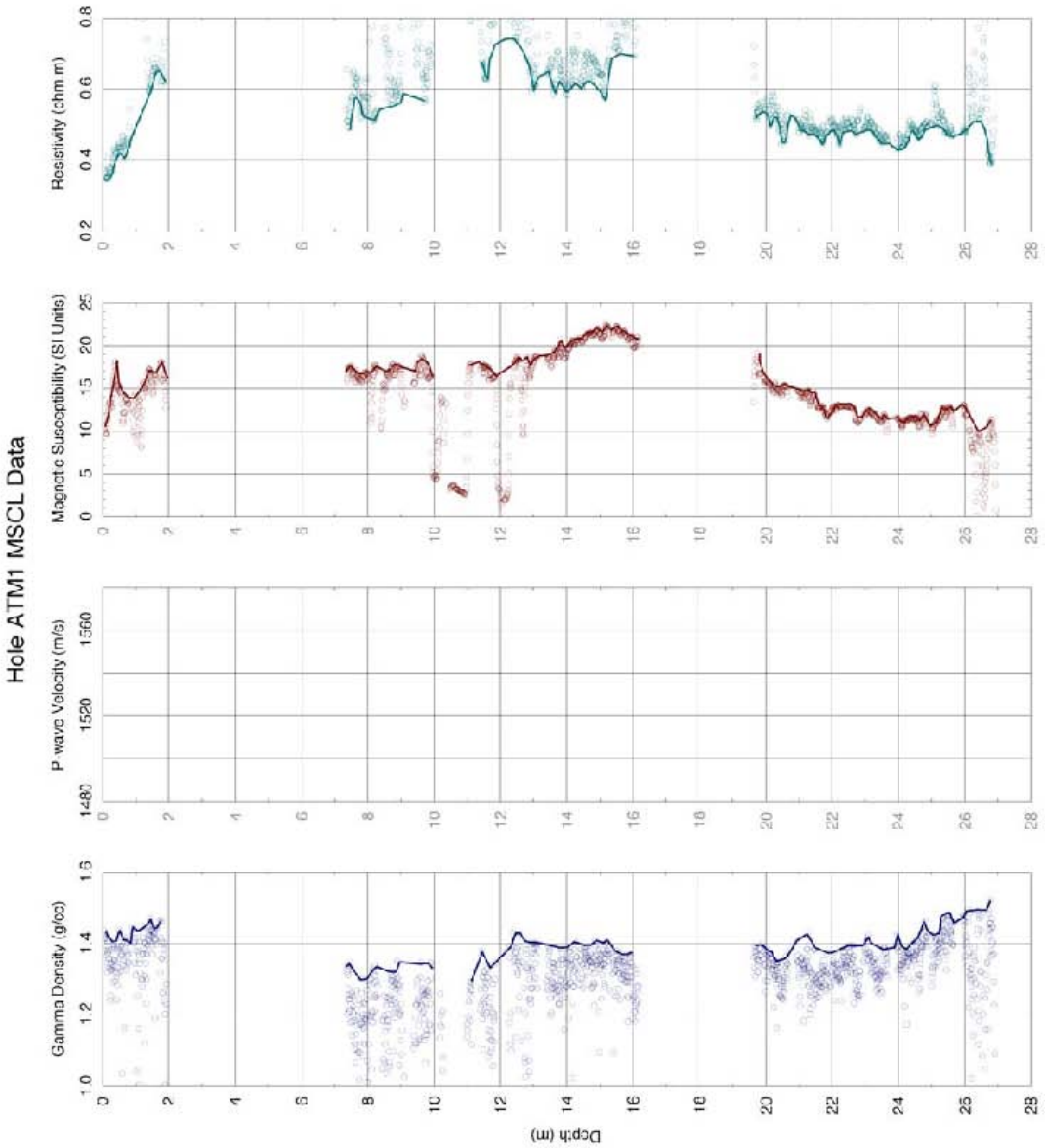

Figure ATM-9. MSCL-S data, including gamma density, P-wave velocity, magnetic susceptibility, and electrical resistivity, for Hole ATM1.

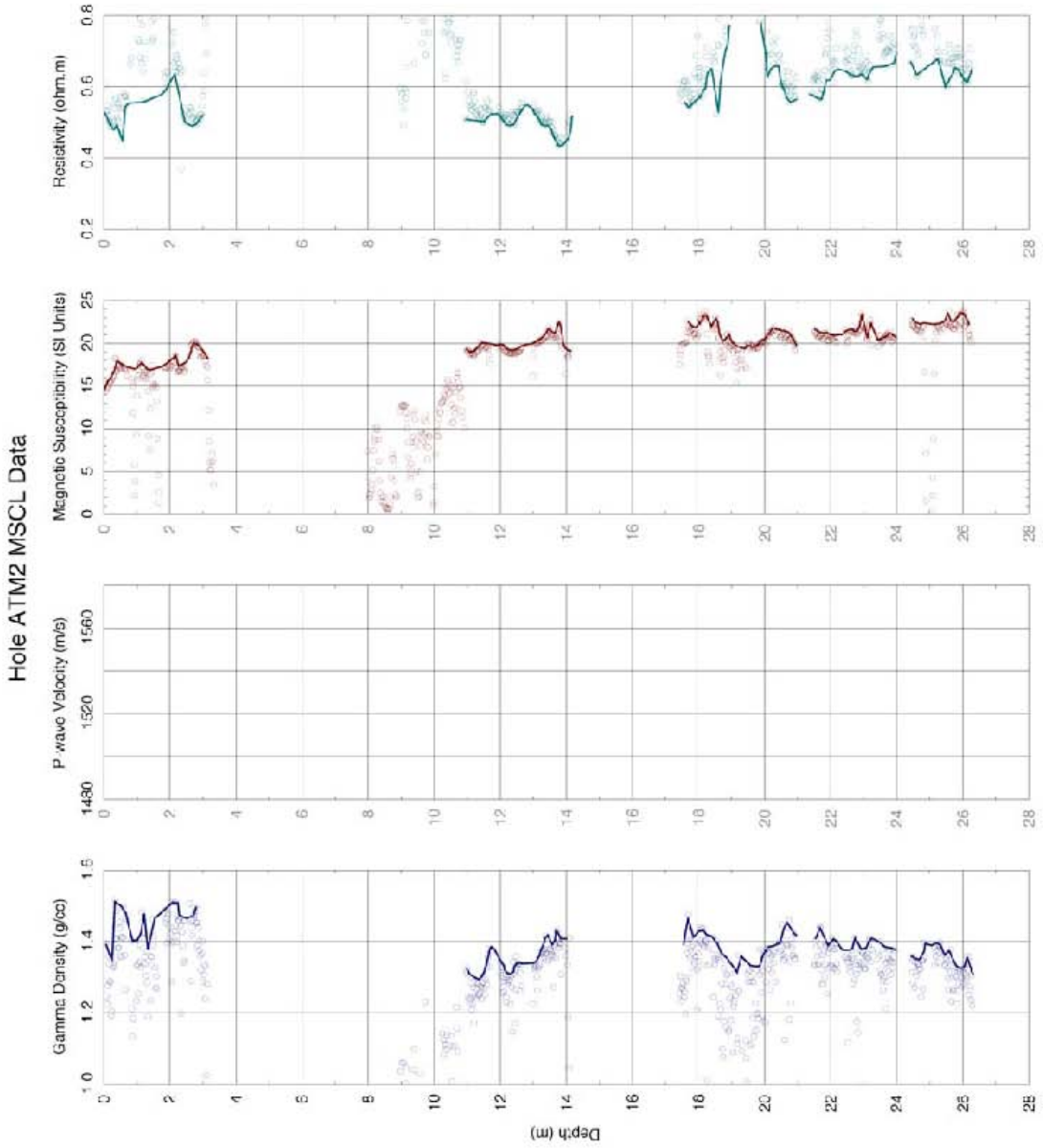

Figure ATM-10. MSCL-S data, including gamma density, P-wave velocity, magnetic susceptibility, and electrical resistivity, for Hole ATM2.

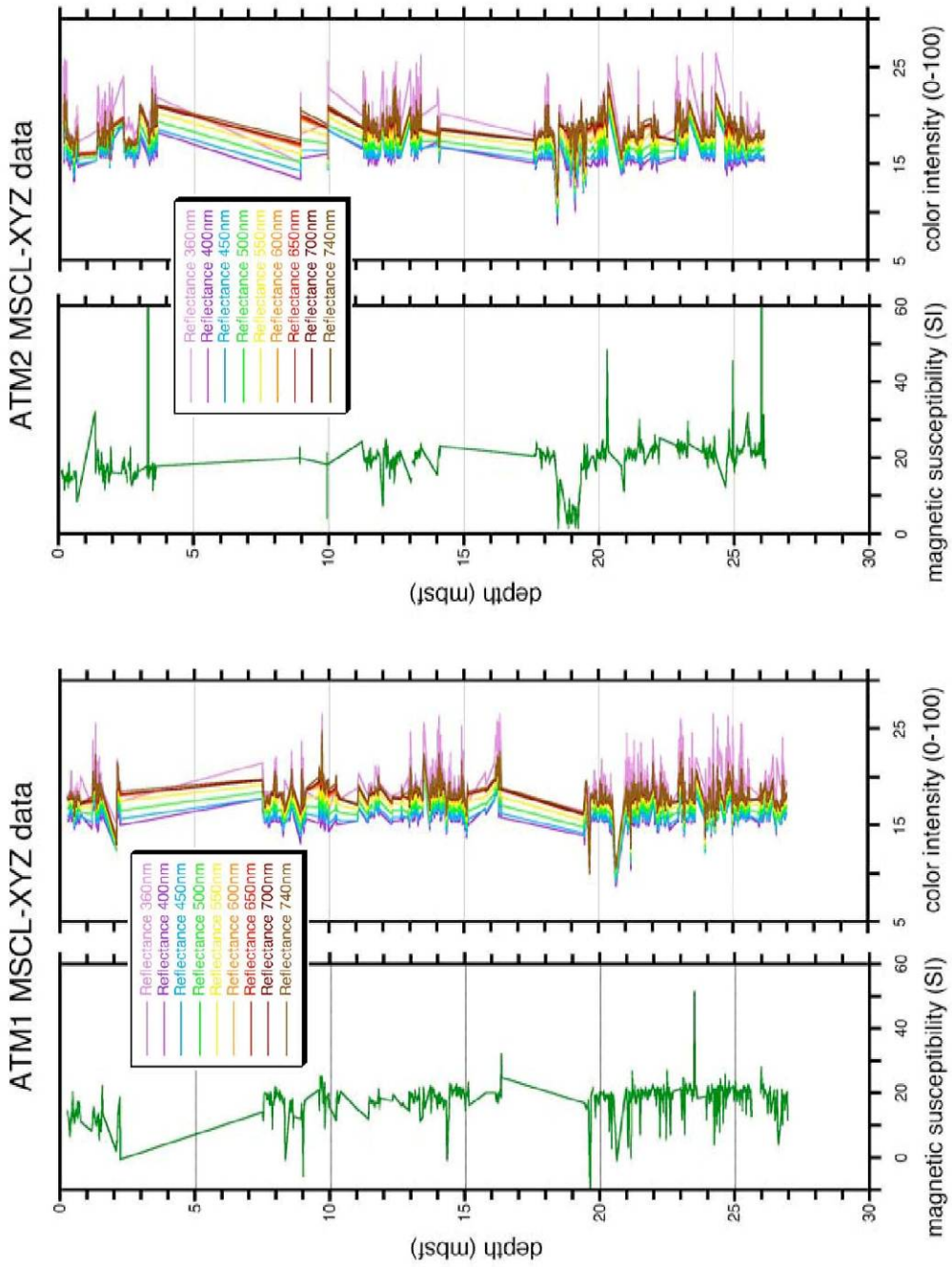

Figure ATM-11. MSCL-XYZ data summary plot, including magnetic susceptibility and color spectrophotometry, for Holes ATM1&2.

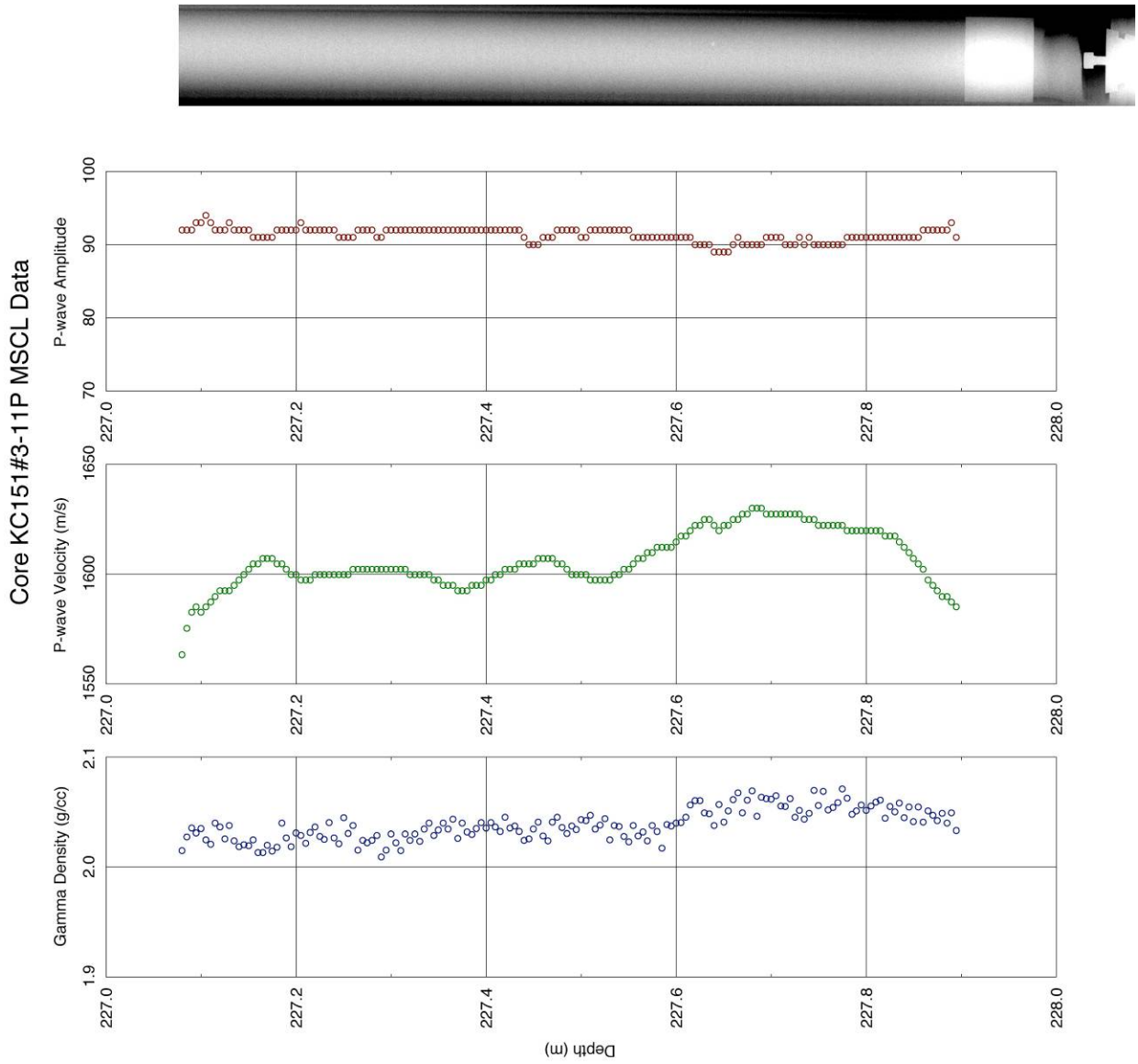

Figure KC151-1. Data from pressure core KC151-3-11P, collected from 227.08 mbsf at a pressure of 160 bar. Figure shows gamma density data, collected in the MSCL-V; P-wave velocity &amplitude, collected in the MSCL-P; and linear X-ray scan, collected in the X-ray CT scanner. Top two-thirds and bottom third of core are distinct in density and velocity.

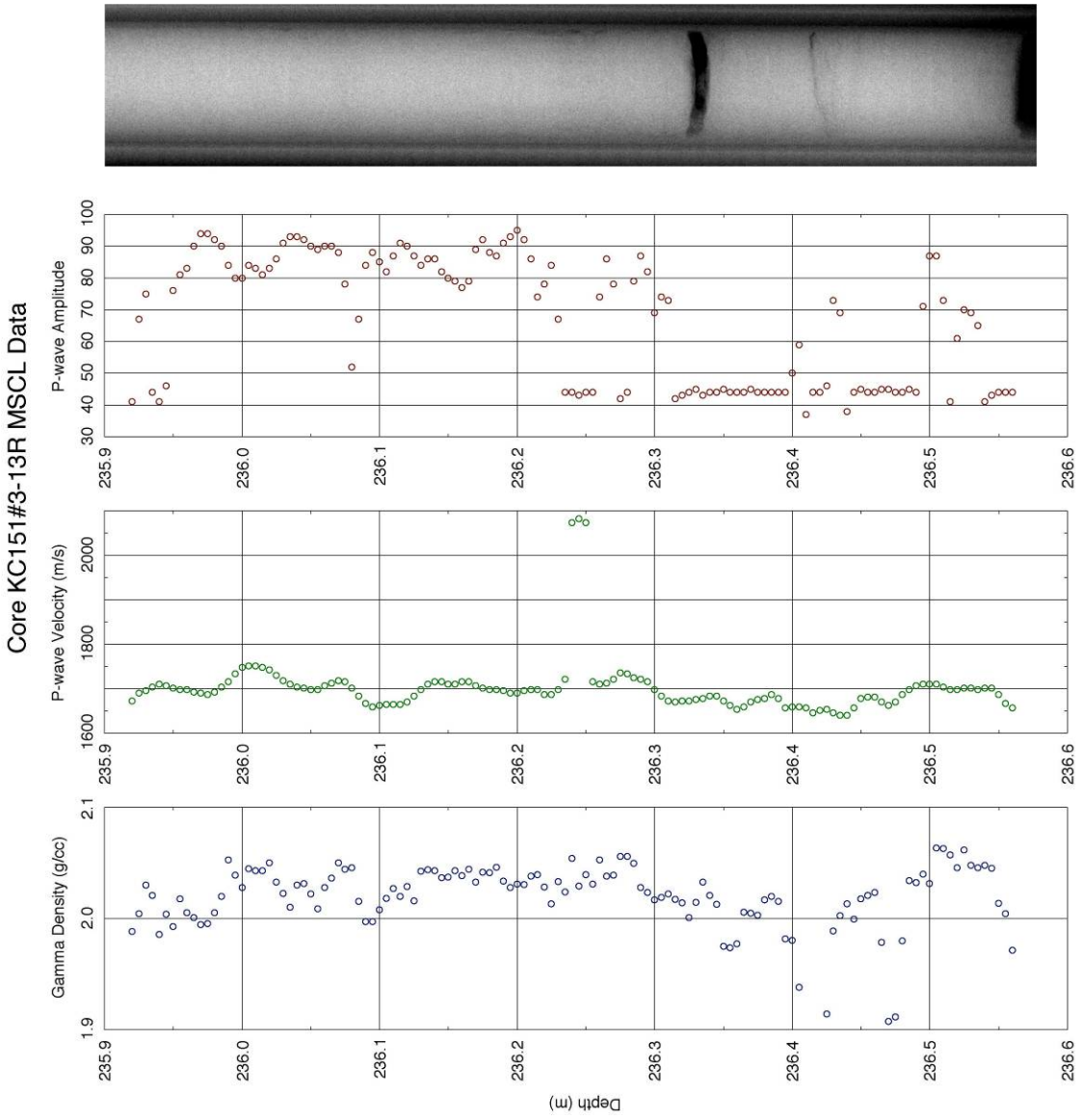

Figure KC151-2. Data from pressure core KC151-3-13R, collected from 235.92 mbsf at a pressure of 160 bar. Figure shows gamma density data, collected in the MSCL-V; P-wave velocity and amplitude, collected in the MSCL-P; and linear X-ray scan, collected in the X-ray CT scanner. Lower half of core is distinguished by low P-wave amplitudes, slightly lower P-wave velocity and more variable density. High-velocity spike at center of core may have been a thin hydrate vein.

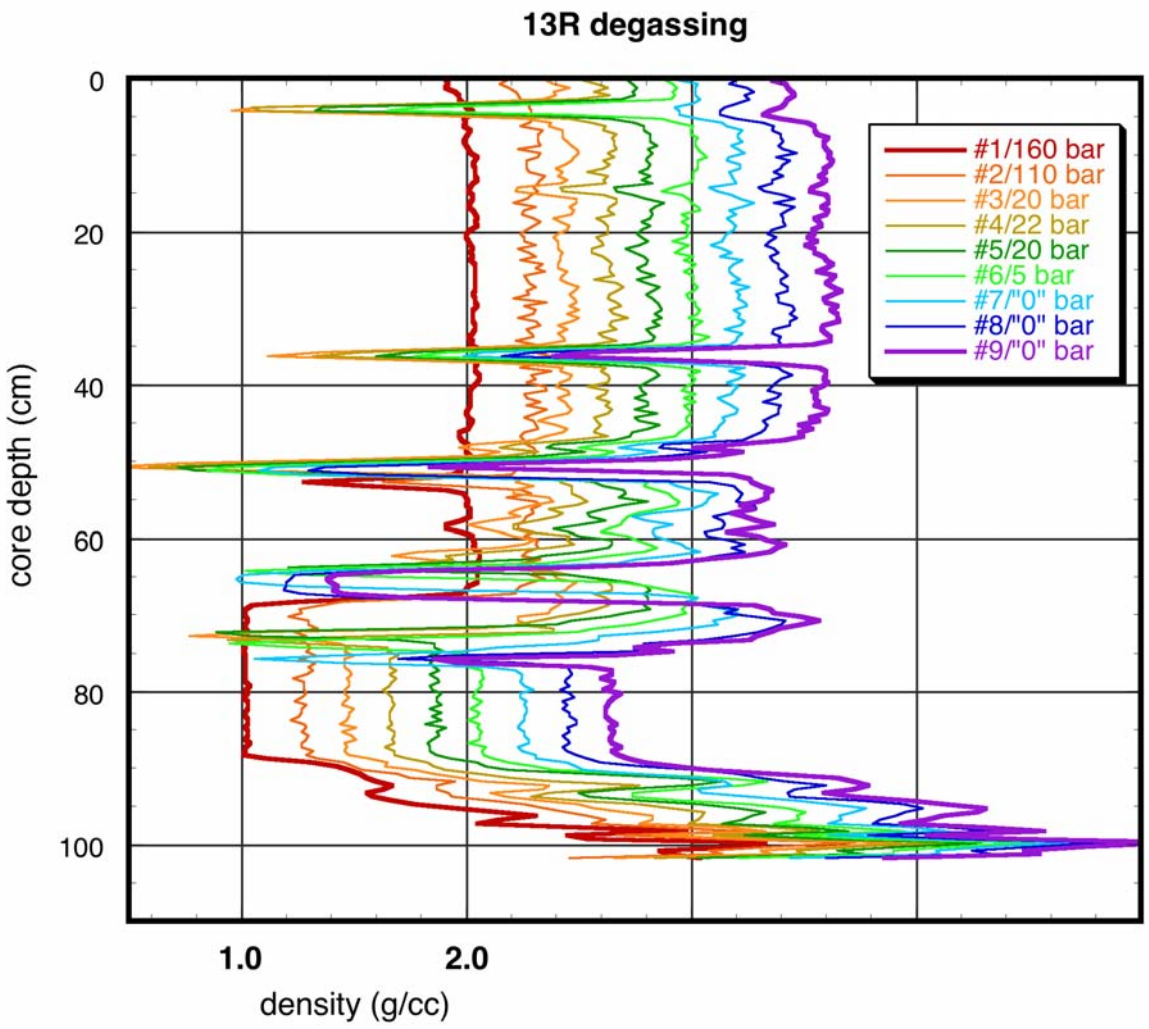

Figure KC151-3. Gamma density data from pressure core KC151-3-13R, collected on repetitive scans during depressurization. Legend shows density scan number and pressure. Each scan is offset from the next by 0.2 g/cc. The high-velocity spike in Figure KC151-2 may correspond to the crack in the core that formed at about 35 cm core depth.

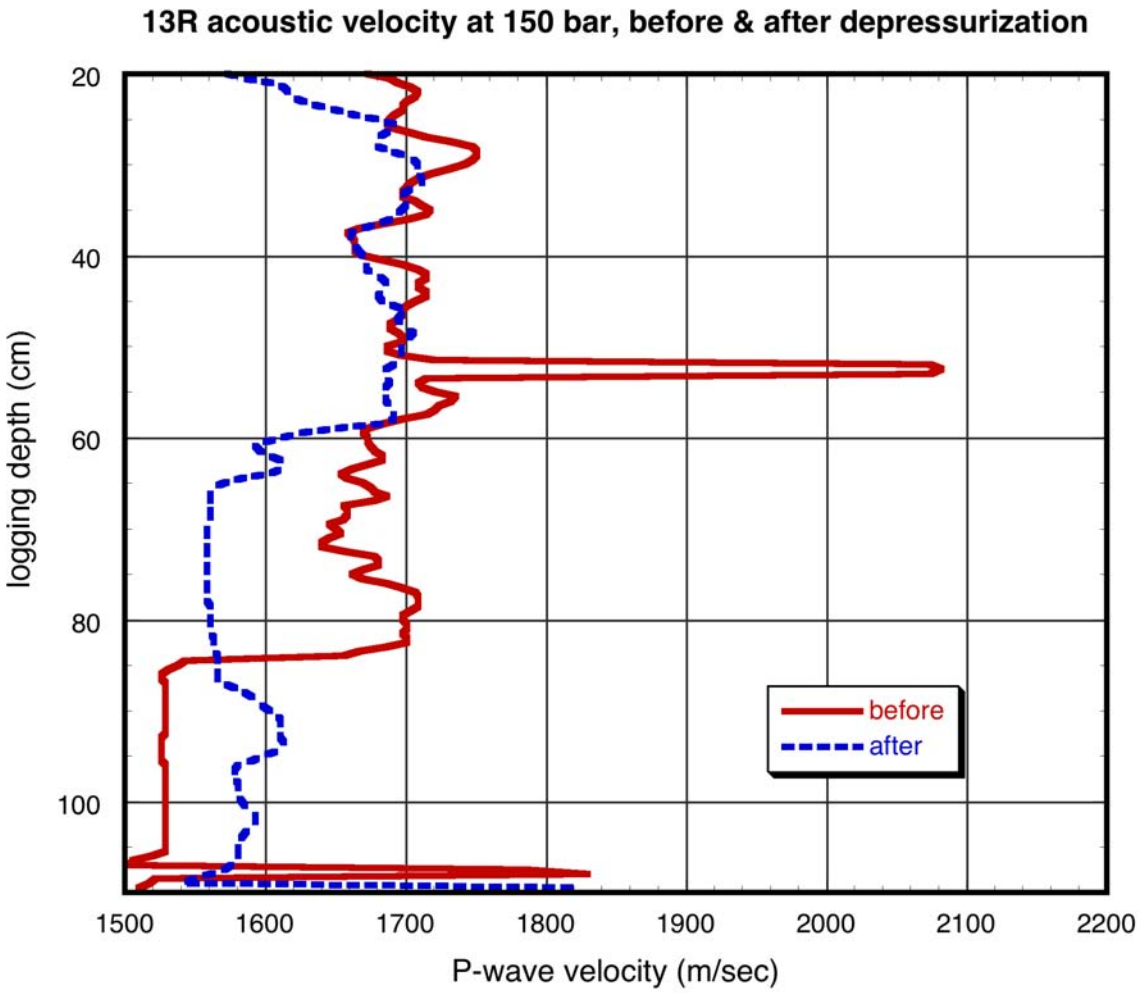

Figure KC151-4. P-wave velocity data from pressure core KC151-3-13R, collected on pristine core and repressurized core, after depressurization. Core starts at about 20 cm logging depth. Note that the high-velocity spike in the center of the core disappeared following depressurization.

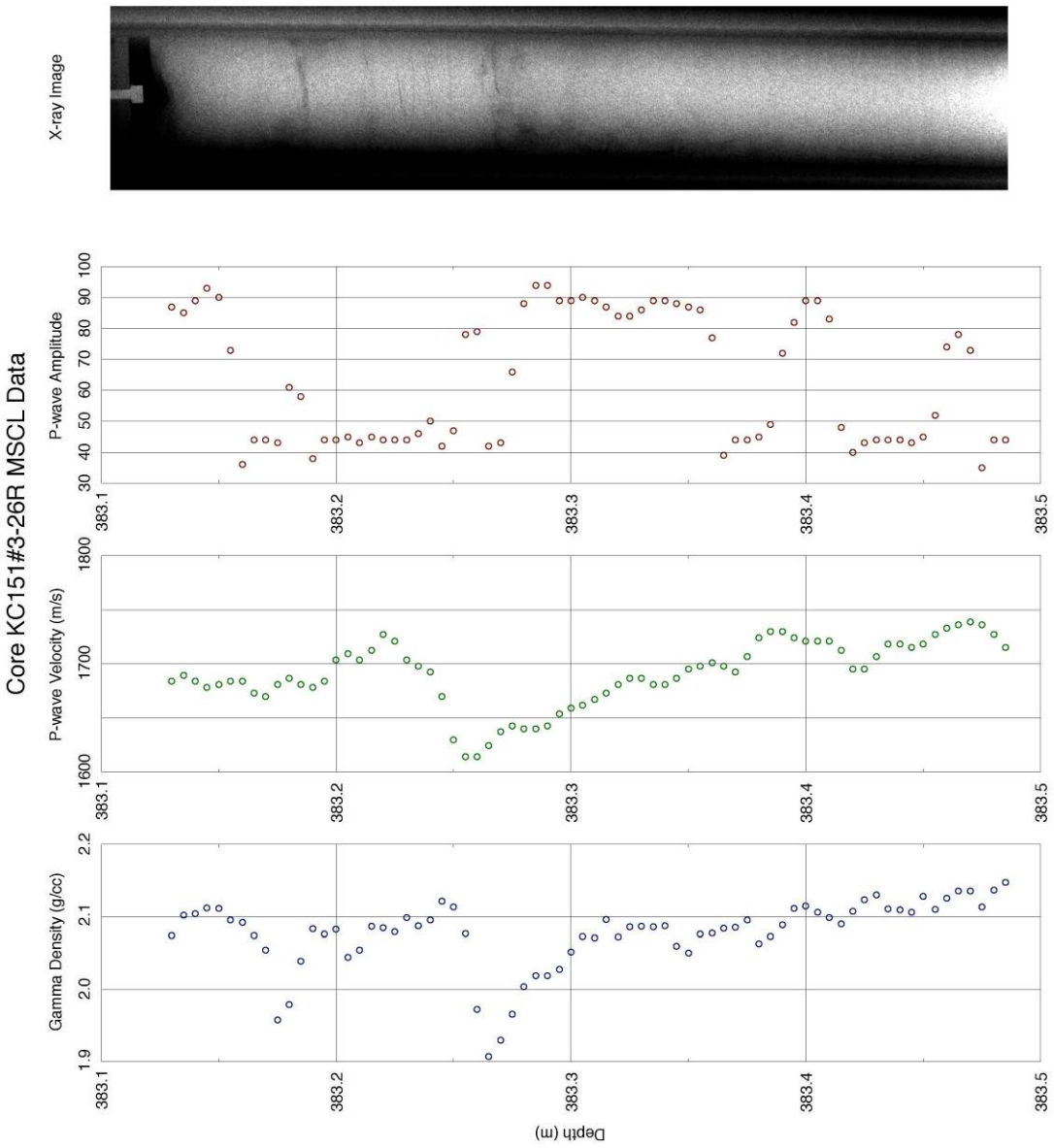

Figure KC151-5. Data from pressure core KC151-3-26R, collected from 383.13 mbsf at a pressure of 180 bar. Figure shows gamma density data, collected in the MSCL-V; P-wave velocity and amplitude, collected in the MSCL-P; and linear X-ray scan, collected in the X-ray CT scanner. Low velocity and densities near center of core and low amplitudes may indicate core disturbance by hydrate dissociation during core recovery.

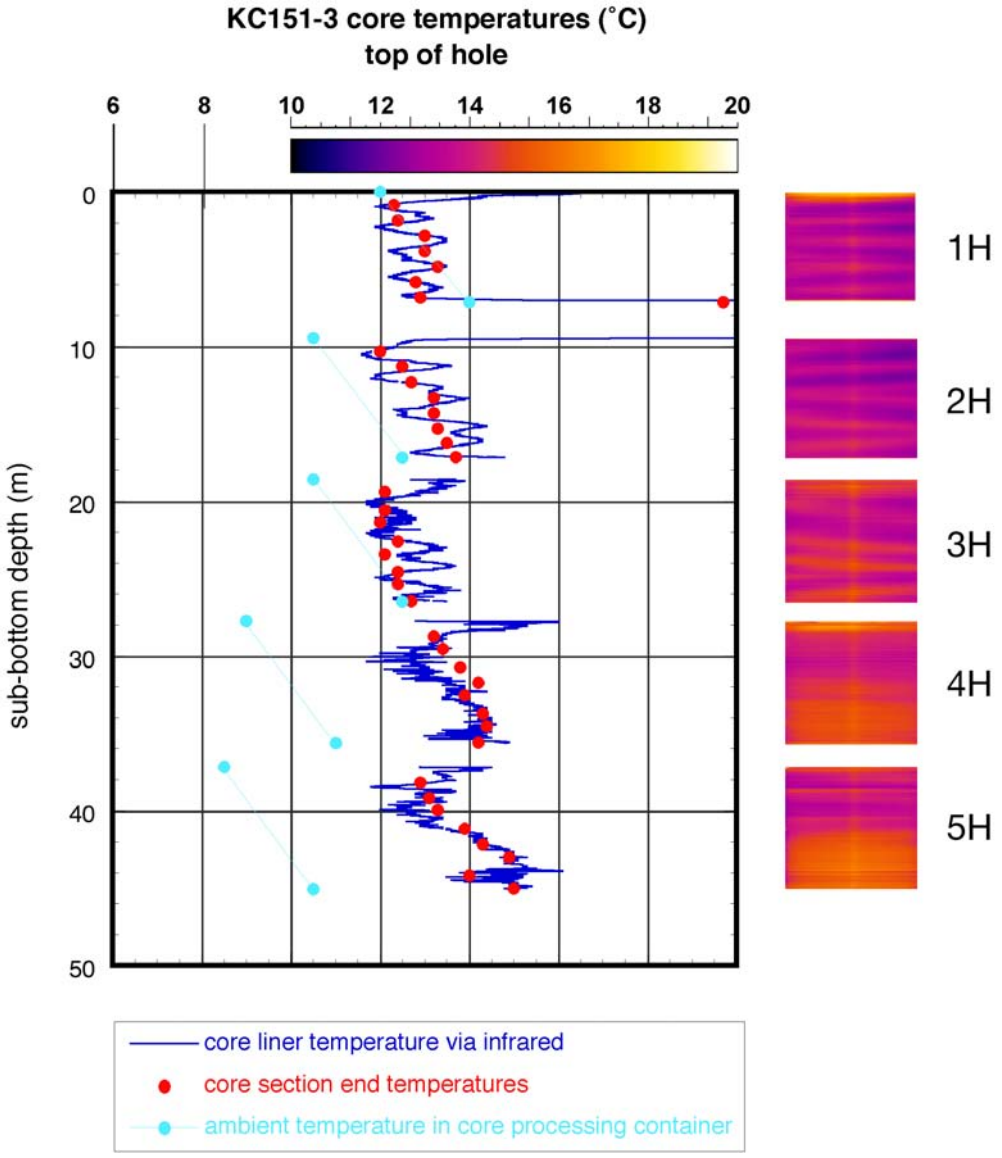

Figure KC151-6. Plot of temperature data from infrared imaging, which takes the temperature of the core liner, and from direct measurement of the center of the core at core section ends for top of Hole KC151-3. Two-dimensional infrared image is shown to the right of the plot.

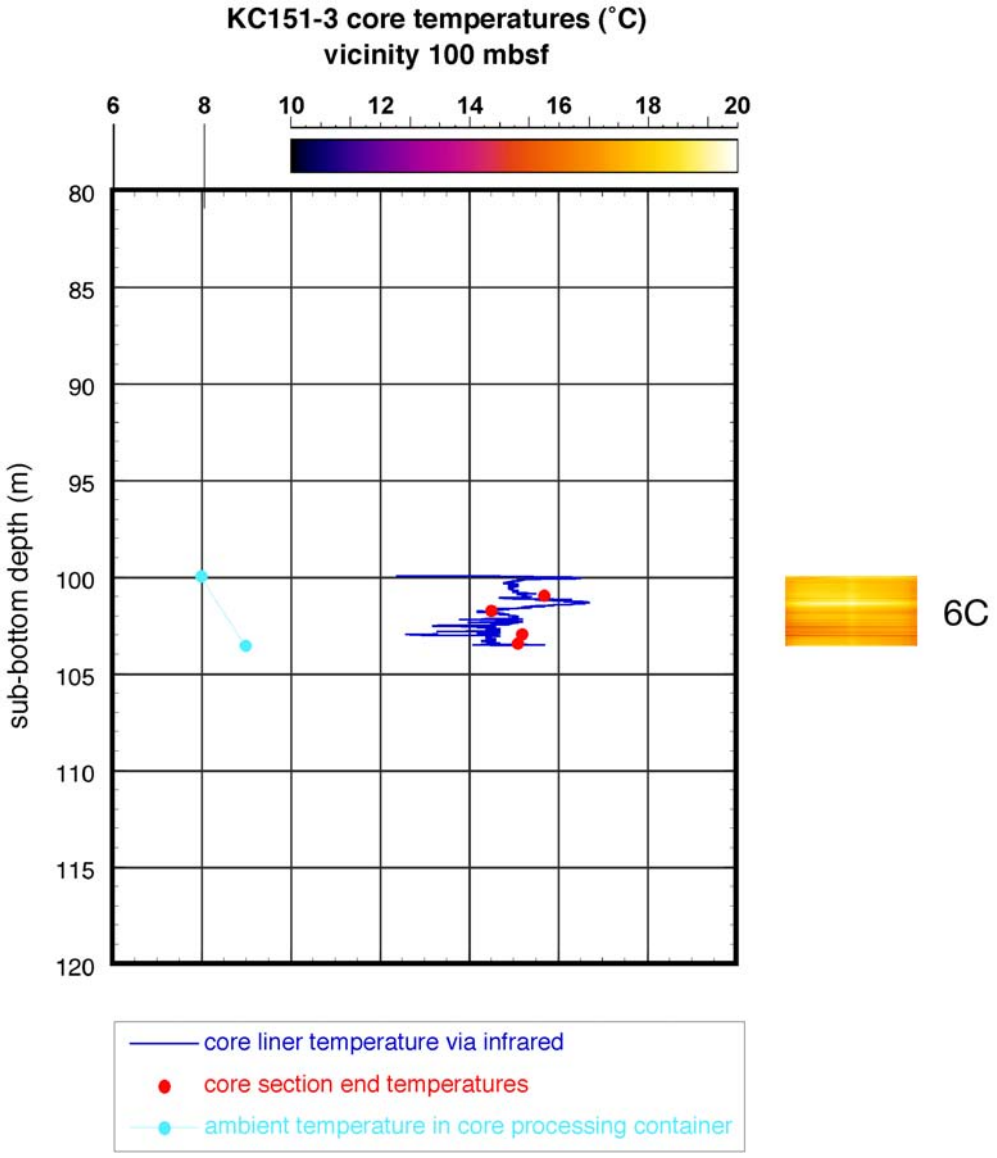

Figure KC151-7. Plot of temperature data from infrared imaging, which takes the temperature of the core liner, and from direct measurement of the center of the core at core section ends for middle of Hole KC151-3. Two-dimensional infrared image is shown to the right of the plot.

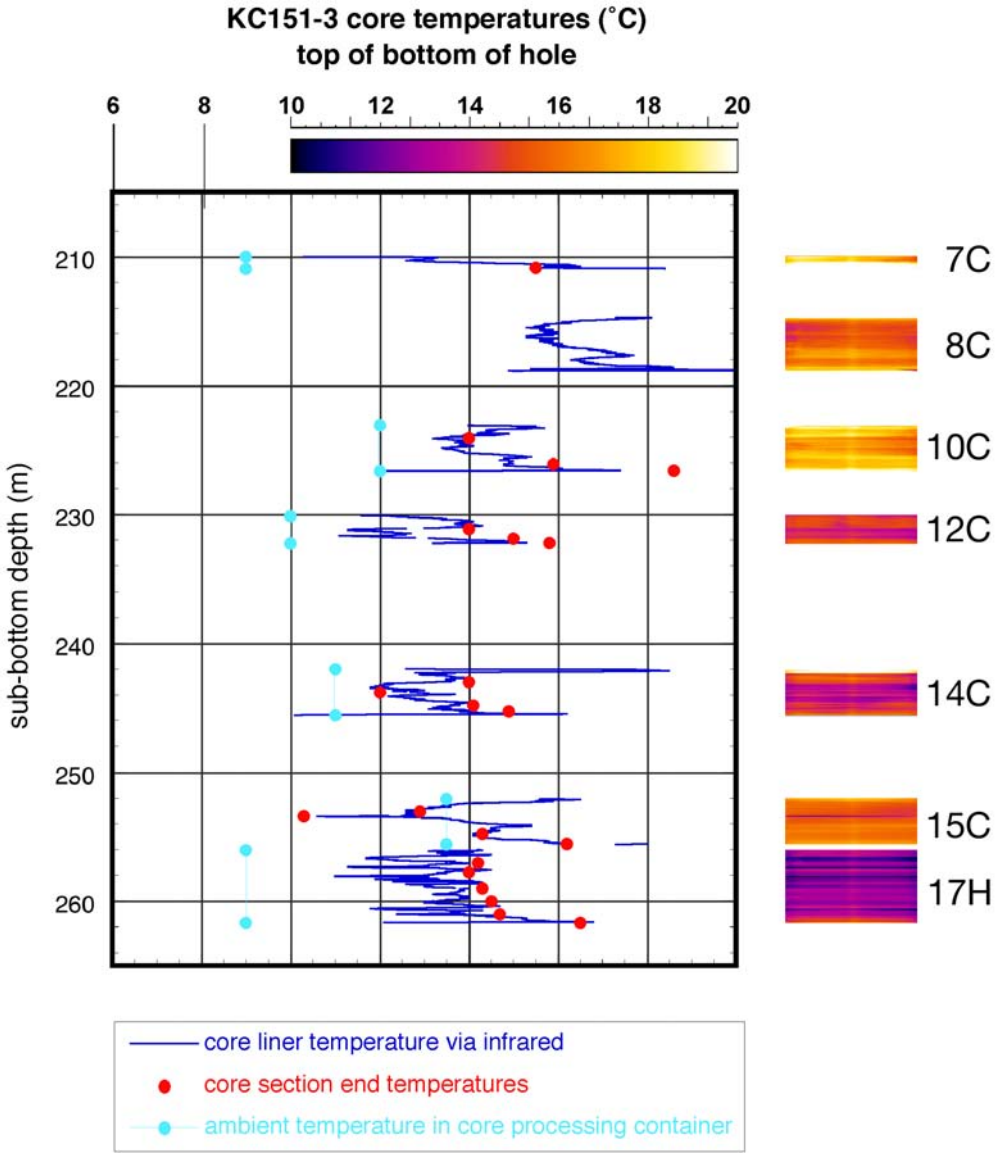

Figure KC151-8. Plot of temperature data from infrared imaging, which takes the temperature of the core liner, and from direct measurement of the center of the core at core section ends for top half of lower portion of Hole KC151-3. Two-dimensional infrared image is shown to the right of the plot.

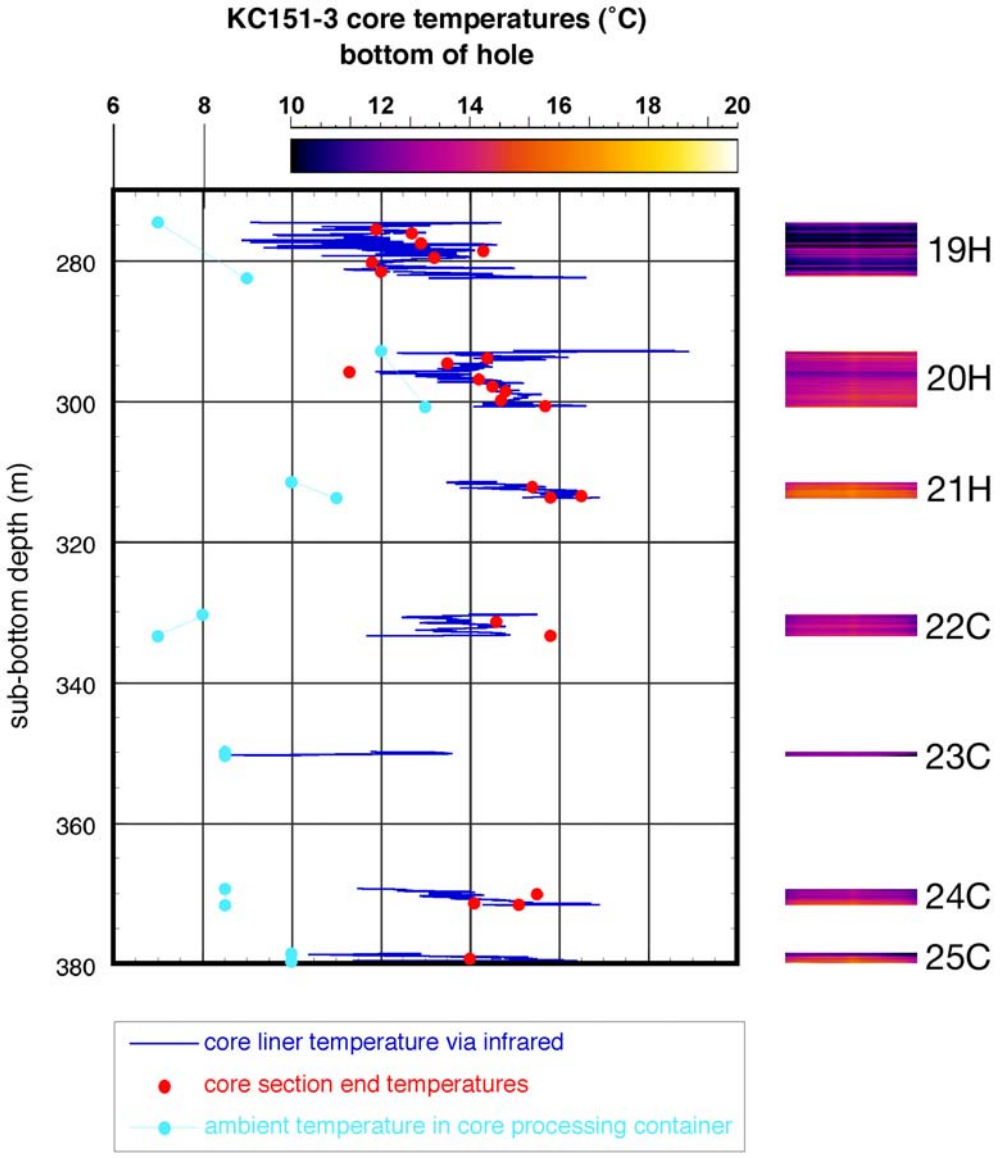

Figure KC151-3-9. Plot of temperature data from infrared imaging, which takes the temperature of the core liner, and from direct measurement of the center of the core at core section ends for bottom half of lower portion of Hole KC151-3. Two-dimensional infrared image is shown to the right of the plot.

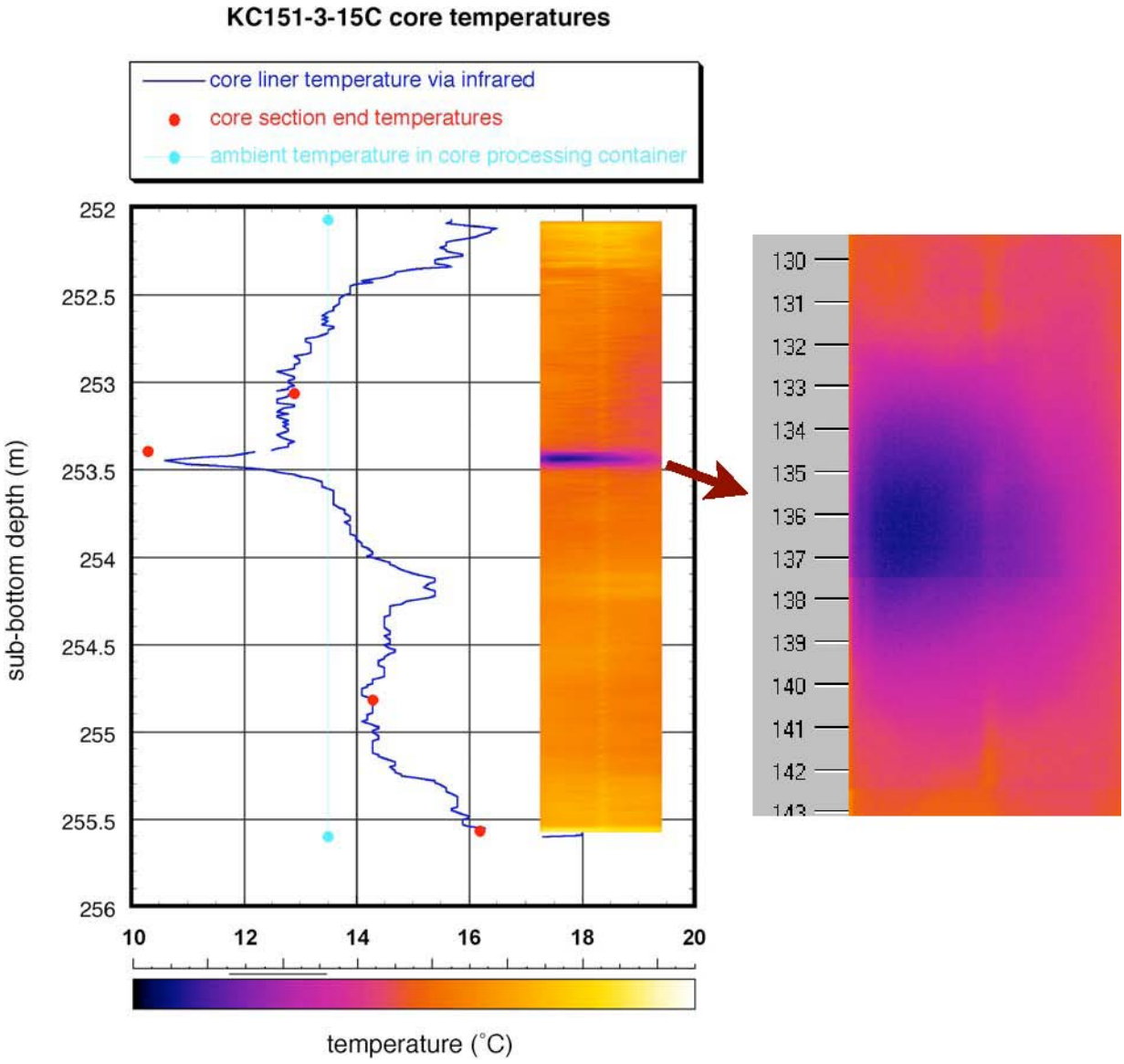

Figure KC151-10. Temperature data for Core KC151-3-15C, including infrared image. The negative thermal anomaly at 253.45 mbsf displayed classic magnitude and morphology for a hydrate generated thermal anomaly. Slight discontinuity at 137.5 cm is a result of joining the adjacent infrared images.

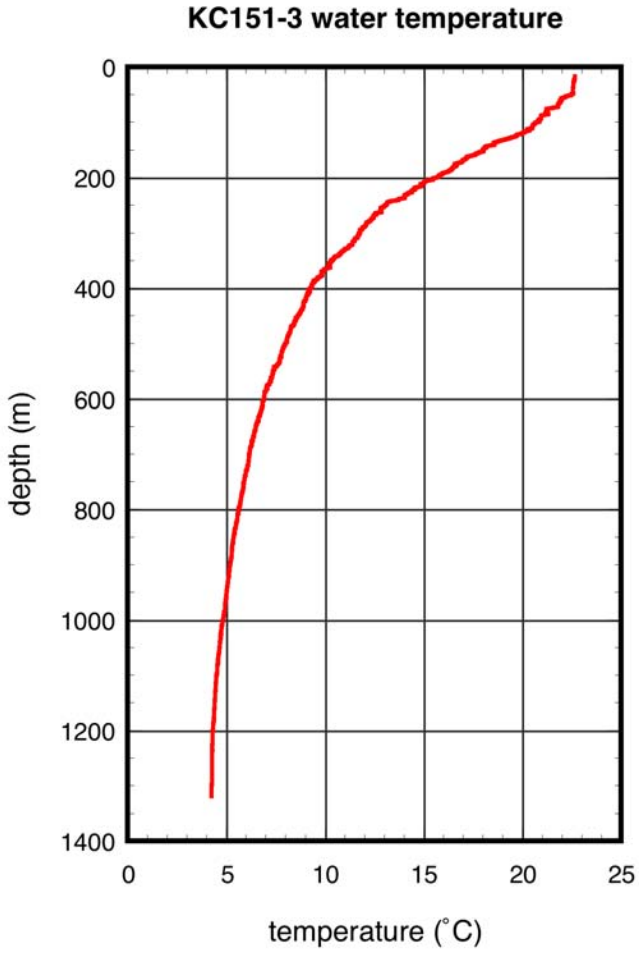

Figure KC151-11. Temperature data from the Seabird CTD cast over Site KC151.

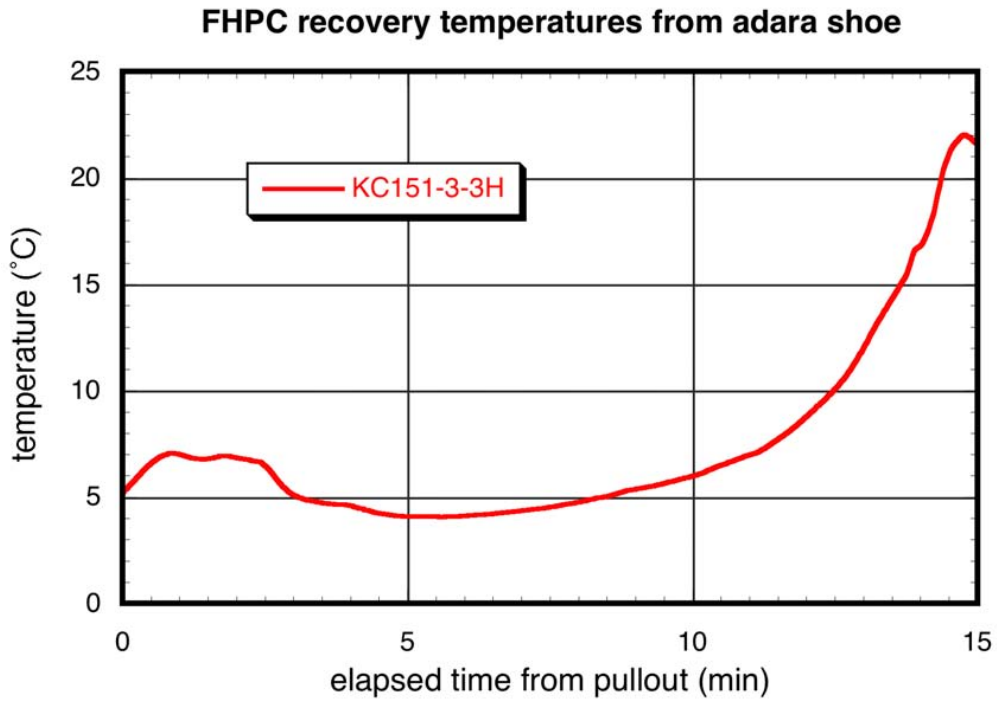

Figure KC151-12. Temperature data from the temperature shoe fitted on the FHPC for core KC151-3-3H.

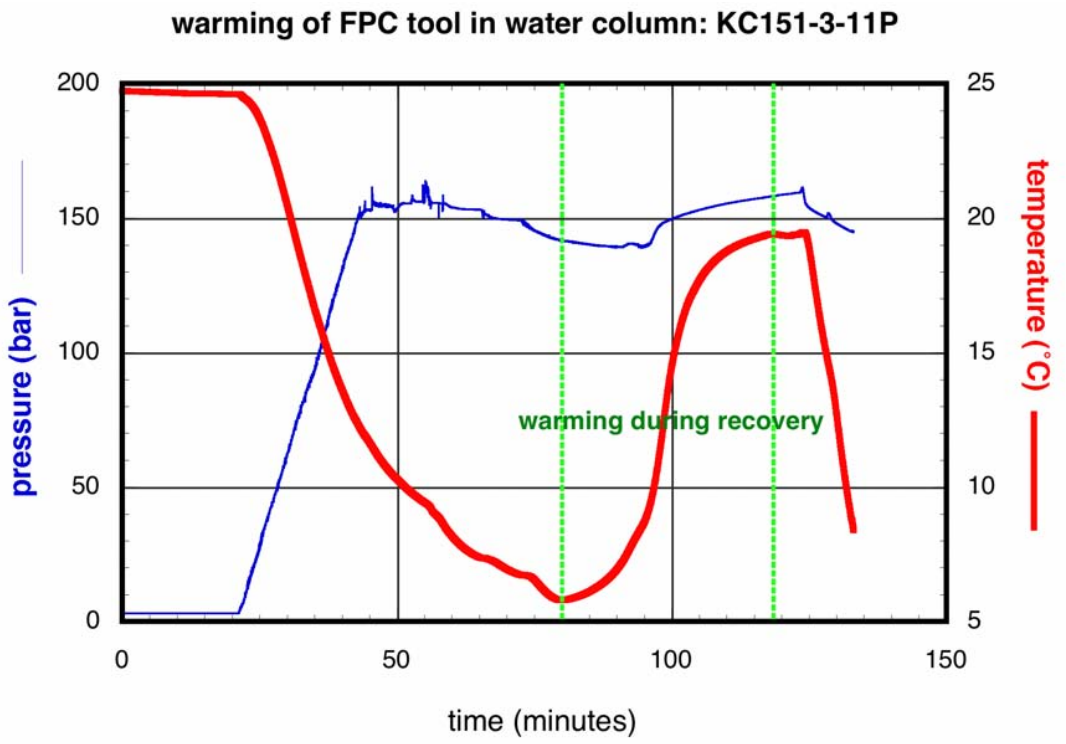

Figure KC151-13. Temperature and pressure data versus time for Core KC151-3-11P. The retrieval of the tool up the drill pipe is bounded by green dashed lines.

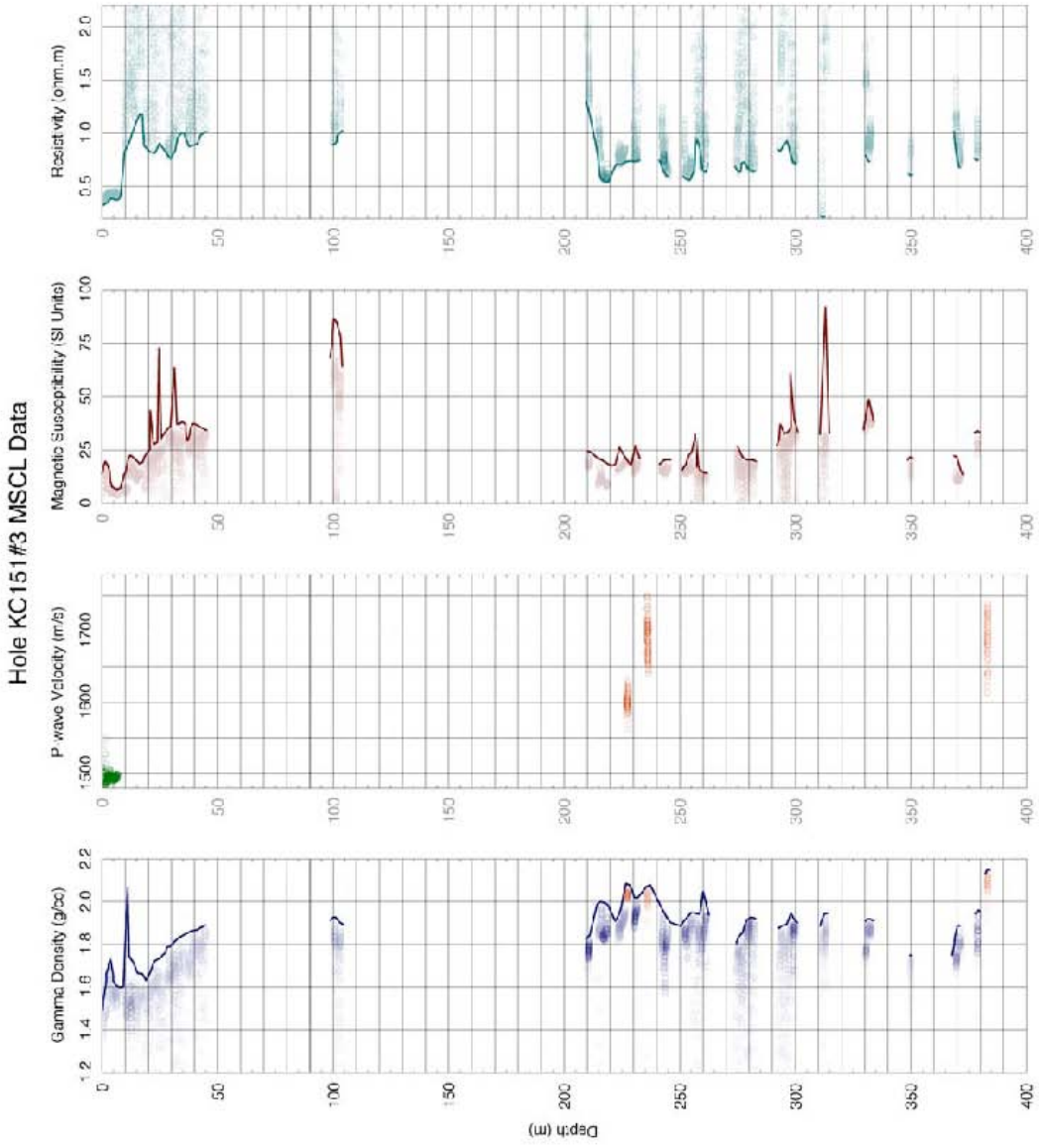

Figure KC151-14. MSCL-S data, including gamma density, P-wave velocity, magnetic susceptibility, and electrical resistivity, for Hole KC151-3. Gamma density and P-wave velocity from pressure cores KC151-3-11P, -13R, and -26R, measured under *in situ* pressure, are included in this composite in orange. High-velocity spike in Core KC151-3-13R of 2074 m/sec is off scale.

Figure KC151-15. Color line scan image of Core KC151-3-20H, 55-65 cm, showing millimeter-thick, sub-horizontal white veins that may be carbonate.

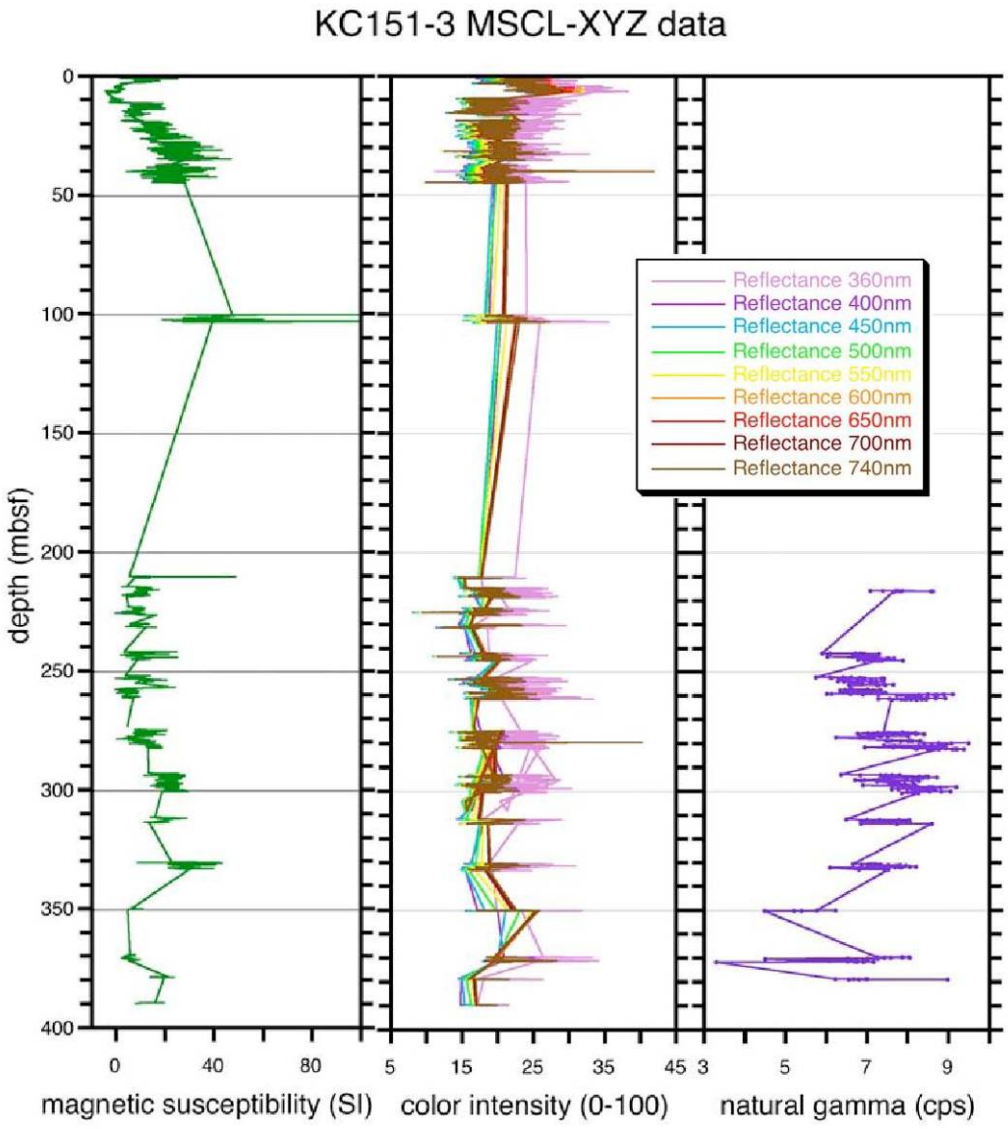

Figure KC151-16. MSCL-XYZ data summary plot, including magnetic susceptibility, color spectrophotometry, and natural gamma radioactivity, for Hole KC151-3. Data for natural gamma was only collected on cores below 200 mbsf.

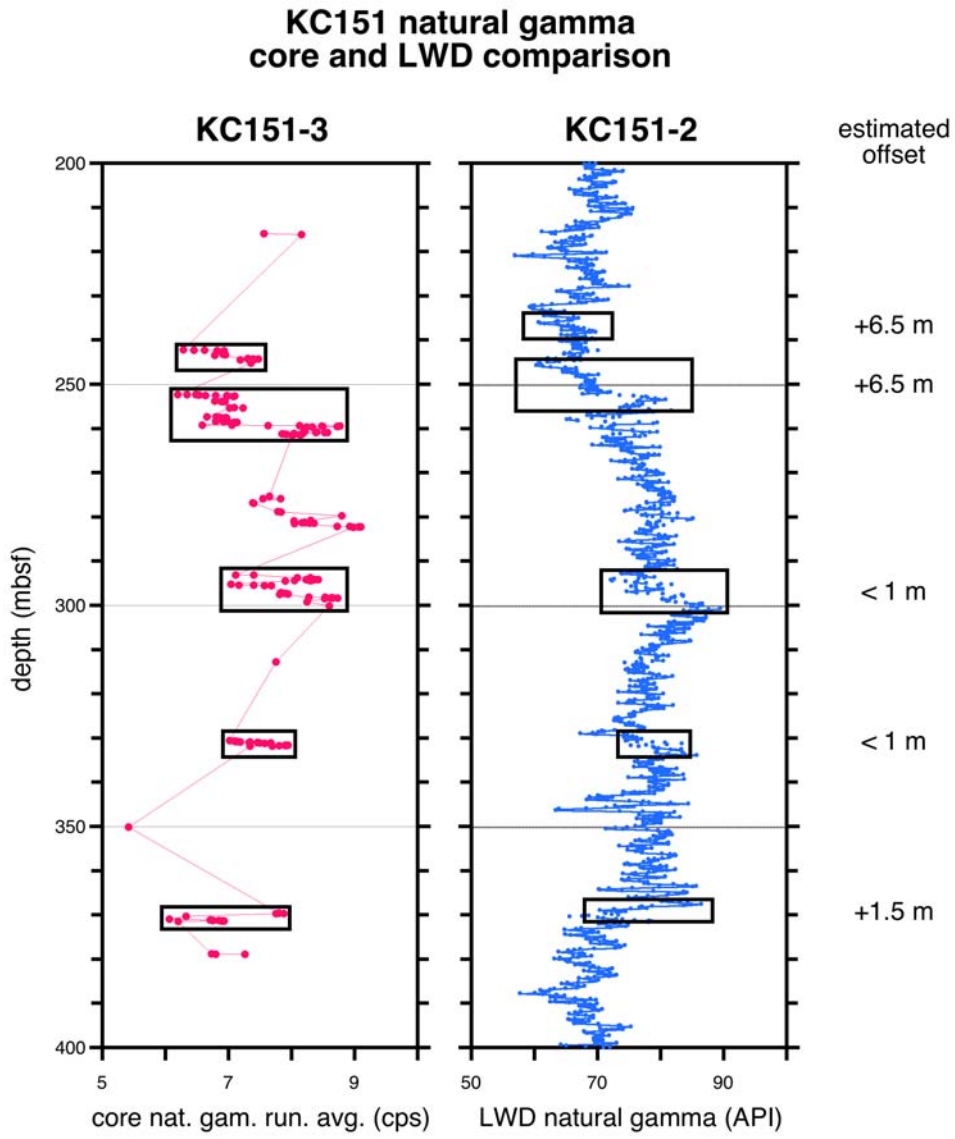

Figure KC151-17. Natural gamma data collected on split cores from KC151-3 compared to logging while drilling natural gamma data from Hole KC151-2. Core data has been smoothed for comparison with the down hole data. Boxed zones are provisional matched strata, and offsets of KC151-3 from KC151-2 are at right.

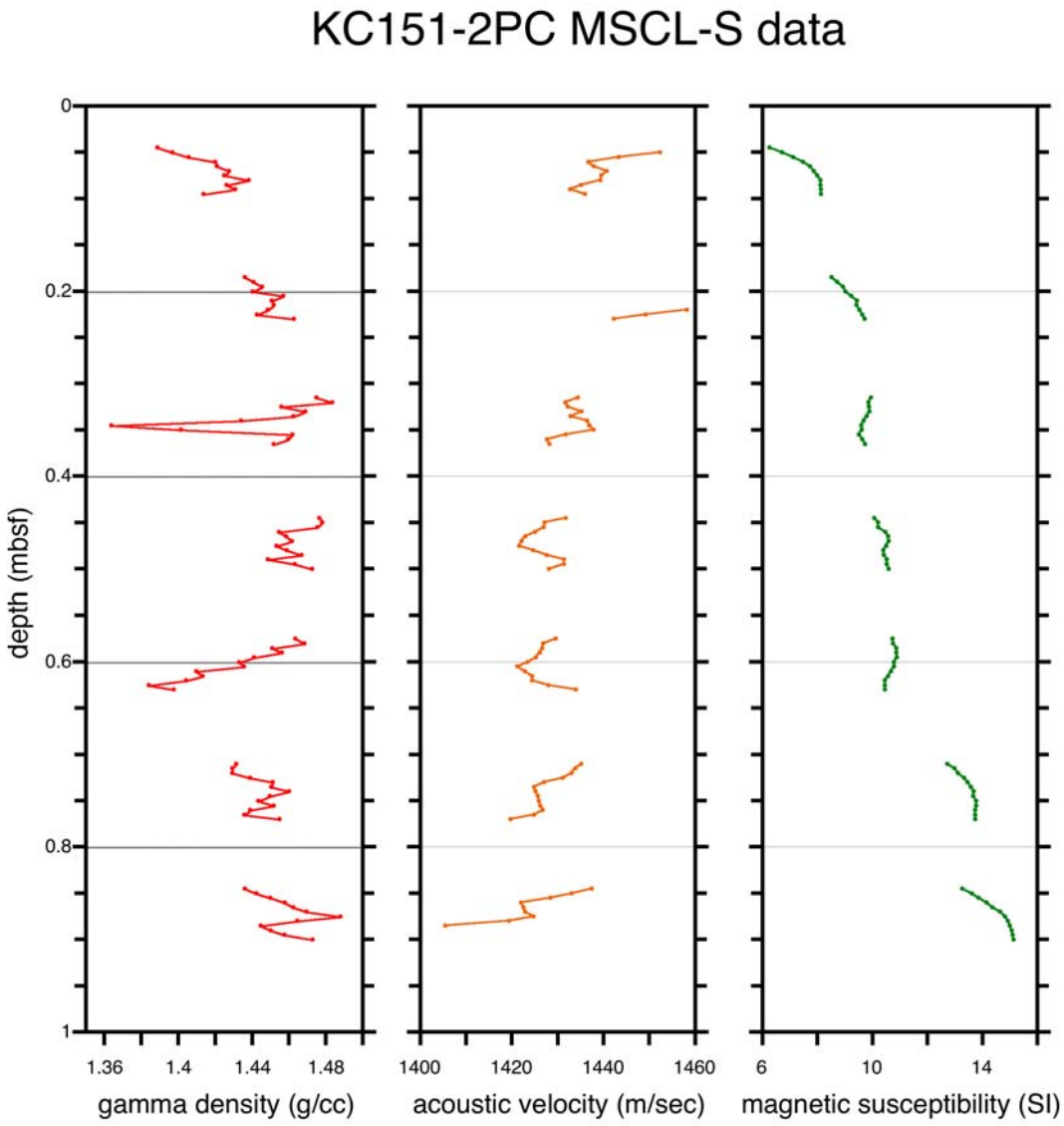

Figure KC151-18. MSCL-S data summary plot, including gamma density, P-wave velocity, and magnetic susceptibility, for push core KC151-2PC.